

MIXED BED ION-EXCHANGE MODELING FOR  
DIVALENT IONS IN A TERNARY SYSTEM

By

SUDHIR K. PONDUGULA

Bachelor of Technology

Andhra University

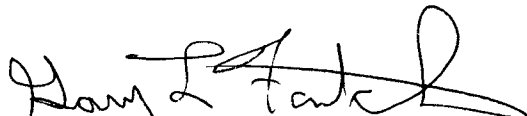
Visakhapatnam, AP, India

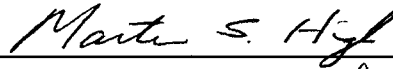
1992

Submitted to the Faculty of the  
Graduate College of  
Oklahoma State University  
in partial fulfillment of  
the requirements for  
the Degree of  
MASTER OF SCIENCE  
May, 1995

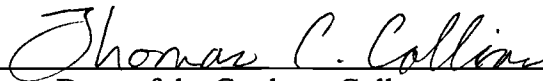
MIXED BED ION-EXCHANGE MODELING FOR  
Divalent Ions in a Ternary System

Thesis Approved:

  
\_\_\_\_\_  
Thesis Adviser

  
\_\_\_\_\_

  
\_\_\_\_\_

  
\_\_\_\_\_  
Dean of the Graduate College

## PREFACE

Film controlled mixed bed simulations for divalent ions in a ternary system were studied in this work. The presence of divalent ions influences the electric field produced as a result of difference in ionic mobilities of the ions. Flux expressions, particle rates, and column material balances are combined and appropriate numerical methods applied to analyze the column effluent concentrations for all the ionic impurities. The model is tested for wide range of conditions. Mathematical modeling was complex and a generalized theoretical model was developed with assumptions where necessary.

I wish to express my deepest appreciation to my major advisor, Dr. Gary L. Foutch, for his guidance, inspiration, patience and invaluable helpfulness throughout my masters program. Grateful acknowledgment is also extended to Dr. Arland H. Johannes and Dr. Martin High for serving on the advisory committee and very helpful suggestions and their technical assistance.

Special gratitude and appreciation are expressed to my parents for their encouragement, understanding, and sacrifice. Particular thanks go to Mr. Vikram Chowdiah for his help and suggestions throughout my study.

Financial assistance from school of Chemical Engineering at Oklahoma State University, and Pennsylvania Power & Light (PP&L) for the completion of this study, are gratefully appreciated.

I would like to express special thanks to all my friends for their encouragement in completing this manuscript.

## TABLE OF CONTENTS

Chapter	Page
I. INTRODUCTION.....	1
Ion Exchange Resin.....	2
Removal of Sulfate by Ion Exchange.....	3
Objective.....	4
II. LITERATURE REVIEW.....	6
Ion Exchange Capacity.....	6
Equilibria and Selectivity.....	6
Kinetics and Mechanism of Ion Exchange.....	14
III. MIXED BED ION EXCHANGE MODELING FOR DIVALENT SPECIES-EFFECT OF SYSTEM PARAMETERS.....	15
Abstract.....	15
Introduction.....	15
Diffusion Coefficients.....	17
Model Development.....	18
Flux Expression.....	19
Interfacial Concentration.....	20
Model Assumptions.....	22
Temperature Effects.....	23
Results and Discussion.....	23
Desulphonation of Strongly Acidic Cation.....	29
Flow Rate Effects.....	33
Reduced Anion Mass Transfer Coefficients Effects.....	38
Effects of Particle Sizes.....	41
Effects of Resin Ratios.....	47
Conclusions and Recommendations.....	47
IV. EFFECT OF PLANT OPERATING PRINCIPLES- RESIN HEEL AND BED CLEANING.....	52
Abstract.....	52
Introduction.....	52
Modeling.....	53
Comparison to Plant Experience.....	54
Bed Cleaning Effects.....	60

Chapter	Page
LITERATURE CITED.....	65
APPENDIX A -ANION FLUX EXPRESSIONS.....	70
APPENDIX B -PARTICLE RATES.....	79
APPENDIX C -COLUMN MATERIAL BALANCES.....	83
APPENDIX D -NUMERICAL METHODS.....	88
APPENDIX E -INLET CONDITIONS AND MODEL PARAMETER VALUES.....	91
APPENDIX F -COMPUTER CODE.....	94

## LIST OF TABLES

Table	Page
II-1 Equilibrium Constants Determined from Binary Experimental data.....	10
II-2. Triangle Rule for Equilibrium Constants.....	11
II-3. Estimates of Equilibrium Constants for Binary Systems at 298° K.....	13
III-1. Conductance as a Function of Temperature.....	18
III-2. Model Assumptions.....	22
III-3 Temperature Effects on Sodium Exchange Parameters Using MBIE Divalent Model.....	24
III-4. Temperature Effects on Calcium Exchange Parameters Using MBIE Divalent Model.....	26
III-5. Temperature Effects on Chloride Exchange Parameters Using MBIE Divalent Model.....	29
III-6. Temperature Effects on Sulfate Exchange Parameters Using MBIE Divalent Model.....	30
D-1. Coefficients of Backward Differentiation Formulas.....	90
E-1. Values Adjusted for Electroneutrality Criteria.....	92

## LIST OF FIGURES

Figure	Page
1. Effect of Temperature on Sodium Concentration profile for a Mixed bed (Cation/Anion ratio of 1.0) Simulation.....	25
2. Effect of Temperature on Calcium Concentration Profile for a Mixed-Bed (Cation/Anion Ratio of 1.0) Simulation.....	27
3. Effect of Temperature on Chloride Concentration Profile for a Mixed-Bed (Cation/Anion Ratio of 1.0) Simulation.....	28
4. Effect of Temperature on Sulfate Concentration profile for a Mixed-Bed (Cation/Anion Ratio of 1.0) Simulation.....	31
5. Reaction Kinetic Constant for Desulphonation of strongly Acidic Cation Ion Exchange Resin.....	32
6. Effect of Flow rate on Sodium Concentration profile for a Mixed-Bed (Cation/Anion Ratio of 1.0) Simulation.....	34
7. Effect of Flow rate on Calcium Concentration profile for a Mixed-Bed (Cation/Anion Ratio of 1.0) Simulation.....	35
8. Effect of Flow rate on Chloride concentration profile for a Mixed-Bed (Cation/Anion Ratio of 1.0) Simulation.....	36
9. Effect of Flow rate on Sulfate concentration profile for a Mixed-Bed (Cation/Anion Ratio of 1.0) Simulation.....	37
10. Effect of Reduced Anion Mass Transfer Coefficient on Chloride with System Parameters at Base Case.....	39
11. Effect of Reduced Anion Mass Transfer Coefficient on Sulfate with System Parameters at Base Case.....	40

Figure	Page
12. Effect of Resin Particle Size on Sodium Concentration Profile for a Mixed Bed Simulation.....	43
13. Effect of Resin Particle Size on Calcium Concentration Profile for a Mixed Bed Simulation.....	44
14. Effect of Resin Particle Size on Chloride Concentration Profile for a Mixed Bed Simulation.....	45
15. Effect of Resin Particle Size on Sulfate Concentration Profile for a Mixed Bed Simulation.....	46
16. Effect of Resin Fraction on Sodium Concentration Profile for a Mixed Bed Simulation.....	48
17. Effect of Resin Fraction on Chloride Concentration Profile for a Mixed Bed Simulation.....	49
18. Effect of Resin Fraction on Sulfate Concentration Profile for a Mixed Bed Simulation.....	50
19. Effect of Resin Heels on Sodium Concentration Profile using MBIE Model for Divalent Ions.....	55
20. Effect of Resin Heels on Calcium Concentration Profile using MBIE Model for Divalent Ions.....	56
21. Effect of Resin Heels on Chloride Concentration Profile using MBIE Model for Divalent Ions.....	57
22. Effect of Resin Heels on Sulfate Concentration Profile using MBIE Model for Divalent Ions.....	58
23. Effect of Bed Cleaning every three weeks on Sodium Concentration Profile using MBIE model for Divalent Ions.....	61
24. Effect of Bed Cleaning every three weeks on Calcium Concentration Profile using MBIE model for Divalent Ions.....	62
25. Effect of Bed Cleaning every three weeks on Chloride Concentration Profile using MBIE model for Divalent Ions.....	63



Figure

Page

26.	Effect of Bed Cleaning every three weeks on Sulfate Concentration Profile using MBIE model for Divalent Ions.....	64
-----	---	----

## CHAPTER I

### INTRODUCTION

Ion exchange has found widespread application in the power and electronic industries. Ion exchange is defined as a reversible exchange of ions between a solid and a liquid in which there is no substantial change in the structure of the solid. Several applications of ion exchange include

- Removal of objectionable cations and anions from drinking and boiler feed water.
- Production of de-ionized water.
- Treatment of trade effluents, both for the purification of liquors and for economic recovery of small amounts of inorganic and organic substances.
- Purification of organic and inorganic chemicals.
- Treatment in analytical chemistry.
- Separation of ion mixtures.
- Others such as determination of the properties of substances in solution for the measurement of the stability of complex ions, medical uses such as in ulcer treatment for neutralization of excess acids by anion exchange resins and sodium removal from the body.

The fundamental principles of ion exchange are based on a few simple facts about the exchange reactions:

1. Ion exchange reactions are stoichiometric.
2. Ions differ in their preference to react with ion exchanging solids. The selectivity is a measurement of the relative preference of one ion to another for a particular material.

3. Ion exchanging materials have the ability to exclude coions. This is known as Donnan exclusion.
4. Very large ions or polymers are subject to a screening effect and are not adsorbed to an appreciable extent.
5. Differences in migration rates of adsorbers substances down a column - primarily a reflection of differences in affinity.
6. Ionic mobility are restricted to the exchangeable ions and counter ions only.
7. Miscellaneous effects include swelling, surface area, and other mechanical properties. These effects may involve basic chemistry of ion exchanger and does have an influence on the overall ion exchange kinetics.

### Ion Exchange Resins

The most common ion-exchange resins are synthetic organic resins; actually a special type of polyelectrolytes. Cross-linked polyelectrolytes can be visualized as an elastic three dimensional hydrocarbon network to which a large number of ion active groups are attached. The most useful hydrocarbon is the copolymerization of styrene and divinylbenzene. This structure gives a maximum resistance to oxidation, reduction, mechanical wear and breakage, and is insoluble in common solvents. The ion active group is always fixed to the high molecular weight polymer and is immobile. The electrical charge of the ion active groups is balanced by oppositely charged ions which are mobile and can exchange with other ions of a similar charge. The chemical behavior of ion-exchange resins is divided into two major classes.

1. Cation resins, which exchange cations or positively charged ions.
2. Anion resins, which exchange anions or negatively charged ions.

Sulphonation of the copolymer with sulfuric acid yields a strong cation resin while amination yields anion resin.

Ion exchange resins are employed to promote reactions which can be catalyzed by conventional acids and bases. Some advantages of solid, substantially insoluble ion-exchange catalysts are; reduction of cost because the catalyst may be used repeatedly and usually without regeneration; increased product yield and efficiency; and elimination of corrosion problems.

Resin properties such as capacity, equivalency of exchange, selectivity, particle size, and crosslinkage effect the exchange kinetics. Other properties which have direct influence on exchange performance in water Purification are (PP&L literature)

1. Surface area per unit volume, which affects kinetics,
2. Terminal settling velocities, which affect the tendency of resins to separate,
3. Bed pressure drop, which affects pumping costs and the bed's capacity to filter insolubles,
4. Backwash/Bed expansion, which affects the ability to clean resins of insoluble materials,
5. Particle distribution, which affects all the above.

### Removal of Sulfate by Ion Exchange

Impurities such as chloride and particularly sulfate in the feed water of boiling water reactors (BWR's) represent the major corrodents in nuclear power plants. Predicting the sulfate levels in the effluent streams requires thorough understanding of the kinetics of divalent exchange. Sulfate occurs in BWR in two ways, as a contaminant in water to system and from materials used in the plant. A primary mechanism is by thermal degradation of cation exchange sites in the polished condensate (desulphonation). Some indications point to the release of organic sulphonates from the cation resin and

release of sulfur species from the vessel liner. While studies are made on the decomposition of cation resin (desulphonation) (PP&L literature) not much information is available on the other two sources of sulfate generation. Other possible sulfate sources are (PP&L literature)

1. Resin leakage from condensate polishers,
2. Condenser leakage with poor anion kinetics,
3. Sulfur containing organics that are not removed by the condensate demineralizers,
4. Resin leakage from reactor water clean up units (RWCU), and
5. Sulfate release from condensate polisher liner.

Sulfate exchange kinetics and equilibria in a ternary system has been studied by Smith and Woodburn (1977). Haas (1987) supplemented it with the concept of ternary interactions. However, little attention is paid to the development of a theoretically based multicomponent multivalent mixed bed ion exchange model that can handle a wide range of operating conditions.

### Objective

Impurities causing intergranular stress corrosion cracking in nuclear power plants can be minimized with the help of ion exchange. Multivalent ions such as sulfate are a common source for corrosion along the grain boundaries on the walls of the units. Other divalents, such as calcium, are likely to be present in condensate (particularly at fresh-water plants), and these can form insoluble deposits on nuclear fuel, resulting in local overheating and corrosion of the fuel cladding. The main objective of this thesis is to develop a theoretically based film diffusion controlled mixed bed ion exchange (MBIE) model which can handle divalent species in a ternary system.

The effect of such plant operating conditions on the overall ionic impurity levels expected, are discussed in the following chapters. Actual plant input is supplied by

Pennsylvania Power & Light. The results are analyzed and compared with plant experience.

## CHAPTER II

### LITERATURE REVIEW

An extensive literature review of ion exchange applied to ultrapure water processing has been carried out by Haub (1984), Yoon (1990), Zecchini (1990) and, more recently, by Lou (1993). This review concentrates on the objectives of this thesis.

#### Ion exchange capacity

Practically, ion exchange processes are considered as pseudo-chemical reactions which require the initial concentrations of exchanging species to be expressed in both phases. Data for the liquid phase are easily obtained, but the corresponding data for the resin phase requires a knowledge of the ion-exchange capacity, which is defined as the number of equivalents of exchangeable ions per unit weight or volume of the resin. The weight or volume of the resin refers to a particular ionic form and is usually the hydrogen form for a cation resin and chloride for an anion resin (Grimshaw and Harland, 1975). For the case of weak acid, weak base, and polyfunctional resins, the maximum degree of exchange depends upon the pH of the liquid phase.

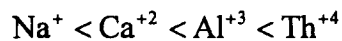
#### Equilibria and selectivity

One of the controlling factors governing the use of ion-exchange separations is the equilibrium distribution of ions between the resin and solution phases. When an ion exchanger or resin bead is placed in an electrolyte solution, equilibrium will be obtained

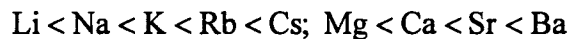
after a certain time. At this point, the ion exchanger and solution both contains the exchanging ions. However, the concentration ratio of the two ions will not be the same in both phases. The preference for one ion over another by the exchanger is known as selectivity. Selectivity depends on the nature of the counterions, the nature of the fixed charges in the matrix, the degree of ion exchanger saturation, the total solution concentration, and the external forces such as temperature and pressure. The ion exchanger prefers counterions that have the higher valence, smaller equivalent volume, greater polarity, and stronger association with fixed ionic groups in the matrix (Helfferich, 1962).

The following observations serve as a guide in predicting and planning ion-exchange systems (Kunin, 1960).

- 1) At low concentrations and ordinary temperatures, the selectivity increases with increasing valency of the exchanging species:

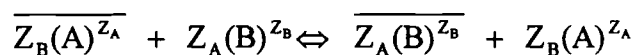


- 2) At low concentrations, ordinary temperatures, and constant valence, the selectivity increases with increasing atomic number of the exchanging species:



- 3) Organic ions of high molecular weight and complex metallic anionic complexes exhibit high exchange capacity.
- 4) Ions with higher activity coefficients have greater exchange capacities.

The stoichiometric exchange between the counterions A in the resin phase and B in the solution phase may be written as



where

$\overline{Z_B(A)^{Z_A}}, \overline{Z_A(B)^{Z_B}}$  = concentrations in resin phase

Z = valence



The selectivity is usually defined in terms of the selectivity coefficient ( $K_A^B$ ), which is the mass action relationship written for the reaction according to a particular choice of concentration units:

$$K_{C_A}^B = \frac{(\bar{C}_B)^{Z_A} (C_A)^{Z_B}}{(\bar{C}_A)^{Z_B} (C_B)^{Z_A}} ; \quad K_{m_A}^B = \frac{(\bar{m}_B)^{Z_A} (m_A)^{Z_B}}{(\bar{m}_A)^{Z_B} (m_B)^{Z_A}} ; \quad K_{X_A}^B = \frac{(\bar{X}_B)^{Z_A} (X_A)^{Z_B}}{(\bar{X}_A)^{Z_B} (X_B)^{Z_A}}$$

where

m = molal

C = molar

X = equivalent ionic fraction

When the exchanging species are all univalent, all three coefficients have the same numerical value i.e.

$$K_{m_A}^B = K_{C_A}^B = K_{X_A}^B$$

A more widely used coefficient in physical chemistry is the distribution coefficient. When any two solutes are contacted by mechanical shaking for several hours with an equal amount of resin and solution, then by comparing the concentration of solute left in the solution with the concentration before exchange, distribution coefficient may be calculated by

$$K_d = \frac{M_s}{M_L} \cdot (\text{volumes of solutions}) / (\text{mass of resins})$$

where

$M_s$  and  $M_L$  are the fraction of the cation M in the resin and liquid phase respectively and  $K_d$  is the distribution coefficient at equilibrium. The ratio of the distribution coefficient of solute A to that of B is defined as the separation factor.

In general, all practical and important ion-exchange processes deal with more than two exchangeable ions. However, most of our knowledge of the behavior of ion-exchange comes from the study of binary systems. Few systematic studies have been done on multicomponent ion exchange because of the complexity of both experimental and theoretical multi-ionic systems.

Prediction of multicomponent ion-exchange equilibrium is needed for the design of exchangers which operate over a wide range of conditions. A theoretical model which allows the equilibrium behavior of multicomponent systems to be predicted would, therefore, be extremely useful. However, little attention has been paid to the influence of resin composition on the affinity of ions in a multi-ionic resin.

de Lucas et al. (1992) studied the cation-exchange equilibria between Amberlite IR-120 resin and aqueous solution of calcium, magnesium, potassium, and sodium chlorides and hydrochloric acid. Experimental data for ion-exchange equilibria of the ternary and quaternary systems are reported in this study. They also developed a model which allows the prediction of multicomponent ion-exchange equilibria from binary data. They concluded that the predictions of ternary and quaternary systems based solely on the binary data are in good agreement with the experimental results. According to this study, methods for the prediction of multicomponent ion-exchange equilibria are classified into four main groups.

- Models assuming ideality of the exchange equilibria (i.e., ideal solutions with negligible effect due to resin swelling and hydration) with a constant separation factor and activity coefficients of all components in the solid phase equal to unity.
- Models assuming regular systems with a linear transformation between the separation factor and the composition in the solid phase.
- Treating ion exchange as a phase equilibrium using standard procedures developed for solution thermodynamics. Surface effects are taken into account

by introducing surface excess variables similar to those used to study adsorption from liquid mixtures on solids.

- Theoretical Models which consider non ideal or real systems, so they should be more accurate in predicting equilibrium behavior.

Among the different models, a model based on the mass action law is applied in this study.

Table II-1 shows the equilibrium-constants determined from experimental data.

Table II-2 shows the triangle rule for ternary system.

Table II-1

Equilibrium constants determined from binary experimental data (de Lucas et al., 1992).

A/B	$K_A^B$	T (K)	$\bar{\epsilon}$ (%)
H <sup>+</sup> /Na <sup>+</sup>	1.760	283	
	1.674	303	7.3
	1.510	323	
H <sup>+</sup> /Ca <sup>2+</sup>	25.70	283	
	29.04	303	6.2
	31.32	323	
Na <sup>+</sup> /Ca <sup>2+</sup>	9.121	283	
	10.86	303	2.6
	12.20	323	

Table II-2

Triangle rule for Equilibrium Constants (de Lucas et al., 1992).

System	283 K	303 K	323 K
$K_{Na}^{Ca} \cdot K_H^{Na^2} \cdot K_{Ca}^H = 1$	1.1	1.05	0.89

Triay and Rundberg (1987) considered the selectivity coefficient distributions by deconvolution of ion exchange isotherms. The ion exchange isotherm is the equilibrium solid-phase concentration of a given ion as a function of the aqueous-phase concentration when the temperature and ionic strength are held constant. The solid-phase concentration increases with aqueous-phase concentration until the exchangeable sites are saturated, provided the structure of the ion exchanger does not change as the adsorbed ions are replaced. The point of saturation (i.e., exhaustion of resin sites) is determined by the ion exchange capacity.

de Bokx et al. (1989) studied the ion-exchange equilibria of alkali-metal and alkaline-earth-metal ions by using surface-sulfonated polystyrene-divinylbenzene resins. This study employs a chromatographic method in which one of the exchanging ions is present in trace quantities only. It was found that the equilibrium coefficient is independent of the concentration of the liquid phase, and therefore specificity in ion exchange is due solely to interactions in the resin phase. The data could be interpreted by enthalpy-entropy compensation. Equations were derived that relate the equilibrium coefficient to a product of the difference between two interaction parameters and a factor that is constant within a class of ions. It was shown that selectivity is determined by the interaction between adsorbed ions and not by the interaction of separate adsorbed ions with the resin.

Horst et al. (1990) believe systems in which equilibria is based on separation factors or equilibrium constants have to be closer to ideal and the predictions aren't good otherwise. This led to study of ion exchange equilibria on weak acid resins by a theoretical approach in which fixed sites and counterions are assumed to form surface complexes. The electric charges of the fixed sites generate an electric field normal to the resin surface. Counterions are located in individual sorption layers which have a certain charge density. Due to the existence of one layer for each kind of counterions, the entire resin phase can be considered as a series of electric capacitors. For the exchange of protons with metal counterions, a set of two characteristic quantities are derived from experiments. By means of this set of quantities, the equilibrium is calculated for a broad range of initial conditions. They applied the relationships of a series of electric capacitors and predicted the multicomponent equilibria using the sets of binary exchange parameters. The assumption that all counterions are located in their characteristic layers led to a simplified mathematical method. This method provided an excellent agreement between experimental and predicted equilibria.

Smith and Woodburn (1978) developed a generalized model to predict multicomponent ion exchange equilibria from binary data. The binary systems used in their study are  $\text{SO}_4^{2-} - \text{Cl}^-$ ,  $\text{SO}_4^{2-} - \text{NO}_3^-$ , and  $\text{Cl}^- - \text{NO}_3^-$  on a strong base anion exchange resin. These systems exhibit non-ideal characteristics in both phases and the experimental characterization is based on the reaction equilibrium constants. Wilson's correlation's for the activity coefficients are used in the model. Table II-3 shows the values of equilibrium constants.

Table II-3

Estimates of equilibrium constants for binary systems at 298 °K (Smith et al., 1978).

Ion exchange reaction	Equilibrium Constant
$R_2SO_4 + 2NO_3 \Leftrightarrow 2RNO_3 + SO_4$	$K_{SO_4}^{NO_3} = 72.939$
$R_2SO_4 + 2Cl \Leftrightarrow 2RCl + SO_4$	$K_{SO_4}^{Cl} = 5.094$
$RCl + NO_3 \Leftrightarrow RNO_3 + Cl$	$K_{Cl}^{NO_3} = 3.780$

The three equilibrium constants are related as

$$K_{SO_4}^{Cl} = K_{SO_4}^{NO_3} / (K_{Cl}^{NO_3})^2$$

Helferich (1967) gave a general analytical solution for systems with an arbitrary number of exchanging species for conditions of local equilibrium, absent axial diffusion and dispersion, with constant separation factors, uniform presaturation, and constant feed. This solution is based on the coherence (stability) of chromatographic boundaries.

Tondeur and Klein (1967) presented a general analytical solution for the simultaneous material balance and constant-separation-factor equilibrium relations pertaining to zones of varying compositions in multicomponent, fixed-bed ion exchange columns. They also provided algebraic and numerical methods determining the constants occurring in the analytical solution, and obtaining the overall concentration profiles of three and four component systems.

Clifford (1982) used a similar approach and calculated the concentration profiles and column histories from a derived set of general rules and equations assuming constant separation factors. He predicted nitrate and sulfate effluent breakthrough curves from weak base anion beds with four-component feed ( $SO_4^{2-}$ ,  $NO_3^-$ ,  $Cl^-$ ,  $HCO_3^-$ ) solutions using multicomponent equilibrium theory. The theory also predicted the length of a run and the final composition of the exhausted bed when treating nitrate-contaminated water.

## Kinetics and Mechanism of Ion Exchange

The rate at which ion-exchange proceeds is a complex function of physico-chemical mechanisms. A high rate of exchange is generally favored by the following conditions:

- 1) small particle size resin,
- 2) efficient resin-solution mixing,
- 3) high solution concentration ,
- 4) high temperature,
- 6) low cross linked resin.

Kitchener (1954) evaluated ion exchange kinetics in detail. The factors mentioned above were considered. A more simplified treatment is to adopt the Nernst film diffusion theory. The solution is considered perfectly mixed. Transport through the Nernst film is treated by Fick's law with a certain equivalent thickness,  $\delta$  (fixed by hydrodynamic factors), for the hypothetical unstirred film. Diffusion inside the resin is the last step.

Overall exchange kinetics is too complicated to analyze mathematically; but a satisfactory method is provided by Boyd, Adamson and Myers (1947), who made use of Nernst (1904) film theory. In film theory, the ion exchange reaction is controlled by two simultaneous diffusion steps - diffusion through the Nernst film, and diffusion through the resin particle. However, many applications use single diffusion processes because either diffusion in the boundary film becomes rate-determining or diffusion through the boundary film is so rapid that the slow step is almost entirely confined to diffusion inside the resin bead.

Results of kinetic studies lead to values for the exchange-diffusion coefficients of a pair of ions in either the resin phase or aqueous phase. However, independent determinations of diffusion coefficients inside resins is possible with the help of radio active tracers (Saldano et al., 1953).

## CHAPTER III

# MIXED BED ION EXCHANGE MODELING FOR DIVALENT SPECIES- EFFECT OF SYSTEM PARAMETERS

### Abstract

A model for ternary mixed bed ion exchange (i.e. six component exchange - three cations and three anions) including divalent species is developed and tested for various system parameters. This model is capable of handling variations in cation-to-anion resin ratio, mass transfer coefficient, particle size, flow rate, and bed composition. The model is extended to address bed cleaning every three weeks whereby average particle loading after cleaning is used as the initial loading for the next three weeks.

### Introduction

The feed water of a boiling water reactor can contain suspended and soluble impurities. The suspended impurities are primarily metal oxides from corrosion, erosion and wear of system materials. They are of concern because they will tend to foul the nuclear fuel. The soluble impurities come from the ingress of cooling water during condenser leaks and from residual regenerants from demineralized water production. Certain of the soluble impurities, particularly chloride and sulfate, will cause or accelerate intergranular stress corrosion cracking (IGSCC) of reactor system materials present at high enough concentration in reactor water. Industry guidelines suggest that chloride and sulfate be maintained well below 5 ppb in reactor water. For a plant with 1% reactor



water cleanup system, this means that the feedwater must contain less than 50 ppt chloride and sulfate. Ion exchange in the condensate polisher must be capable of removing impurities from condensate down to these levels. Minimizing these impurities will reduce the growth rate of the cracks once they are formed. The principle sources of corrosion products in the feed water of BWR's results from condenser leakage and resin leachability (source of sulfate release). The condensate/feed water impurities must be kept low to maintain reactor water purity. Nuclear power plants often experience difficulty in meeting low impurity levels (usually 5 ppb for corrosion products). Ion exchange is the most suitable unit operation for this purpose.

Many attempts have been made to develop general, multicomponent, ion exchange models for non ideal behavior. Klien et al. (1987) considered only ideal components of a ternary system. Soldatov and Bychkova (1970) described the ternary system  $K^+ - NH_4 - H^+$  based on activity coefficients in the binary mixture calculated from experimental data and applied to the ternary mixture. For accurate results, the treatment requires that the main binary system be close to ideal.

Danes and Danes (1972) proposed a method for calculating ion exchange equilibria of polyionic systems where the molar excess free mixing enthalpy of the resins is expressed as a polynomial. The predictive power of the method is limited to systems which obey ideal or regular solution rules.

Basic principles of ion exchange coupled with kinetics of individual species are applied in developing the current model. Because of the presence of divalent species, however, some complications arise in the mathematical modeling. Assumptions and conditions are applied at appropriate junctures where necessary.

The objective of this work is to develop a film controlled neutralization model for MBIE that includes divalent species in a ternary system. The diffusion coefficients (given in Table III-1) for the ionic species use the limiting mobilities given by Robinson

and Stokes (1959). Non-ionic mass transfer coefficient correlation's are applied in this work to account for the effect of differing mobilities of the ions on the overall exchange process. Data from Pennsylvania Power & Light (PPL) is used in the model and computer predictions are analyzed.

### Diffusion Coefficients:

In an electrolyte solution the solute is in the form of ions, either cations or anions. The relative mobility of all ions depends on their size. However, all the ions present must also satisfy the overall charge balance. The Nernst (1888) equation provides a simple and accurate method for predicting diffusion coefficients in electrolyte solutions by relating the diffusion coefficients to electrical conductivities:

$$D_{AB}^{\circ} = \left( \frac{RT}{F^2} \right) \left( \frac{\lambda_{+}^{\circ} \lambda_{-}^{\circ}}{\lambda_{+}^{\circ} + \lambda_{-}^{\circ}} \right) \left( \frac{Z_{-} + Z_{+}}{Z_{-} Z_{+}} \right) \quad 3-1$$

$$D_i^{\circ} = (RT / F^2) \lambda_i^{\circ} \quad 3-2$$

where

$\lambda_i^{\circ}$  = electrolyte conductance at infinite dilution, (A / cm<sup>2</sup>)(cm / V)(cm<sup>3</sup> / g – equiv.)

T = absolute temperature, °K

Equation 3-1 is used to relate temperature to the ionic diffusion coefficients. The Nernst equation has been verified experimentally for dilute solutions (Divekar et al., 1987). Temperature and equivalent conductance are correlated by least squares at infinite dilution (given in Table III-1).

Table III-1

Conductance as a Function of Temperature (Divekar et al., 1987).

---

$\lambda_{\text{H}}^{\circ} = 221.7134 + 5.52964 T - 0.014445 T^2$	3-3
$\lambda_{\text{OH}}^{\circ} = 104.74113 + 3.807544 T^2$	3-4
$\lambda_{\text{Na}}^{\circ} = 23.00498 + 1.06416 T + 0.0033196 T^2$	3-5
$\lambda_{\text{Cl}}^{\circ} = 39.6493 + 1.39176 T + 0.0033196 T^2$	3-6
$\lambda_{\text{S}}^{\circ} = (35.76 + 2.079 T)/2$	3-7
$\lambda_{\text{Ca}}^{\circ} = (23.27 + 1.575 T)/2$	3-8

---

Combining eq 3-1 and 3-2 - 3-7 provides expressions to relate the effect of temperature on the diffusion coefficients of ions of the form

$$D_i = (RT / F^2) (A_i + B_i T + C_i T^2) \quad 3-9$$

### Model Development

The exchange of divalent species in a film controlled homogeneous MBIE is addressed in this model. The film diffusion fluxes are described using the Nernst-Planck equation combined with the continuity equation for the film. Basic assumptions relevant to the model are used in developing the interfacial concentrations. Final effluent concentrations are determined by using the column material balance combined with the rate expressions which are solved numerically. Numerical methods were based primarily on stability rather than computationally faster methods. These are discussed in detail in APPENDIX D.

## Flux Expression

Zecchini et al. (1990) discussed the ternary interactions in univalent ions. Divalent ions affect the electroneutrality and no net current flow expressions in the model development. The electric field produced as a result of difference in ionic mobilities, changes significantly in the presence of divalent ions. This has a direct influence on the flux expression which is needed to determine particle rates. Electroneutrality and no net current flow criteria are used in simplifying the continuity equation for a liquid film controlled process.

$$C_n + C_h + 2C_b = C_c + C_o + 2C_s \quad (\text{electroneutrality}),$$

$$J_n + J_h + 2J_b = J_c + J_o + 2J_s \quad (\text{no net current flow}),$$

$$J_n = J_h = J_b = 0 \quad (\text{anion exchange; no coion flux}),$$

$$J_c = J_o = J_s = 0 \quad (\text{cation exchange; no coion flux})$$

Combining the above four relations and eliminating the electric potential,  $\phi$ , in the Nernst-Planck equation for each of the ions and considering that reactions are restricted to bulk phase neutralization (i.e., changes in flux w.r.t. radial position is negligible):

$\frac{dJ_i}{dr} = 0$  yields a linear profile for coion concentration within the film of the form

$$C_p = \frac{C_p^o - C_p^*}{\delta} r + C_p^*$$

where

$$C_p = C_h + C_n + C_b$$

Combining this expression with Nernst-Planck equation and integrating from the bulk phase to the film yields a final flux expression of the form

$$-J_i \delta = (1 - Z_i) D_i \left( \frac{1 - \left(\frac{C_p^*}{C_p^o}\right) \left(\frac{C_i^*}{C_i^o}\right)}{1 + \left(\frac{C_p^*}{C_p^o}\right) \left(\frac{1}{C_i^o}\right)} \right)$$

This expression is used for all the individual ions to determine the effective diffusivity.

The static film model combined with the flux of the species results in

$$\frac{d \langle C_i \rangle}{dt} = K_i' a_s (C_i^o - C_i^*) = -J_i a_s$$

resin phase fractional concentration can be written as

$$y_i = \langle C_i \rangle / Q,$$

and the liquid phase as

$$x_i = C_i / C_T$$

Particle rates are developed by combining the flux expression and static film model.

Final particle rate for divalent ion results as

$$\frac{\partial y_i}{\partial \tau} = 9R_s \frac{K_s}{K_c} (x_s^o - x_s^*)$$

### Interfacial Concentrations

Interfacial concentrations for the ions are developed using the basic principles of ion exchange using the Nernst-Planck equation. A simultaneous solution of electroneutrality, no net current flow, no coion flux, and Nernst-Planck equations using the principles of film diffusion controlled process, leads to an expression for interfacial concentration in terms of the known parameters.

A final expression eliminating the flux terms is of the form

$$\begin{aligned} \frac{d}{dr} (D_c C_c^2 + (2D_c + 2D_o) C_o C_c + (4D_c + 6D_s) C_s C_c + D_o C_o^2 \\ + (4D_o + 6D_s) C_o C_s + 6D_s C_s^2) = 0 \end{aligned}$$

This is an expression which relates the concentrations in bulk phase to the concentrations at interface at any given time. This transforms the above expression from bulk phase concentrations to interfacial concentrations. Selectivity coefficients for each of the species can be written as:

$$K_o^c = \frac{y_c C_o^*}{y_o C_c^*} \quad K_o^s = \frac{y_s C_o^{*2}}{y_o^2 C_s^*} Q \quad K_c^s = \frac{y_s C_c^{*2}}{y_c^2 C_s^*} Q$$

These expressions are used to eliminate the chloride and hydroxide interfacial concentrations in favor of sulfate. The final equation for sulfate interfacial concentration is of the form

$$A C_s^{*2} + B C_s^{*3/2} + E C_s^* - \text{RHS} = 0$$

where

$$A = 6D_s$$

$$B = \frac{((4D_c + 6D_s)K_c^{s/2} y_c + (4D_o + 6D_s)K_o^{s/2} y_o)}{y_s^{1/2} Q^{1/2}}$$

$$E = \frac{(D_c K_c^s y_c^2 + (2D_c + 2D_o)K_o^{s/2} K_c^{s/2} y_o y_c + D_o y_o^2 K_o^s)}{y_s Q}$$

$$\begin{aligned} \text{RHS} = & (D_c C_c^{o2} + (2D_c + 2D_o)C_o^o C_c^o + (4D_c + 6D_s)C_s^o C_c^o + D_o C_o^{o2} \\ & + (4D_o + 6D_s)C_o^o C_s^o + 6D_s C_s^{o2}) \end{aligned}$$

Chloride and hydroxide interfacial concentrations are obtained using selectivity coefficients.

**Assumptions:**

The presence of divalent species led to complex mathematical modeling. Assumptions have been minimized to develop a generalized theoretically based divalent model. Table III-2 lists the assumptions that have been applied.

Table III-2  
MODEL ASSUMPTIONS

- 
1. Film diffusion control
  2. The Nernst-Planck equation incorporates all interactions among diffusing ionic species.
  3. Pseudo steady state exchange (Variations of concentration with space are much more important than with time)
  4. Local equilibrium at solid-film interface
  5. No coion flux across the particle surface
  6. No net coion flux within the film
  7. No net current flow
  8. Reactions are instantaneous when compared with the rate of exchange
  9. Ternary system with divalent species exchange
  10. Curvature of the film is negligible
  11. Uniform bulk and surface compositions
  12. Activity coefficients are constant and unity
  13. Negligible axial dispersion
  14. Isothermal, isobaric operation
  15. Negligible particle diffusion resistance
  16. Selectivity Coefficients are constant and temperature independent
-

The major assumption underlying this model is the film diffusion controlled process which is most accurate for dilute solutions (<5 ppb). Selectivity coefficients are assumed constant and independent temperature. Electroneutrality criteria for the inlet concentrations is fixed by adjusting the pH.

### **Temperature Effects**

An MBIE model for divalent species has been developed and tested for temperature effects on equilibria and kinetics of ion exchange. Divekar et al. (1987) modified the model developed by Haub and Foutch (1986) to account for temperature effects for univalent species. The current model for divalent exchange was tested for temperatures ranging from 32.2 to 60° C.

Expressions for the temperature dependent terms (ionic diffusion coefficients, ionization constant for water, bulk solution viscosity) were obtained from the literature. Variations in temperature affects many system parameters like solution viscosity, ionic diffusion coefficients, selectivity coefficients, and ionization constant of water. This model calculates all of these temperature dependent parameters except selectivity coefficients which were not available in the literature for the desired species.

### **Results and Discussion**

The effect of temperature on concentration profiles were tested at 32.2, 48.9, and 60° C. This was done for a cation to anion ratio of 1:1 by volume, and a flow rate of 42.7 gpm/ft<sup>2</sup>. All other conditions were at the base case (Appendix E). Diffusion coefficient, mass transfer coefficient, and solution viscosity were calculated as a function of temperature. The effect of increase in temperature from 32.2° C to 60° C increases the ionization constant of water from 1.8E-14 to 10E-14 (i.e., both hydrogen and hydroxyl



ion concentrations increase in the bulk phase. Divekar et al, 1986). This results in a reduced concentration gradient for the mass transfer of the hydrogen and hydroxyl ions and consequently poor overall rate exchange is observed at higher temperatures.

**Sodium:** Table III-3 shows the calculated values for sodium, at the different temperatures considered. A decrease in temperature from the base case (at 60° C) to 32.2° C, causes the effluent equilibrium leakage of sodium concentration to decrease by 45.8%. As shown in Figure 1, the breakthrough curves are steeper at higher temperatures. Breakthrough occurs 200 days earlier for sodium when the process is operated at 60° C compared to 32.2° C.

Table III-3  
Temperature Effects on Sodium Exchange parameters Using  
MBIE Divalent Model.

Temperature ° C	Diffusion Coefficient (cm <sup>2</sup> /s)	Mass Transfer Coefficient (cm/s)	Effluent Leakage Values (ppb)	% Change of Effluent Leakage from value at 60° C
32.2	0.165E-4	0.023	0.026	-45.8
48.9	0.238E-4	0.031	0.035	-27.1
60.0	0.294E-4	0.037	0.048	

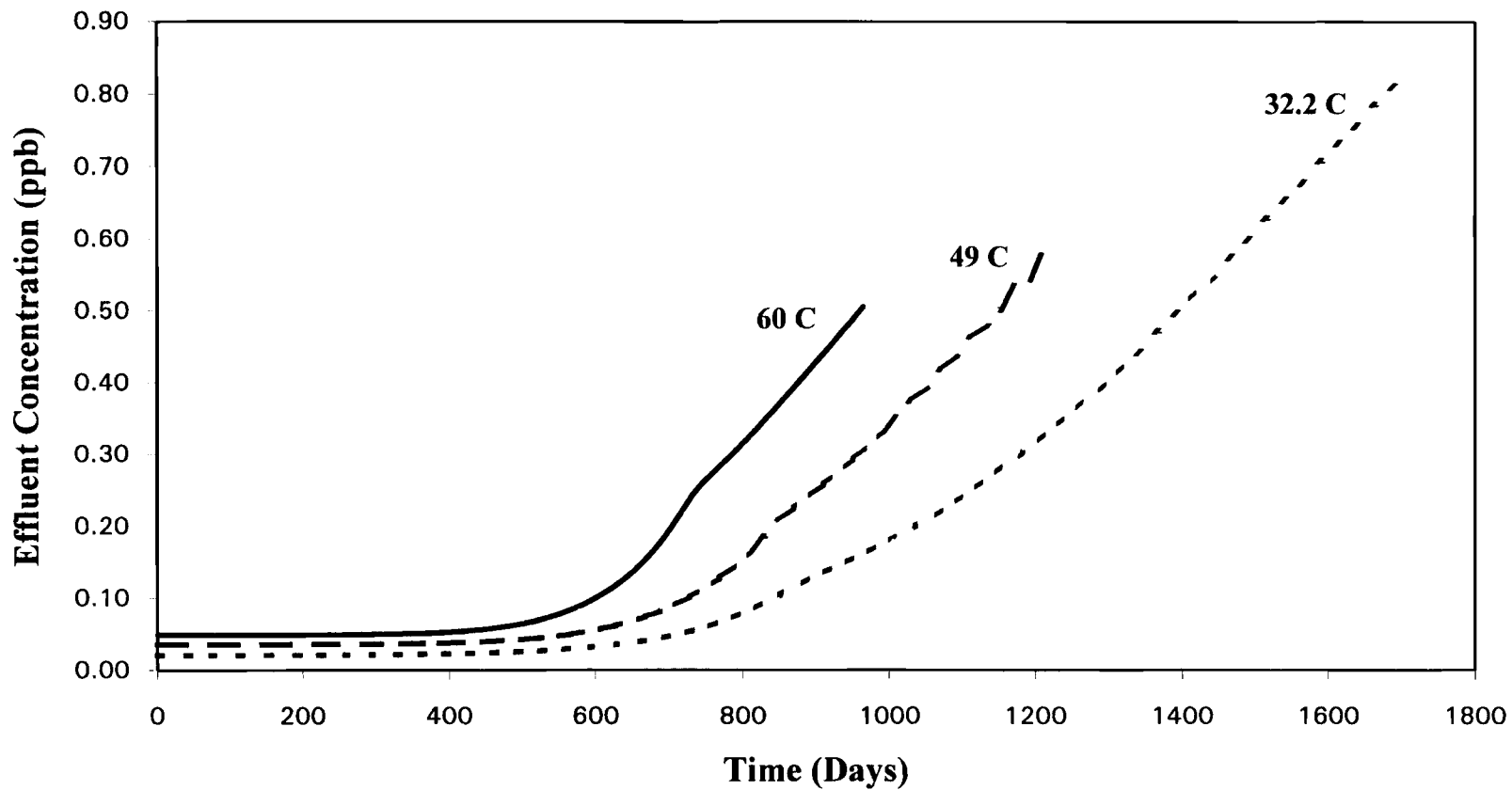


Figure 1. Effect of Temperature on Sodium Concentration Profile for a Mixed-Bed (Cation/Anion Ratio of 1.0) Simulation

**Calcium:** Table III-4 shows the calculated values for calcium, at the three temperatures considered. A decrease in temperature from base case (at 60° C) to 32.2° C, causes the effluent equilibrium leakage of calcium to decrease by 76%. As shown in Figure 2, the breakthrough curve is steeper when the process is run at 32.2° C.

Table III-4  
Temperature Effects on Calcium Exchange Parameters using  
MBIE Divalent model.

Temperature ° C	Diffusion Coefficients (cm <sup>2</sup> /s)	Mass transfer Coefficient (cm/s)	Effluent Leakage Values (ppb)	% Change of Effluent Leakage from value at 60° C
32.2	0.100E-4	0.1671E-1	0.841E-8	-76.0
48.9	0.144E-4	0.2247E-1	0.186E-7	-46.7
60.0	0.175E-4	0.2660E-1	0.349E-7	

**Chloride:** Table III-5 shows the calculated values for chloride, at the three temperatures considered above. A decrease in temperature from base case (at 60° C) to 32.2° C, causes the effluent equilibrium leakage of chloride to decrease by 57.7%. As shown in Figure 3, the breakthrough curves of chloride are more steeper compared to sodium. Breakthrough occurs 100 days earlier when the system is run at 60° C compared to 32.2° C.

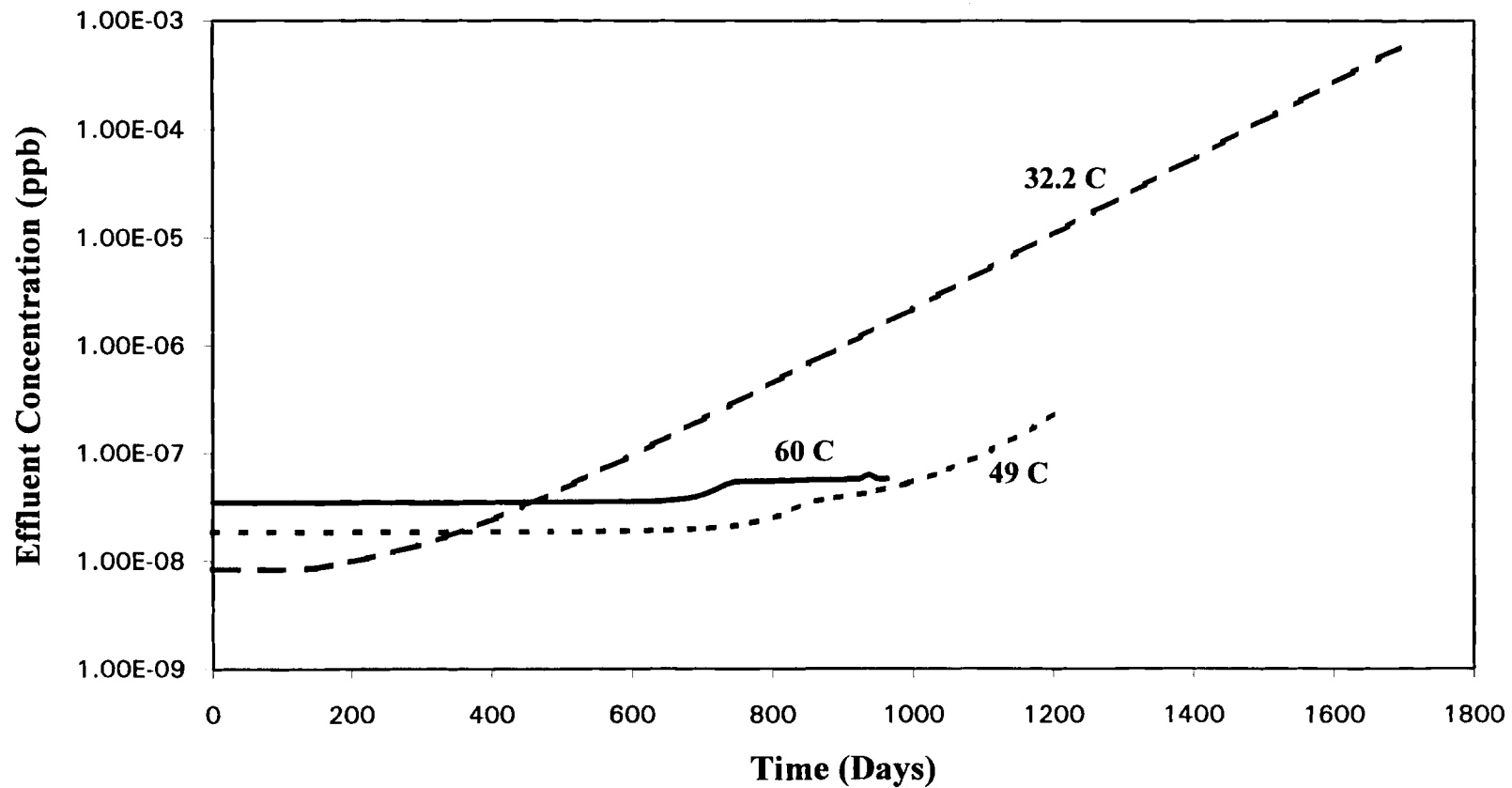


Figure 2. Effect of Temperature on Calcium Concentration profile for a Mixed-Bed (Cation/Anion Ratio of 1.0) Simulation

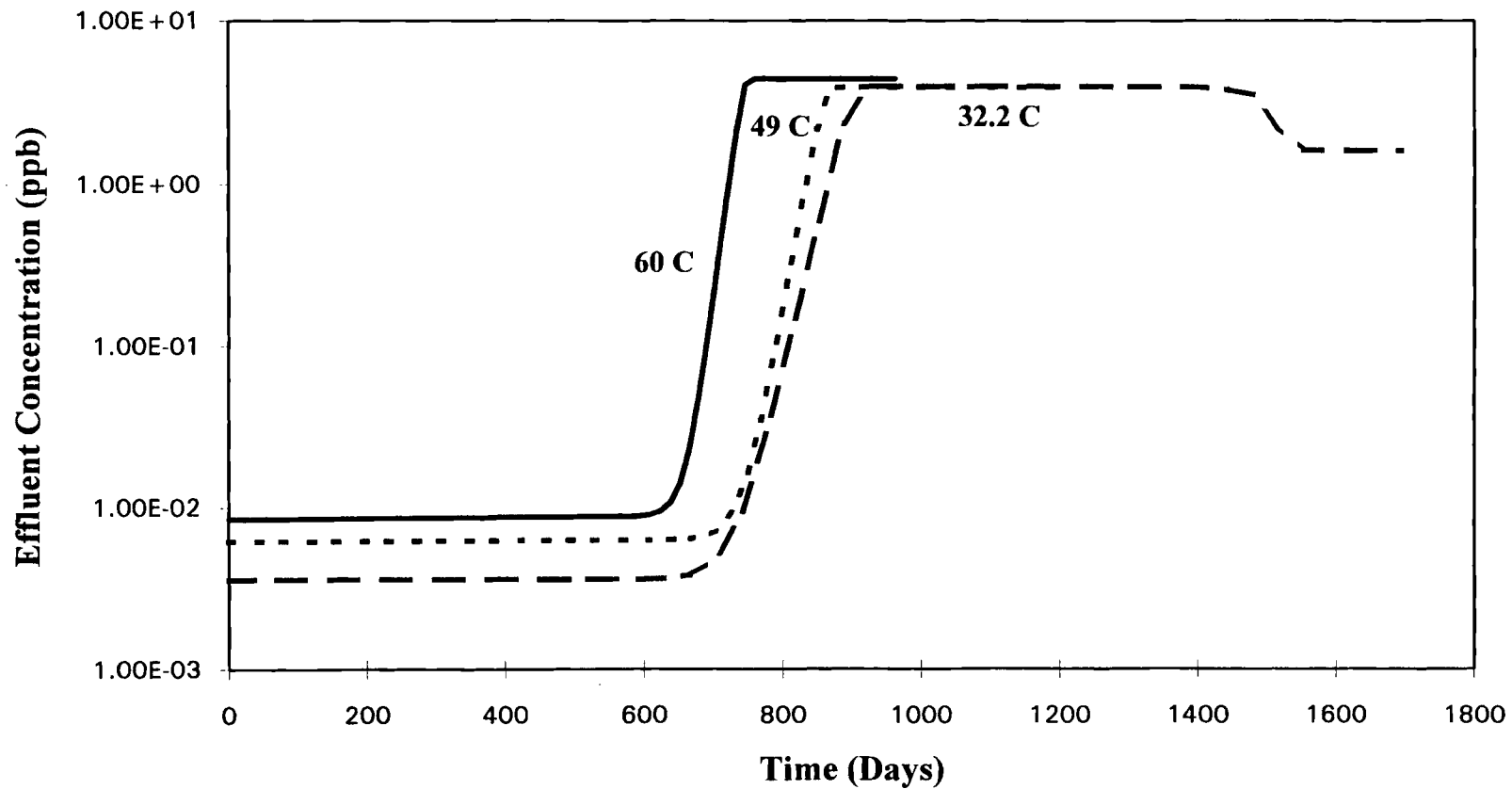


Figure 3. Effect of Temperature on Chloride Concentration profile for a Mixed-Bed (Cation/Anion Ratio of 1.0) Simulation

Table III-5  
Temperature Effects on Chloride Exchange Using  
MBIE Divalent Model.

Temperature ° C	Diffusion Coefficients cm <sup>2</sup> /s	Mass Transfer Coefficient (cm/s)	Effluent Leakage Values (ppb)	% Change of Effluent Leakage from value at Base Case (60° C)
32.2	0.239E-4	0.343E-1	0.358E-2	-57.7
48.9	0.332E-4	0.453E-1	0.619E-2	-27.0
60.0	0.402E-4	0.534E-1	0.848E-2	-

**Sulfate:** The main sources of sulfate in the reactor units of industries are due to

- a) Desulphonation of the cation resin (release of sulfate),
- b) Release of organic sulfonates from the cation resin, and
- c) Release of sulfur species from the vessel liner.

The model addresses the desulphonation effect.

**Desulphonation of strongly acidic cation ion exchange resin (release of sulfate):**

The decomposition of cation resin has been studied by several investigators (Fisher 1993, Fejes 1969, Marinsky and Potter 1953). Most of the data available has been developed at temperatures much higher than that employed in power plant condensate polishing. The rate constant for desulphonation versus 1/T for several of these studies is available in the literature (Fisher 1993). A least squares method is employed to obtain the rate constant as a function of temperature.

$$K = 7.5e + 6 \text{EXP}(-10278.6 / (T + 273.16)) \quad (3-10)$$

where

K is a first order rate constant in  $\text{hr}^{-1}$

T is in  $^{\circ}\text{C}$ .

Sulfate throw is assumed constant from each slice. The whole bed is considered as a finite set of slices. For the base case at  $60^{\circ}\text{C}$ , desulphonation increases the effluent sulfate concentration by five orders of magnitude ( $10^{-7}$  ppb to  $10^{-2}$  ppb). As shown in Figure 4, the effect of temperature has the greatest effect on sulfate. A decrease of temperature from base case (at  $60^{\circ}\text{C}$ ) to  $32.2^{\circ}\text{C}$ , causes effluent equilibrium leakage sulfate concentration to decrease by 90.5%. Breakthrough for sulfate did not occur for both the higher temperatures for the current column conditions. At a temperature of  $32.2^{\circ}\text{C}$ , a steep increase in the curve is observed after twelve hundred days. Table III-6 shows calculated values in sulfate for the three temperatures considered above. Figure 5 shows the plot of rate constant for desulphonation versus  $1/T$ .

Table III-6  
Temperature Effects on Sulfate Exchange Parameters Using  
MBIE Divalent Model.

Temperature $^{\circ}\text{C}$	Diffusion Coefficients ( $\text{cm}^2 / \text{s}$ )	Mass Transfer Coefficient ( $\text{cm/s}$ )	Effluent Leakage Values (ppb)	% Change of Effluent Leakage from $60^{\circ}\text{C}$
32.2	0.140E-4	0.240E-1	0.343E-3	-90.5
48.9	0.197E-4	0.320E-1	0.147E-2	-59.4
60.0	0.238E-4	0.377E-1	0.362E-2	-

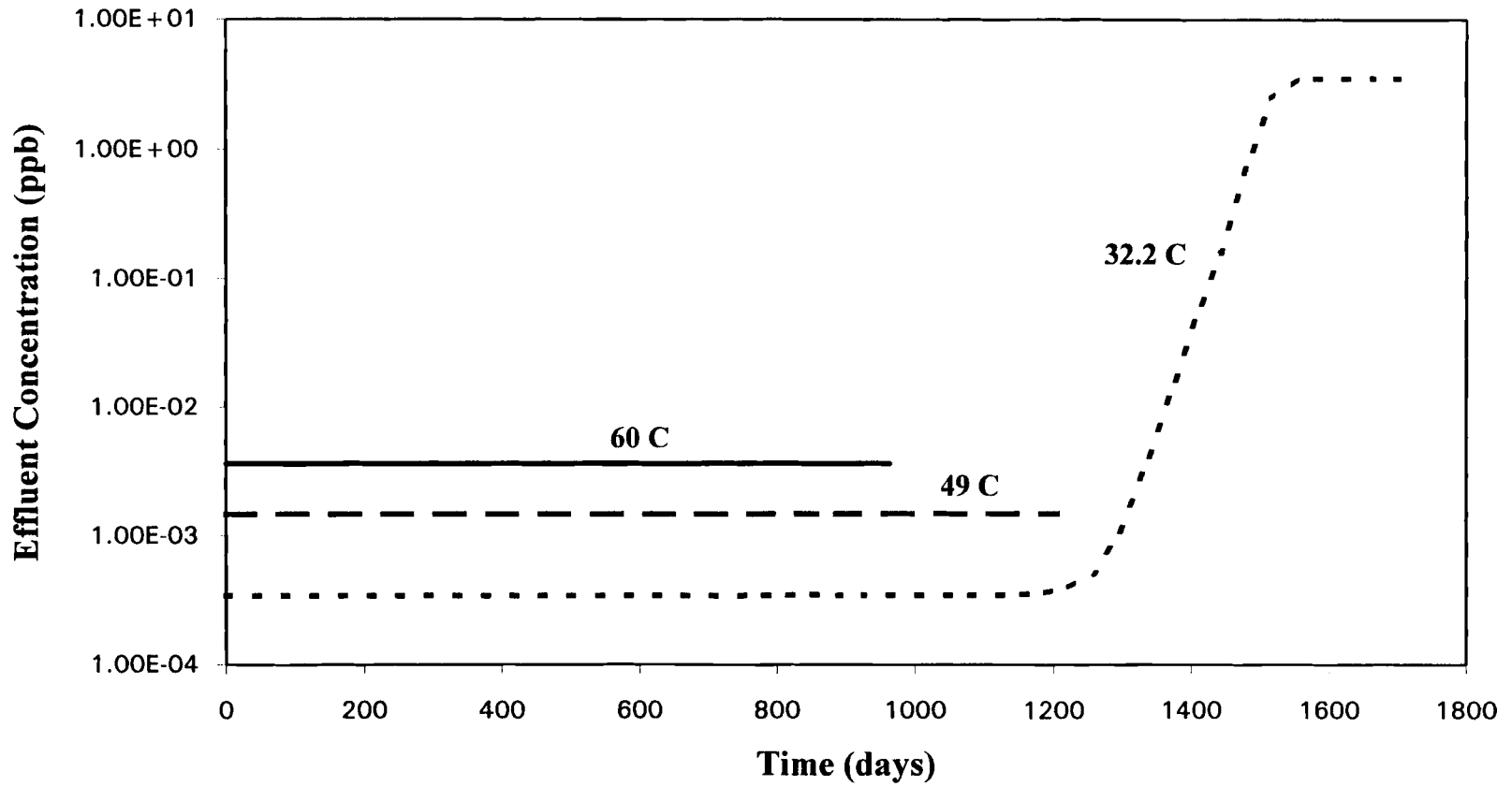


Figure 4. Effect of Temperature on Sulfate Concentration profile for a Mixed-Bed (Cation/Anion Ratio of 1.0) Simulation



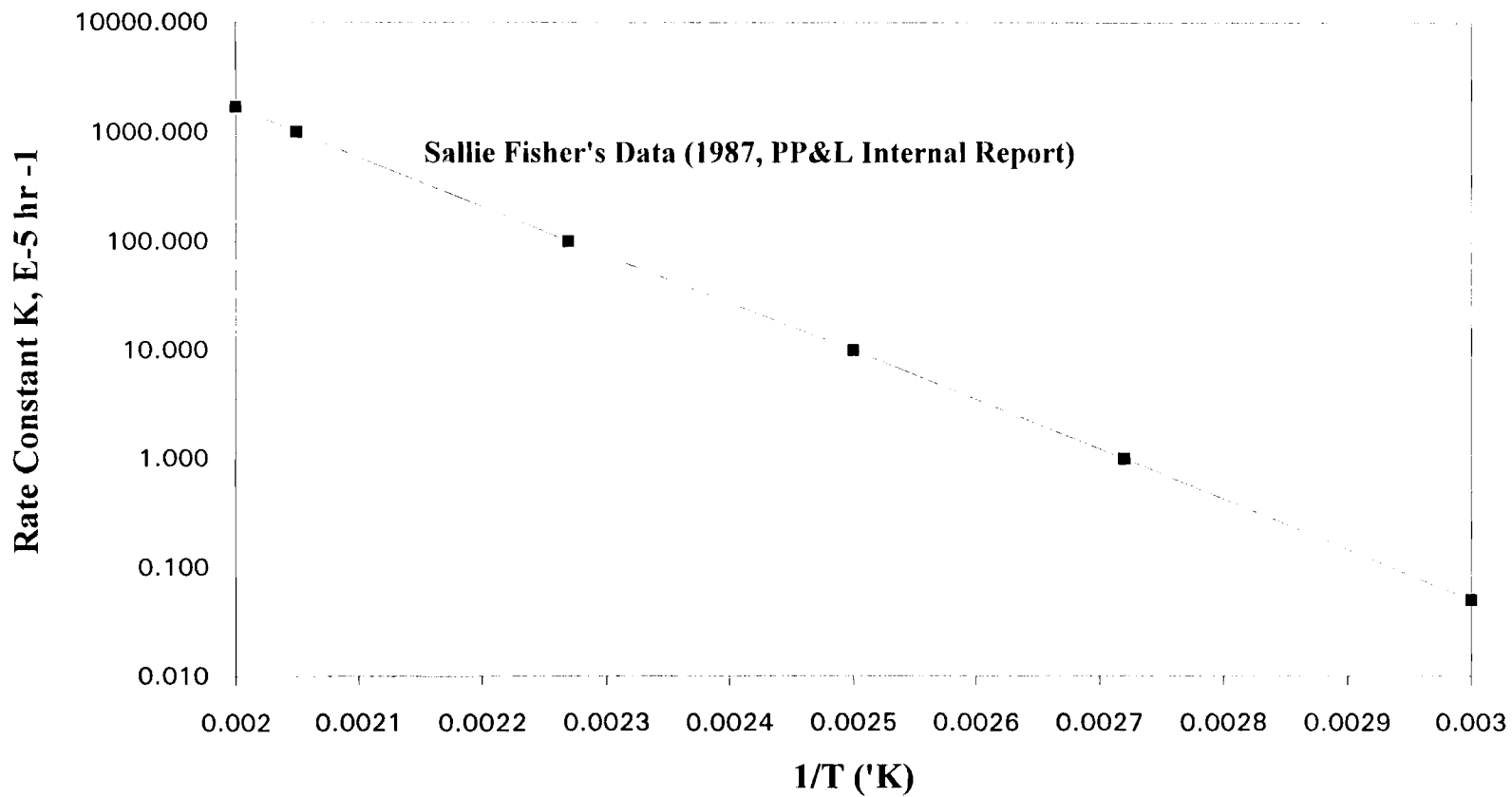


Figure 5. Reaction Kinetic Constant for Desulphonation of strongly Acidic Cation Ion Exchange Resin.

### Flow Rate Effects

Figures 6 through 9, show the effect of change in flow rate on predicted effluent profiles. The flow rates used were 42, 50 and 57 gpm/ft<sup>2</sup>. All simulations were conducted at 60°C (base case).

**Sodium:** Figure 6 shows that effluent equilibrium leakage values are not affected by varying the flow rate. Sharp curves and early breakthrough occurs for higher flow rates. By increasing the flow rate from 42 gpm/ft<sup>2</sup> (base case) to 57 gpm/ft<sup>2</sup>, breakthrough occurs earlier by 200 days. By operating with a higher flow rate of 57 gpm/ft<sup>2</sup>, the bed is saturated approximately 200 days earlier than that observed for base case.

**Calcium:** Calcium exhibits a trend similar to sodium but the effluent concentrations are much less. Figure 7 shows equilibrium leakage values do not get affected by variation in flow rates. By increasing the flow rate from 42 gpm/ft<sup>2</sup> (base case) to 57 gpm/ft<sup>2</sup>, breakthrough occurs earlier by 180 days. The curves get steeper at higher flow rates.

**Chloride:** Figure 8 shows the predicted effluent equilibrium leakage of chloride. A trend similar to sodium curve is seen in the case of chloride. Equilibrium leakage values for all three cases are the same. Breakthrough is characterized by steep curves in all three cases. For a flow rate of 57 gpm/ft<sup>2</sup>, breakthrough is approximately 180 days earlier compared to the base condition at 42 gpm/ft<sup>2</sup>.

**Sulfate:** Unlike sodium, calcium and chloride, sulfate effluent leakage values shows a strong function of the flow rate. Higher flow rates decrease the effluent leakage values. A 13.4% decrease in effluent leakage value is observed when the flow rate is increased from 42 gpm/ft<sup>2</sup> (base case) to 57 gpm/ft<sup>2</sup>. The Primary reason for this behavior is seen

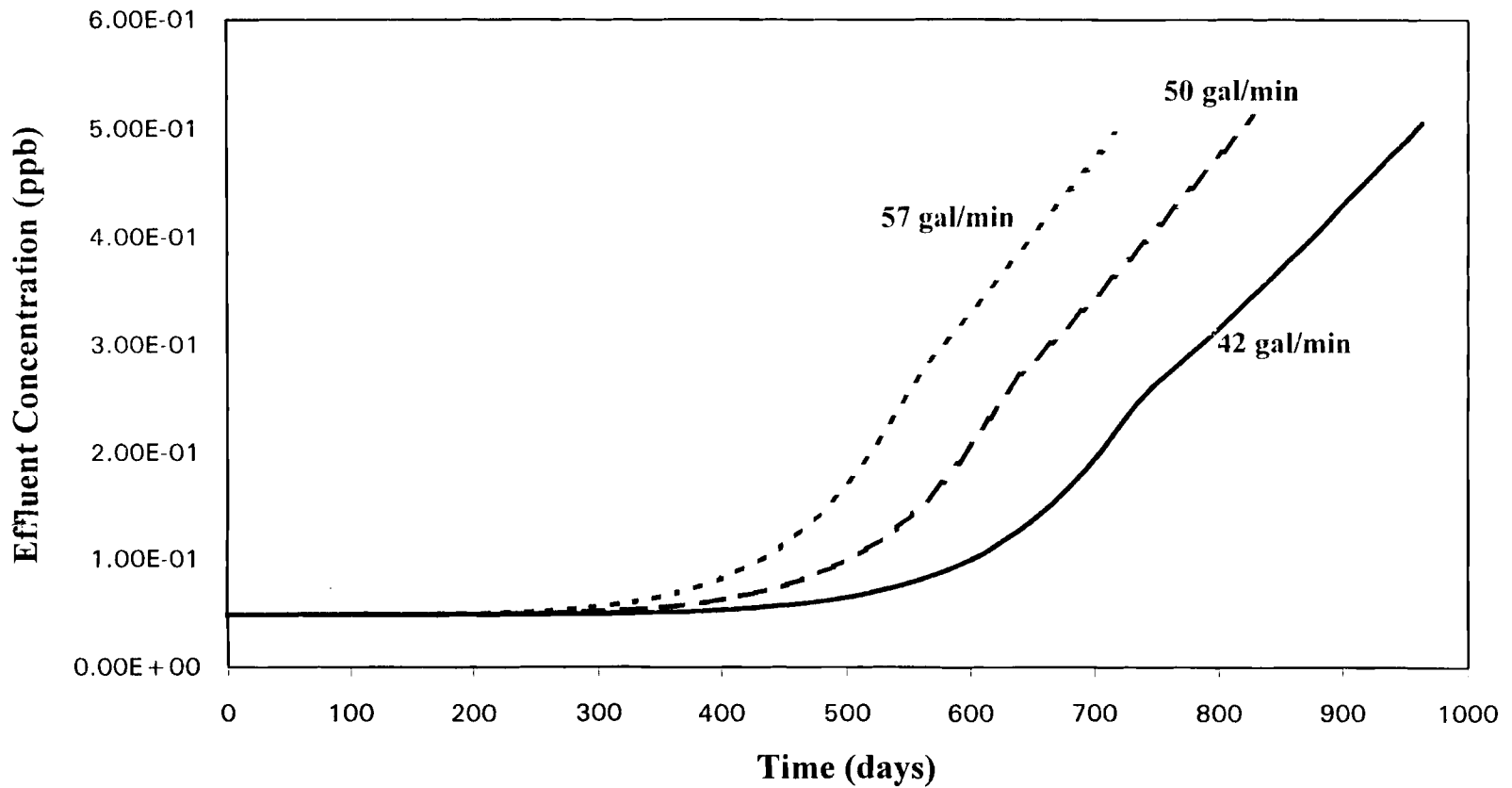


Figure 6. Effect of Flow rate on Sodium Concentration profile for a Mixed-Bed (Cation/Anion Ratio of 1.0) Simulation

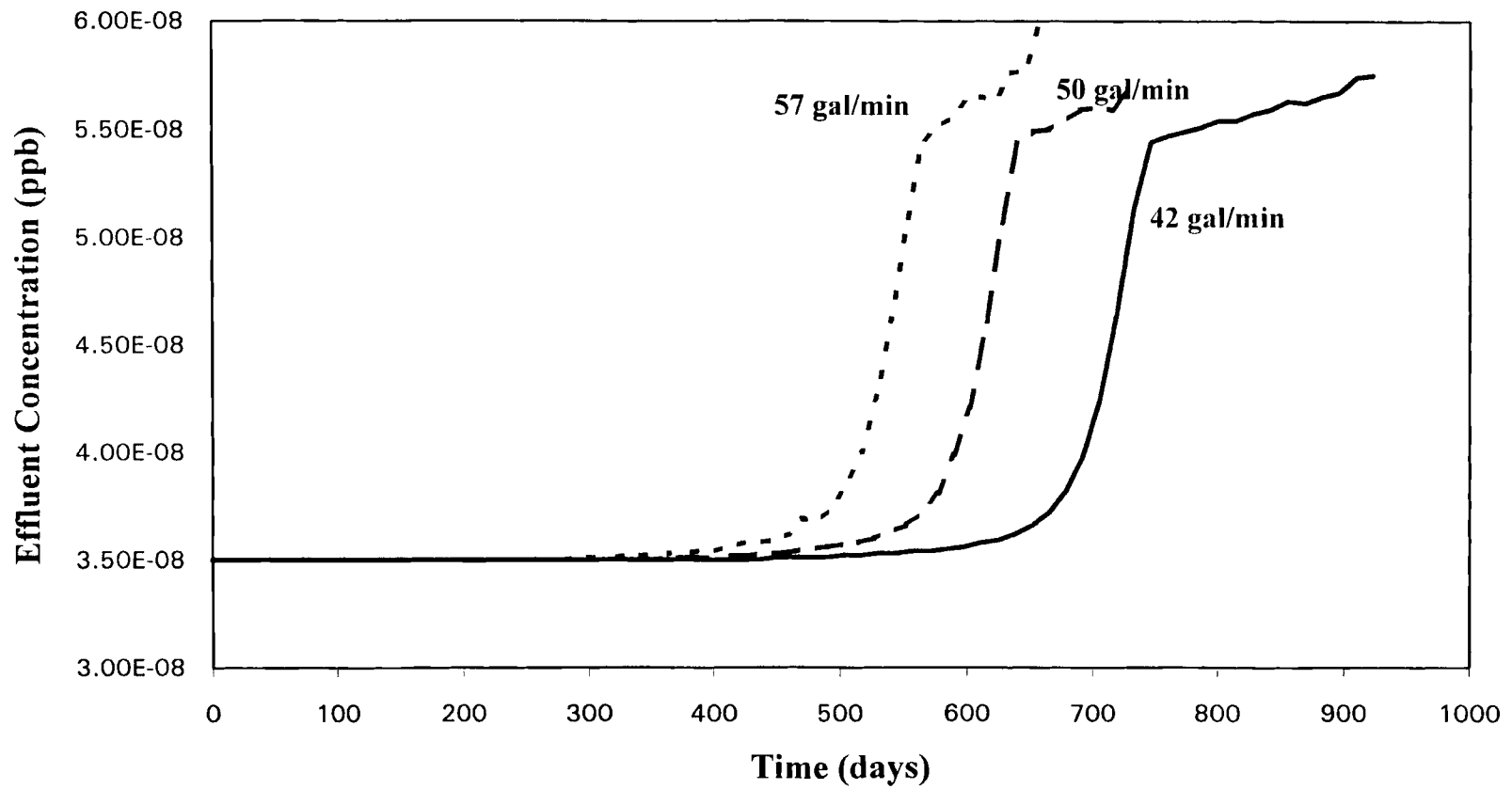


Figure 7. Effect of Flow rate on Calcium Concentration profile for a Mixed-Bed (Cation/Anion Ratio of 1.0) Simulation

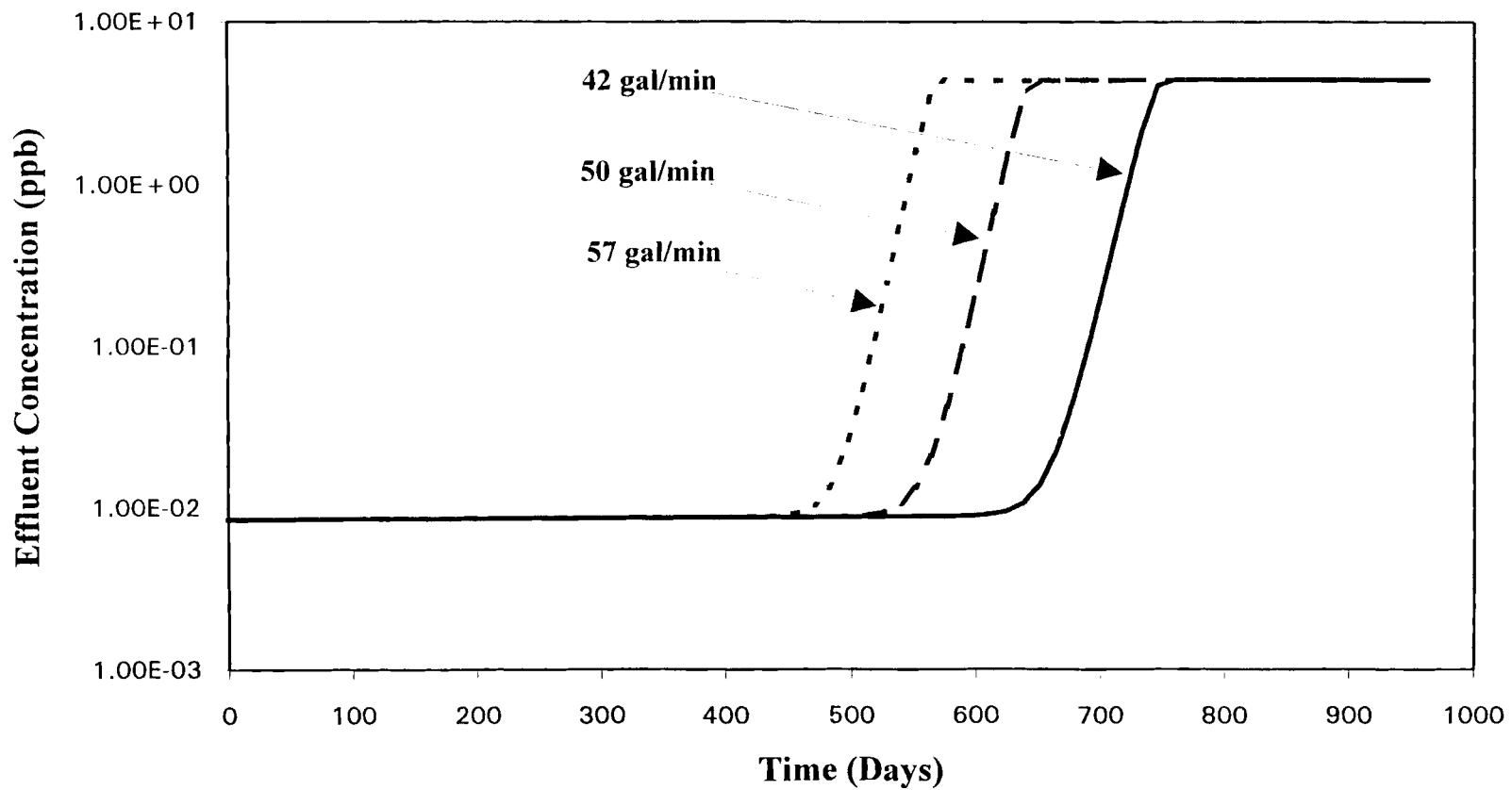


Figure 8. Effect of Flow rate on Chloride concentration profile for a Mixed-Bed (Cation/Anion Ratio of 1.0) Simulation

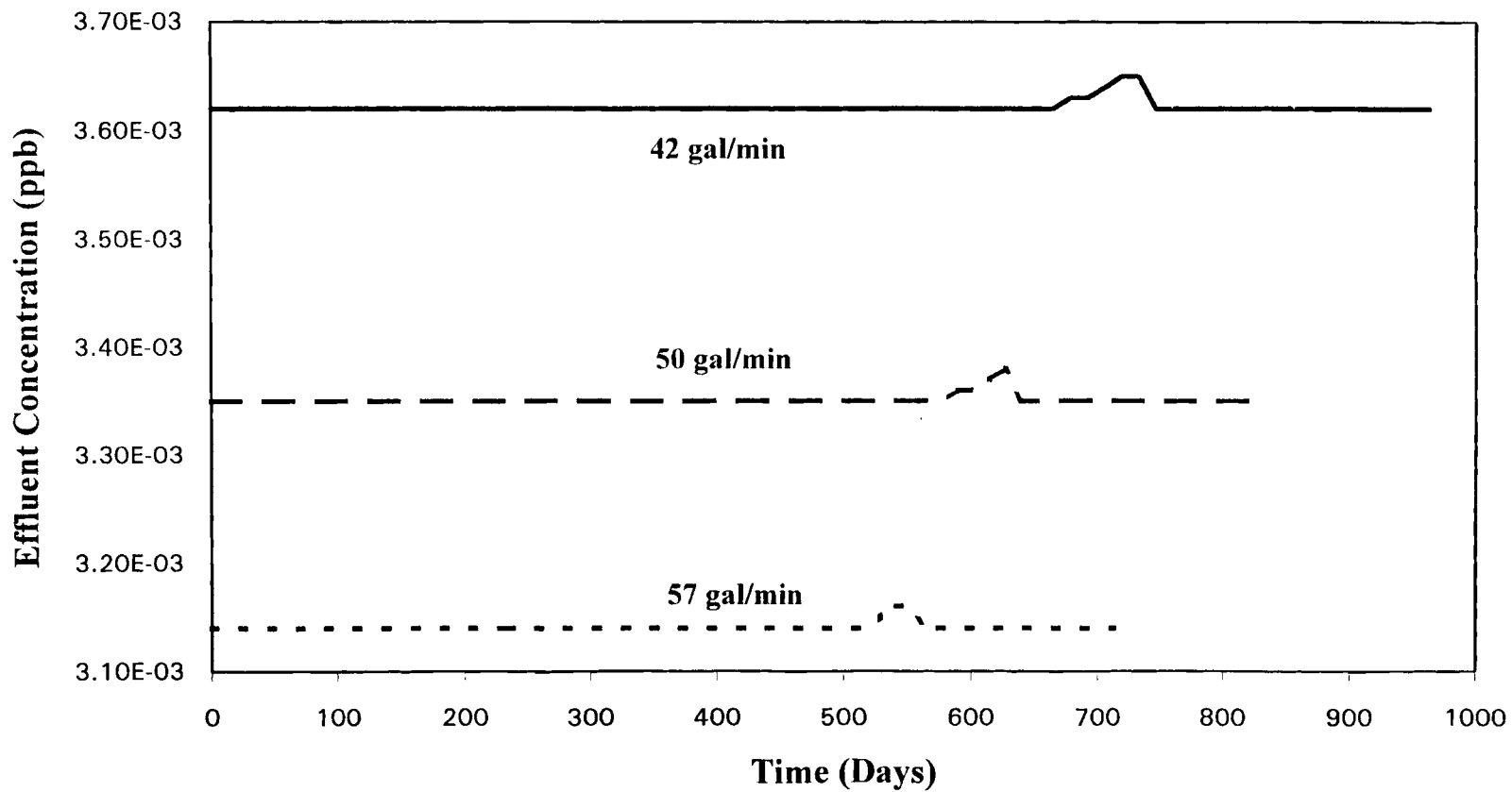


Figure 9. Effect of Flow rate on Sulfate concentration profile for a Mixed-Bed (Cation/Anion Ratio of 1.0) Simulation

in the generation term for sulfate which is a function of flow rate. Small 'peaks' of the order of  $0.3E-3$  ppb are observed in the concentration profiles. This interval corresponds to chloride breakthrough. This could be attributed to numerical instability.

### **Reduced Anion Mass Transfer Coefficient Effects**

The mass transfer coefficients of chloride and sulfate are reduced by half to note the changes in the concentration profile values at base case conditions. Mass transfer coefficients of sodium and calcium are not changed. All the other system parameters are maintained at the base condition.

**Chloride:** Figure 10 shows that equilibrium leakage effluent concentrations are not affected by reducing the mass transfer coefficient by half. Higher mass transfer coefficients exhibit sharper breakthrough curves as shown in the figure. Reducing the mass transfer coefficient by half caused an earlier breakthrough by approximately 100 days. Higher mass transfer coefficients exhibit sharp curves.

**Sulfate:** Unlike chloride, the equilibrium leakage effluent concentrations of sulfate showed a 100 % ( $0.36E-2$  ppb to  $0.72E-2$  ppb) increase by reducing the sulfate mass transfer coefficient by half. Breakthrough didn't occur in both the cases. The leakage values were fairly constant throughout the operation in both the cases. One reason for the sudden increase in effluent concentrations is associated with the desulphonation effect. The sulfate throw from each slice is assumed constant and the expression given as:

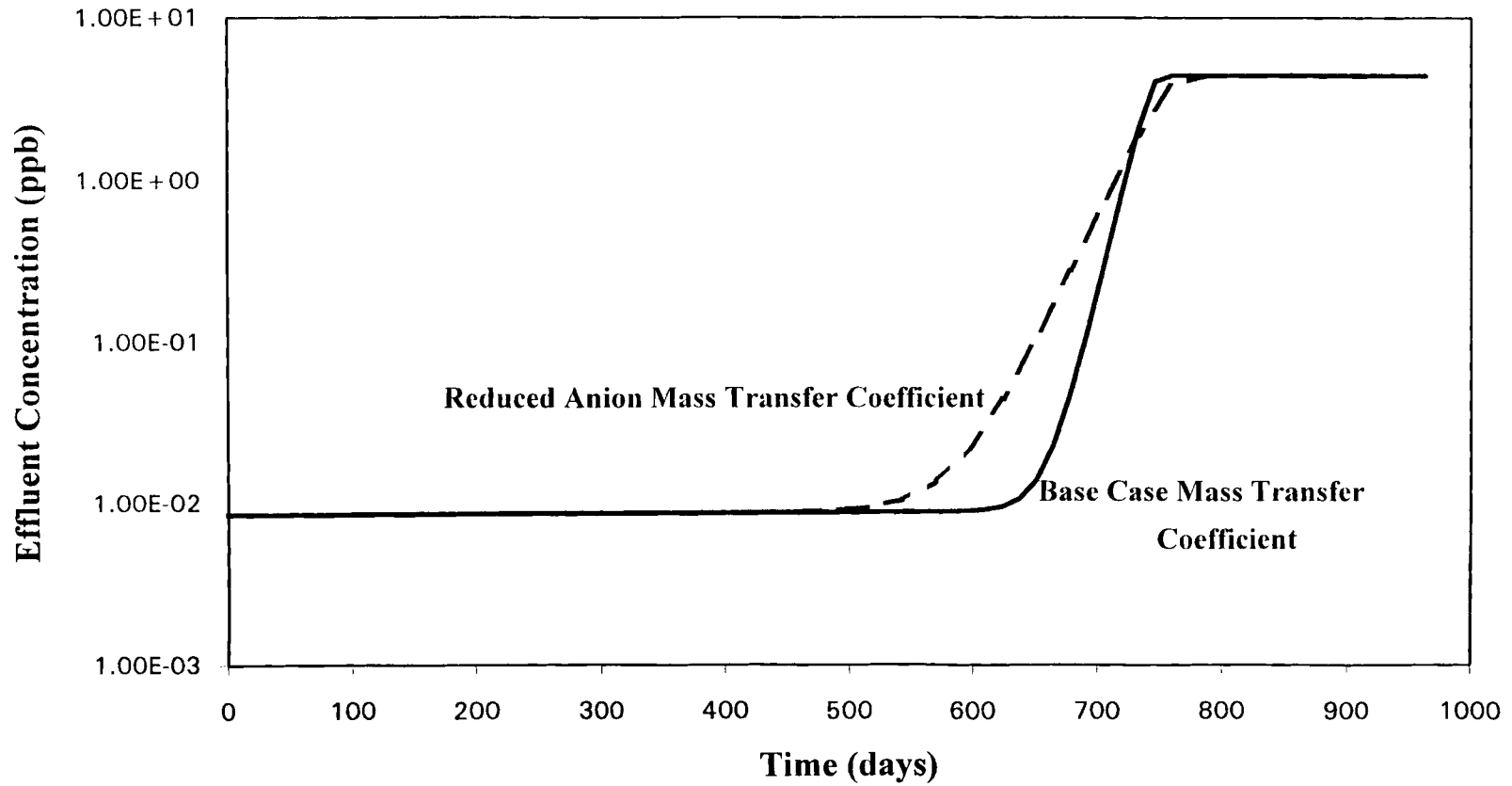


Figure 10. Effect of Reduced Anion Mass Transfer Coefficient on Chloride with System Parameters at Base Case



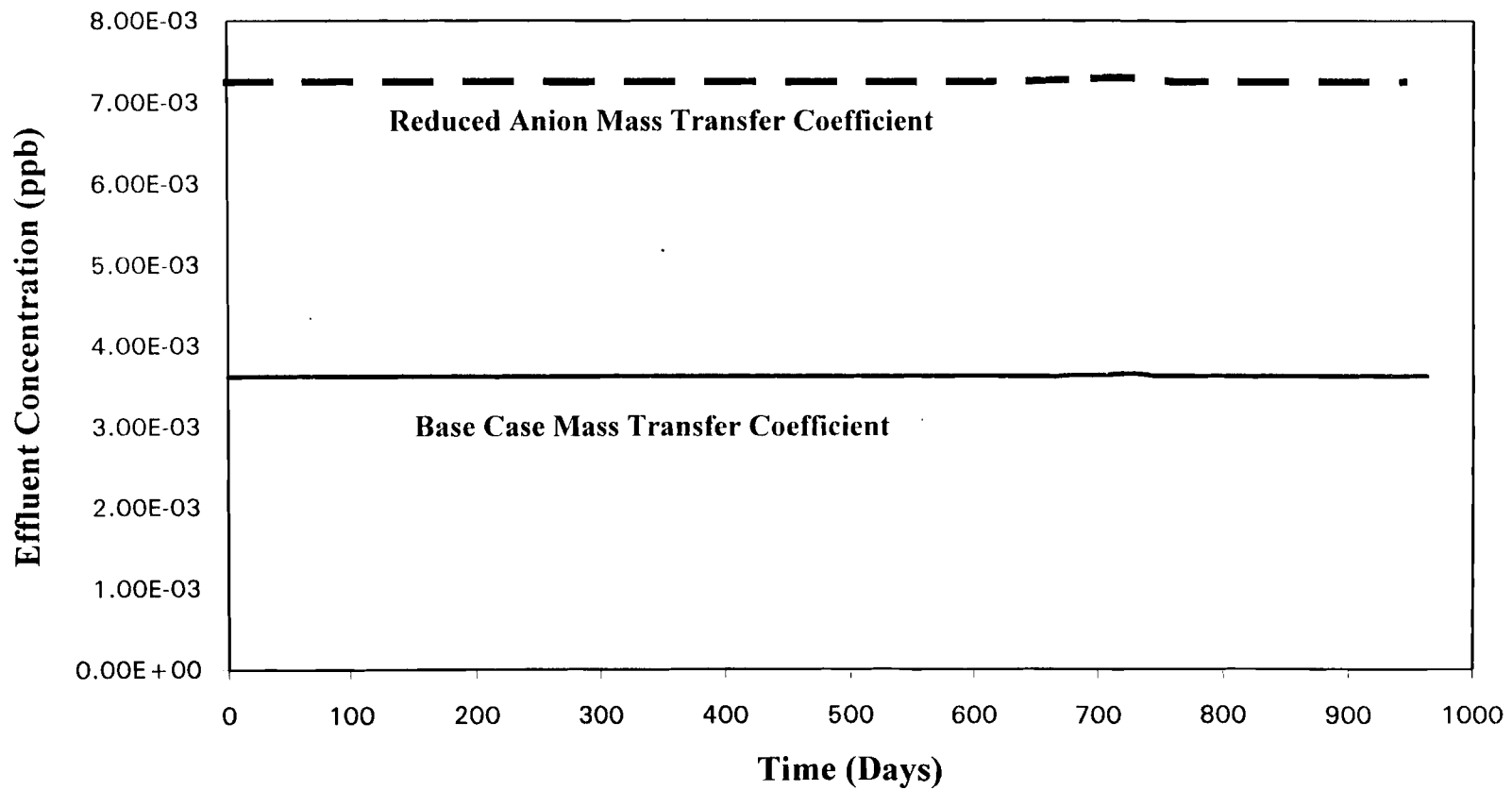


Figure 11. Effect of Reduced Anion Mass Transfer Coefficient on Sulfate with System Parameters at Base Case

$$\begin{aligned}
 DS = & (7.5e + 6\text{EXP}(-10278.6 / (T(^{\circ}\text{C}) + 273.16)) \\
 & \times HT \times 3.1415(D^2) \times q_c)(vs \times d_{pa}) \times \text{FCR} \\
 & / (NT \times 3600 \times \text{FR} \times \text{KLC} \times (1 - \text{VD}))
 \end{aligned}
 \tag{3-11}$$

where

DS= desulphonation (meq/ml)

HT = height of the column in cm

D = diameter of the column in cm

VS = superficial velocity through the bed

$d_{pa}$  = anion particle diameter in cm

FCR = fraction of cation resin in the bed

NT = number of distances steps along the column

FR = flow rate in  $\text{cm}^3/\text{s}$

KLC = chloride mass transfer coefficient

VD = bed void fraction

DS (eq. 3-11) is the desulphonation transformed into consistent units to be used in the computer code. Reduction in the mass transfer coefficient of chloride has an inverse effect on the desulphonation. This increased uniform desulphonation throughout the bed causes higher leaching and consequently higher effluent leakage sulfate concentrations are observed.

### Effects of Particle sizes

The effects of resin particle size on the predicted effluent concentrations were tested for the following two categories.

a) Cation particle = 0.8 cm; Anion Particle = 0.6 cm

b) Cation Particle = 0.65 cm; Anion Particle = 0.55 cm

All the other parameters are at base case.

Figure 12 shows that equilibrium effluent leakage sodium concentrations are not affected by change in particle size. The bed saturation time is the same in both cases. Mass transfer coefficients effect the breakthrough curves. Higer mass transfer coefficients give sharper breakthrough curves. Mass transfer coefficients are calculated using Kataoka and Carberry correlations and are related to particle size as:

$$K_i \alpha (d_p)^{-0.5} \text{ for } Re \geq 20, \text{ and}$$

$$K_i \alpha (d_p)^{-2/3} \text{ for } Re \leq 20$$

Also, the sodium rate expression is proportional to the ratio of anion to cation particle size.

Figure 13 shows the effluent calcium leakage concentrations. A similar trend to sodium is observed.

Figure 14 shows the effluent leakage chloride concentrations. Chloride is taken as the reference ion in the divalent model and consequently the chloride rate expression is independent of mass transfer coefficient and ration of particle size. The observed change in the effluent chloride concentration profile is due to sulfate exchange kinetics.

Unlike sodium, calcium, and chloride, Sulfate effluent leakage concentrations are a strong function of particle size. As shown in Figure 15, a 12.2% decrease in the effluent equilibrium leakage is observed when the particle sizes are reduced. This change is due to the desulphonation effect which is directly proportional to the particle size.

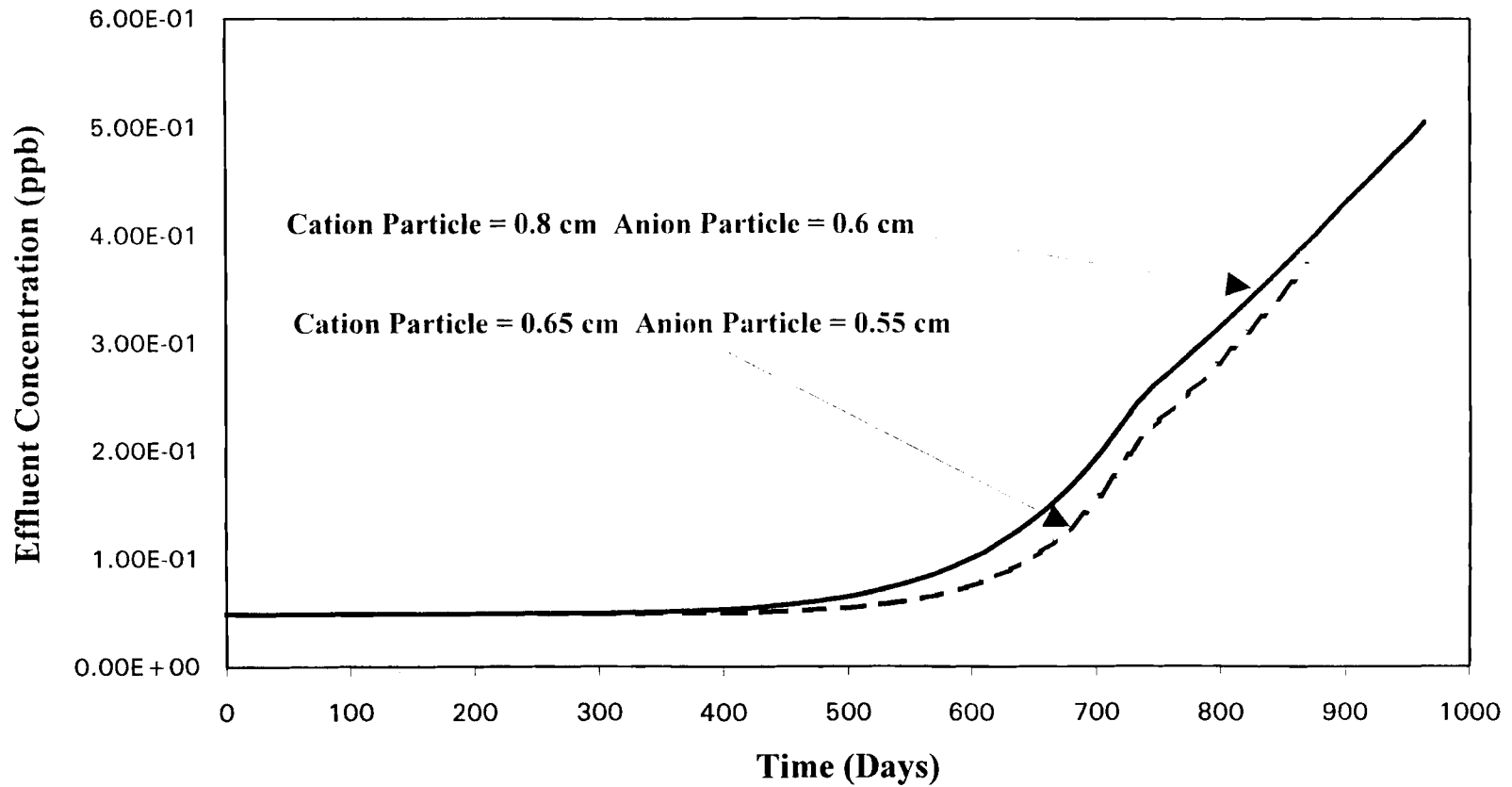


Figure 12. Effect of Resin Particle Size on Sodium Concentration Profile for a Mixed Bed Simulation Using Divalent Model

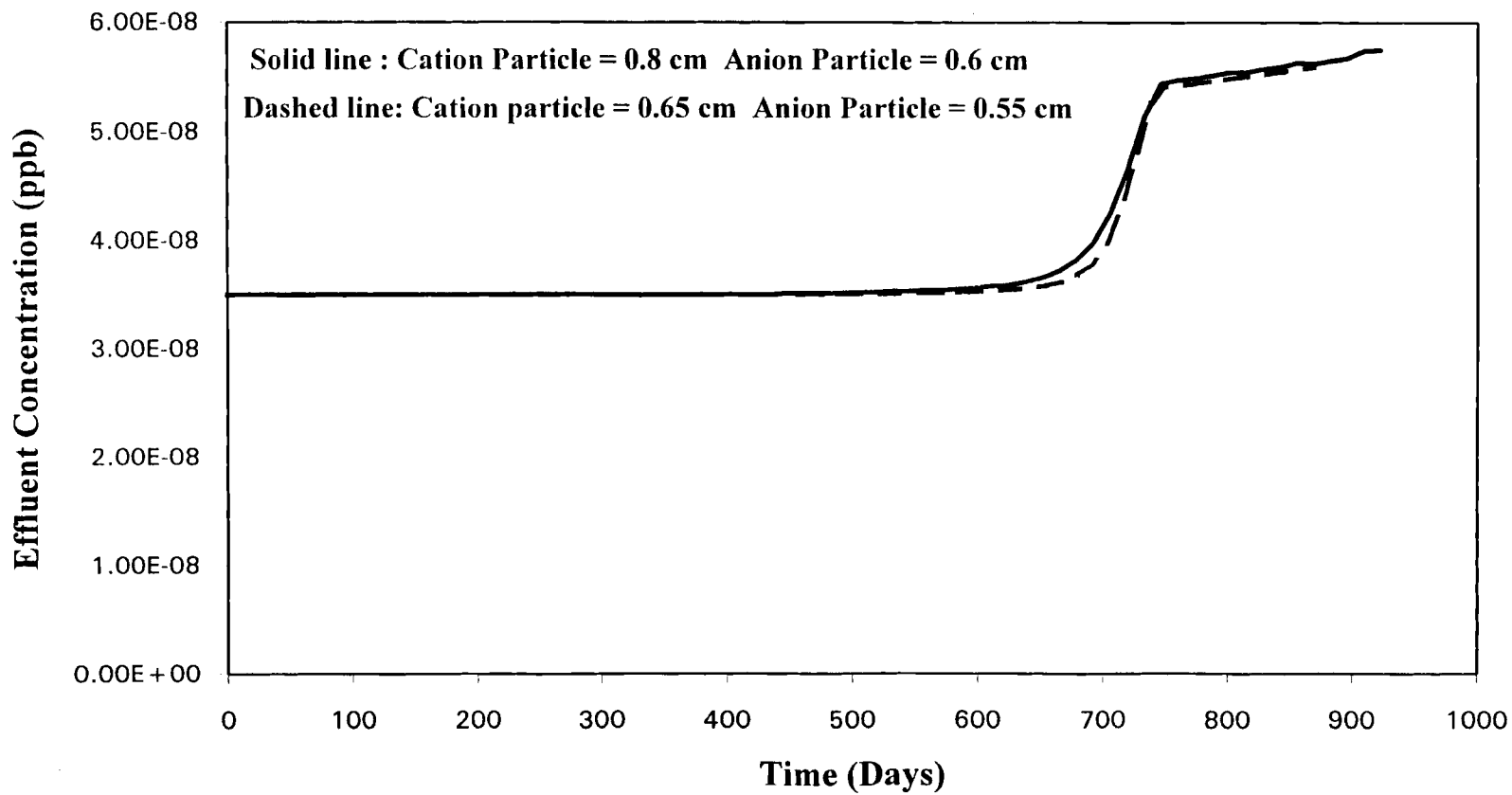


Figure 13. Effect of Resin particle Size on Calcium Concentration Profile for a Mixed Bed Simulation Using Divalent Model

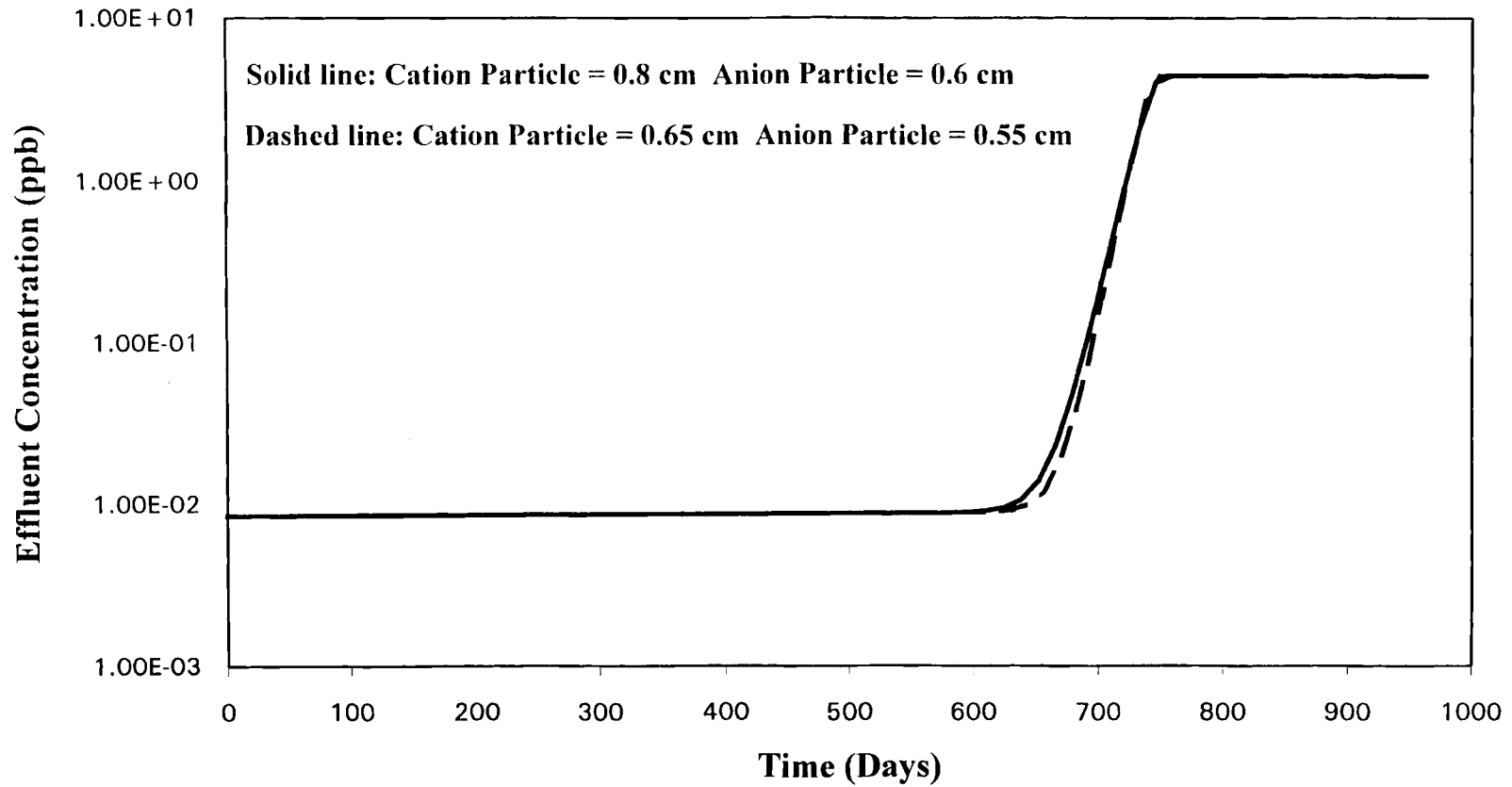


Figure 14. Effect of Resin Particle Size on Chloride Concentration Profile for a Mixed Bed Simulation Using Divalent model

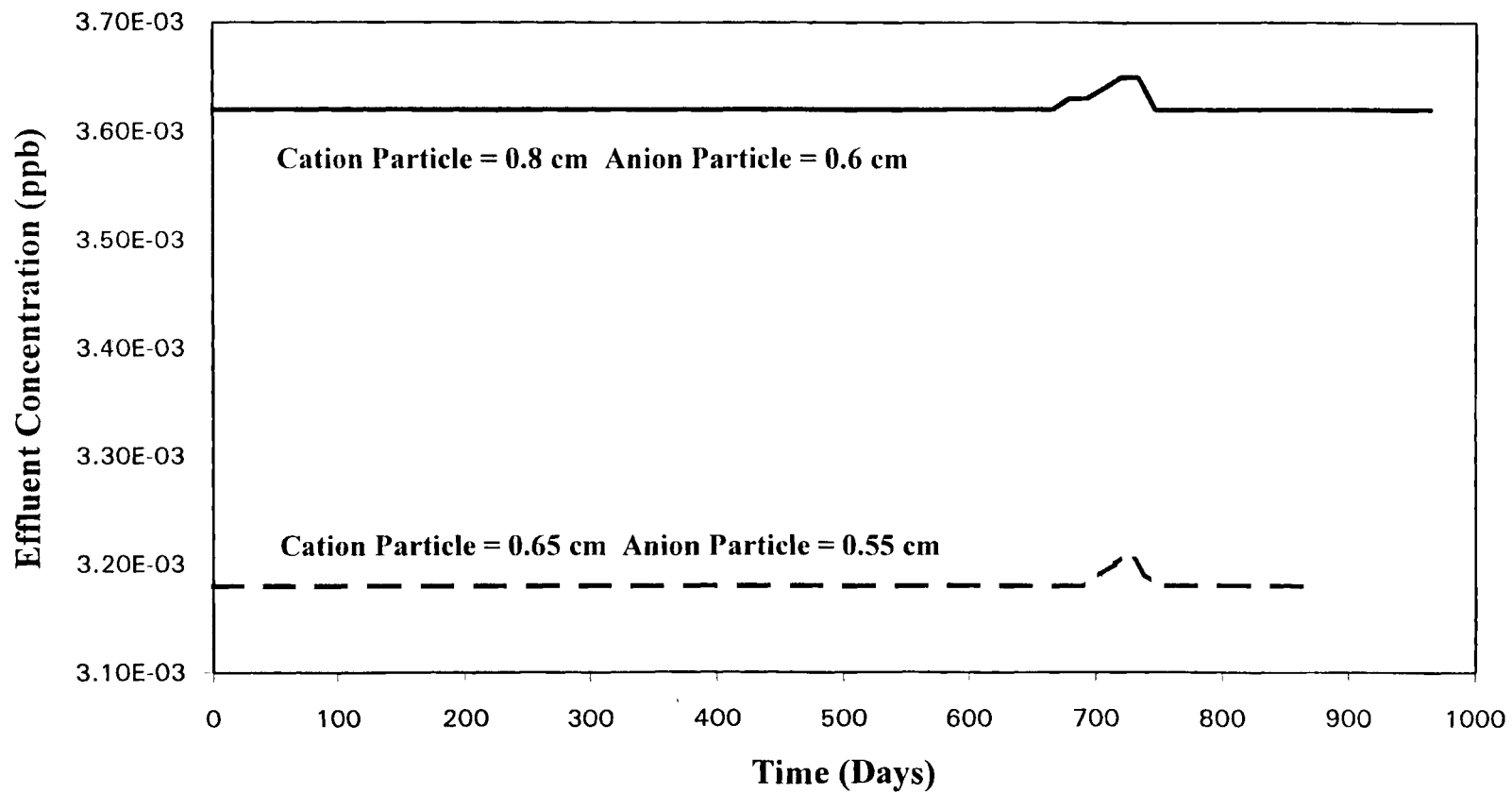


Figure 15. Effect of Resin Particle Size on Sulfate Concentration Profile for a Mixed Bed Simulation Using Divalent Model

## Effects of Resin Ratios

Figures 16 through 18 shows the effect of resin ratios on the predicted effluent concentration profiles. Resin ratios used were

- a) Cation: Anion = 1.5:1,
- b) Cation: Anion = 1:1, and
- c) Cation: Anion = 1:1.5.

All the other parameters are maintained at base condition.

As shown in Figure 16, the effluent leakage sodium concentrations are not affected by change in resin ratios. The effluent concentrations change after 200 days. An earlier breakthrough by 180 days occurs for a cation/anion ratio of 1.0/1.5 compared to cation/anion resin ratio of 1.5/1.0. Figure 17 shows the chloride effluent concentration profile for varying resin ratios. There is no change in the effluent leakage concentrations. Steepness of the breakthrough curves did not change for cation/anion ratio of 1.5/1.0 and cation/anion ratio of 1.0. Breakthrough was not observed for cation/anion ratio of 1.0/1.5. Figure 18 shows the sulfate effluent leakage concentrations. The effluent leakage concentrations shows a significant change for different resin ratios. By changing the cation/anion ratio from 1.5/1.0 to 1.0/1.5, a 55.5% decrease in the effluent sulfate leakage concentrations is observed. This is due to the desulphonation effect of cation resin.

## Conclusions and Recommendations

The divalent model developed here can be used for a wide range of conditions. Data on selectivity coefficients for divalent exchange as a function of temperature is not available in the literature and improved predictions are expected when they are



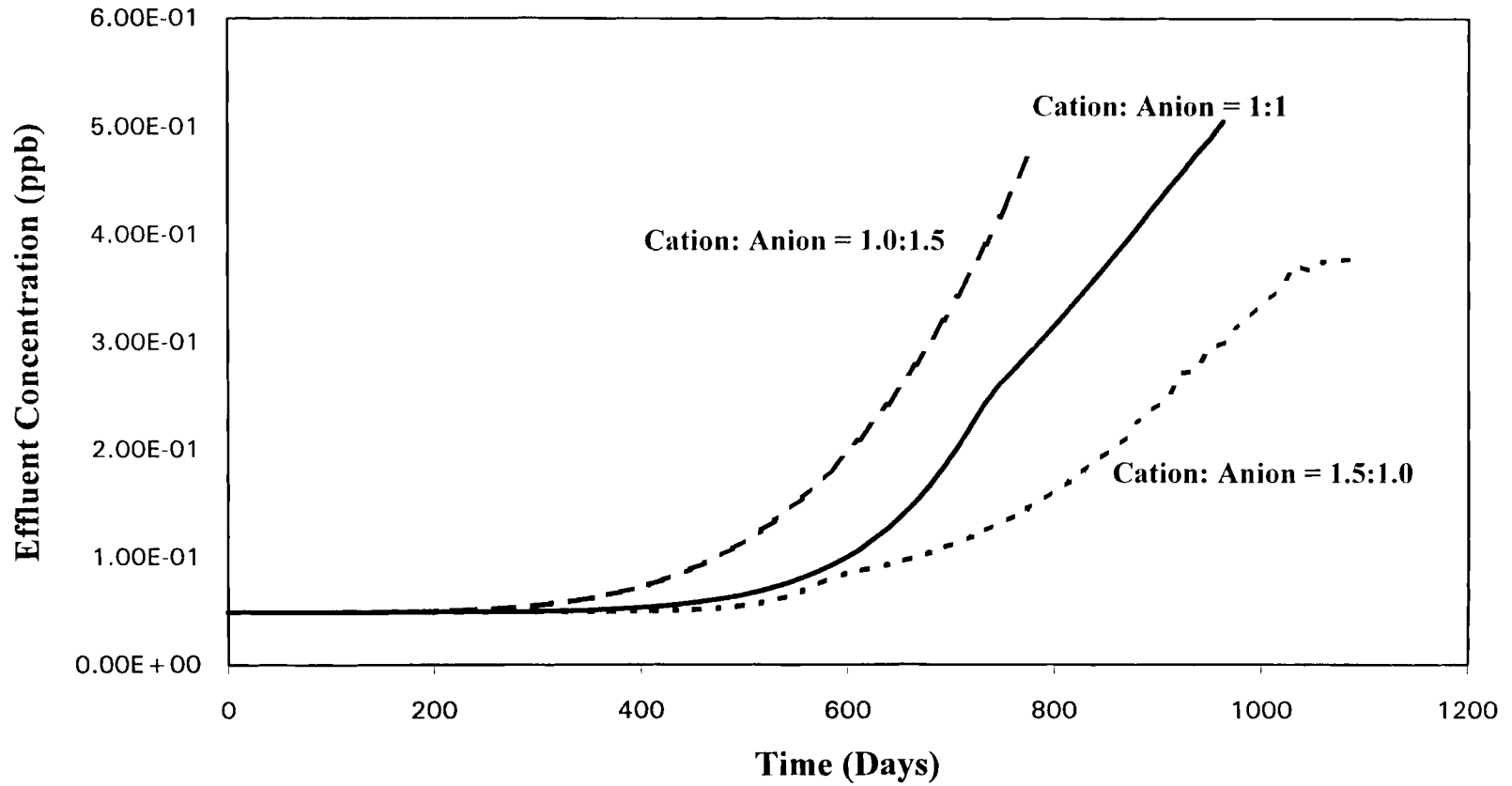


Figure 16. Effect of Resin Ratios on Sodium Concentration Profile for a Mixed Bed Simulation Using Divalent Model

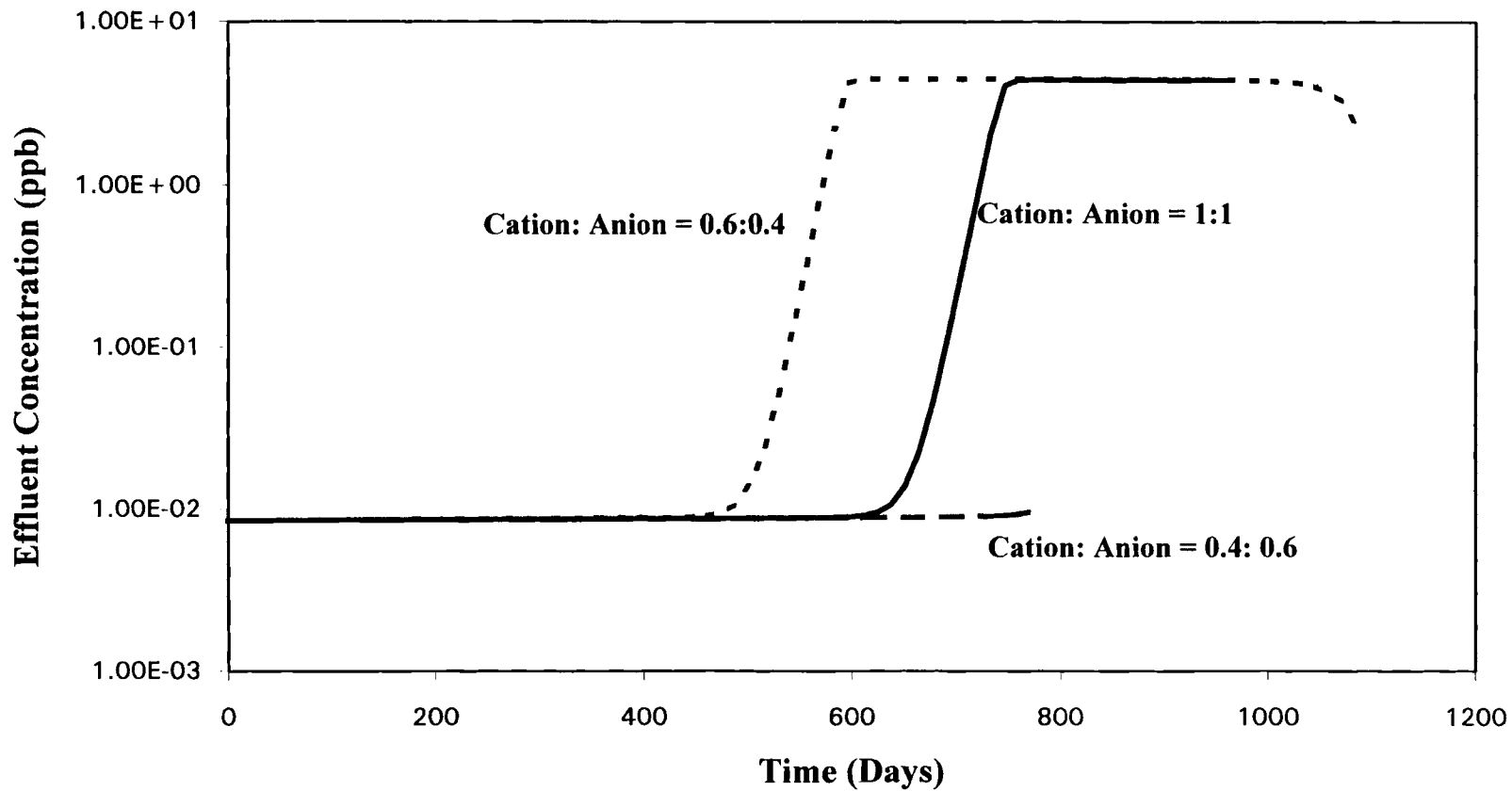


Figure 17. Effect of Resin Ratios Chloride Concentration Profile for a Mixed Bed Simulation Using Divalent Model

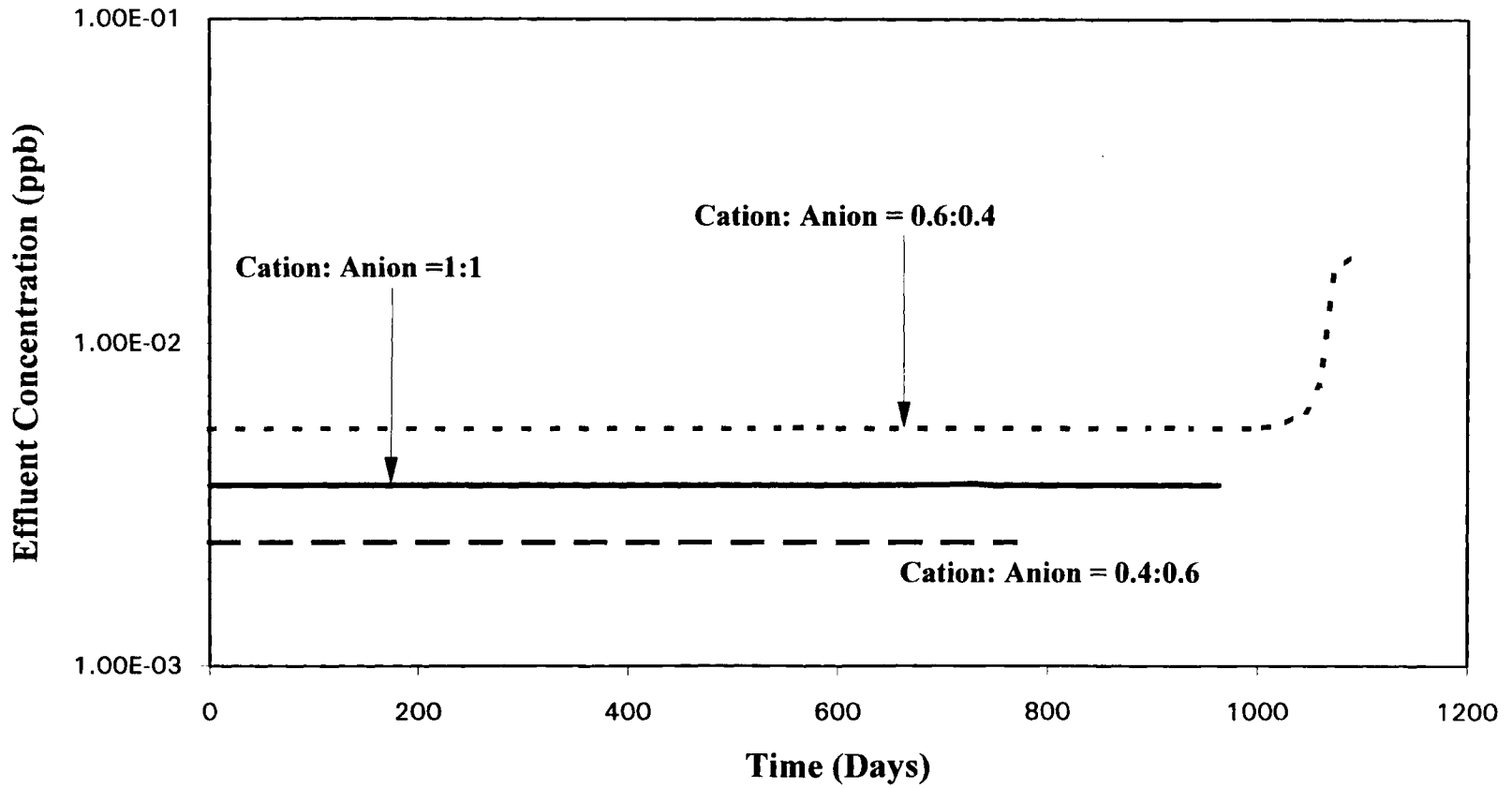


Figure 18. Effect of Resin Ratios on Sulfate Concentration Profile for a Mixed Bed Simulation Using Divalent Model

incorporated in the model. Desulphonation effects were incorporated into the model and its predictions agreed with plant data qualitatively. Effect of system parameters on desulphonation changes sulfate leakage significantly. Sulfate release into the effluent stream is primarily due to desulphonation. Plant data indicated the presence of  $\text{HCO}_3^- / \text{CO}_3^{2-}$  in high quantities along with other impurities ( $\text{Mg}^+, \text{Cu}^+$ ) with anion equivalent ratios of  $0.3\text{SO}_4^{2-} : 0.5\text{HCO}_3^- / \text{CO}_3^{2-} : 0.2\text{Cl}^-$ . Divalent model does not currently handle bicarbonate predictions. Actual plant data comparisons can be made when the divalent model is modified to multicomponent model which can predict the effluent concentrations of  $\text{HCO}_3^- / \text{CO}_3^{2-}$ .

Calcium concentrations are quite lower than expected. Kinetic corrections can be developed to improve equilibrium relations and its predictions in a multicomponent exchange and applied to all divalent species.

## CHAPTER IV

### EFFECT OF PLANT OPERATING PRINCIPLES - RESIN HEEL AND BED CLEANING

#### Abstract

An MBIE Model for divalent ions is tested for the effects of resin heel (i.e. uneven distribution of resin in the bed). The model is then extended to address bed cleaning every three weeks whereby average particle loading after cleaning is used as the initial loading for the next three weeks. The predictions agree with plant experience.

#### Introduction

Ion exchange in deep bed polishers is optimum when the cation and anion resins are homogeneously mixed. The effluent stream will contain minimal quantities of ionic and organic impurities and near neutral water. However, in practice, it is difficult to achieve a well mixed bed in service vessels. Thermal degradation of cation resin exchange sites for sulfate release (discussed in chapter III ) into BWR's is a serious problem. In addition, the resin is transferred out of the bed for ultrasonic cleaning at approximately three week intervals. About 10% of the bed, primarily in the form of cationic resin (due to its weight), classifies at the bottom of the bed. One approach to avoid this situation has been to replace the cationic heels with an anionic underlay. The expected result for this underlay is an increase in organic amines released from the bed,

but these amines would decompose in the BWR to ammonia, organic acids, nitrogen oxides and carbon dioxide. All of these products are volatile and would not be expected to concentrate in the reactor. Reduction in the overall ion exchange performance was expected.

## Modeling

An MBIE model for divalent ions is used to evaluate the ionic removal performance of the bed containing an anionic rich underlay. The base case used 1:1 cation to anion resin ratios by volume throughout the bed. Sulfate concentration fed to the column was 3.3 ppb (including 3.0 ppb as a condenser leak). Cation equivalent ratios of 0.2 Na<sup>+</sup>: 0.8 Ca<sup>+2</sup> were used. Chlorine was adjusted to meet electroneutrality criteria.

Water flowrate was 42 gallons per minute per foot square of cross-sectional area, and the system was operated at an isothermal temperature of 140°F. The bed was 3.35 m in diameter and 1.0 m deep. Resin properties, selectivity coefficients, and initial particle loading are given in APPENDIX F. Diffusion coefficients and pH are a function of temperature. Mass transfer coefficients are calculated using correlation's by Kataoka or Carberry depending on flow conditions.

In addition, the model included a sulfate generation term for the cationic resin. An expression for the kinetic rate constant was used based on data supplied to PP&L by Fisher and Burke (fig.27). The expression used in the code was

$$K = 7.5E + 6 \times e^{(-10278/(T+273.16))}$$

Where K is a first order reaction rate constant with units of hr<sup>-1</sup>, and T is the temperature of the bed in °C.

Using this equation, localized sulfate generation throughout the bed is assumed constant for an isothermal system. Also, sulfate release is a strong function of flow

conditions and water oxygen content. Fisher and Burke's data were generated in beakers exposed to air. Additional data have been presented in PP&L literature.

To approximate the bed underlay, the same total resin capacity is used, but a 5:1 anion rich layer is assumed for the bottom 5 cm of the bed (the total anion to cation resin ratio in the column is 1.07/1.0). Figure 18 through 21 presents the predicted effluent concentration curves for sodium, calcium, chloride, and sulfate for these simulations. Sodium and calcium follow a similar trend and curves become steeper for anionic heels though not significantly. Chloride breakthrough starts 20 days later for simulation with anionic heels. Of particular note is the reduction in the sulfate equilibrium leakage from  $2.2 \times 10^{-2}$  (base case) to  $0.7 \times 10^{-3}$  ppb. This suggests that using an anionic underlay has the potential to reduce sulfate leakage from the bed significantly when compared to an ideal mixed bed. The improvement is even greater when compared to a bed operating with cationic heels. The effluent concentrations were an order of magnitude higher ( $1.40 \times 10^{-2}$  ppb) when operating with a 5 cm cationic heel.

### **Comparison to Plant Experience**

An in-plant test of anion underlays has been performed by PP&L. Ion exchange units are normally operated with cation-rich heel at the outlets. Each of the seven condensate polisher vessels was cleaned and an underlay installed while the plant operated at 100% power. As the number of vessels with underlays increased (they were brought on-line one at a time), sulfate reactor water gradually dropped from 6-8 ppb to 3-4 ppb.

The reactor water cleanup system (which limits impurity concentrations in reactor water) processes at 1% of the feed water flow rate. Therefore, the decrease observed in reactor water sulfate is equivalent to a decrease in the available sulfur in polished effluent of about 0.03-0.04 ppb as sulfate.

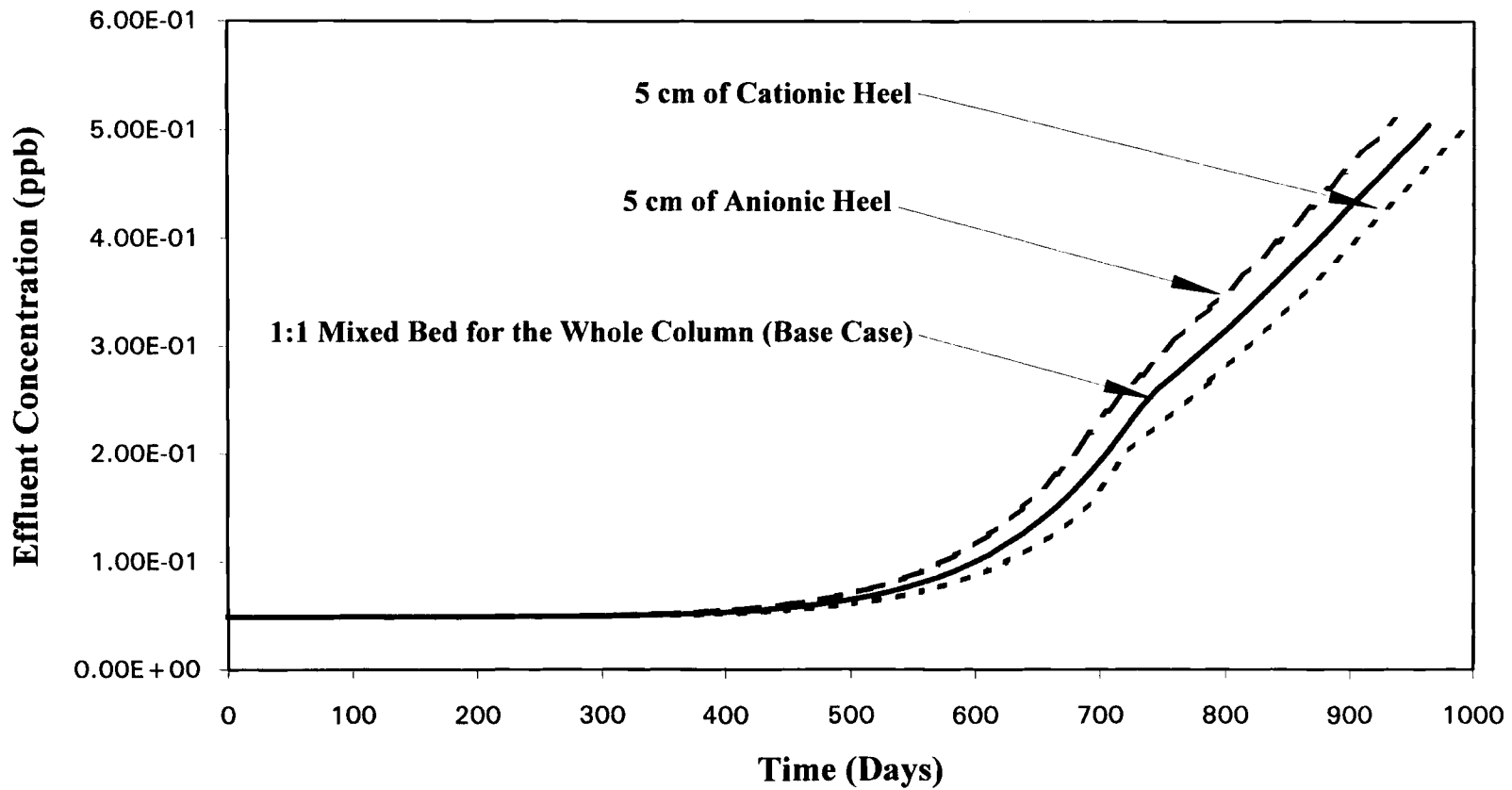


Figure 19. Effect of Anion Resin Underlay on Sodium Concentration Profile Using MBIE Model for Divalent Ions.



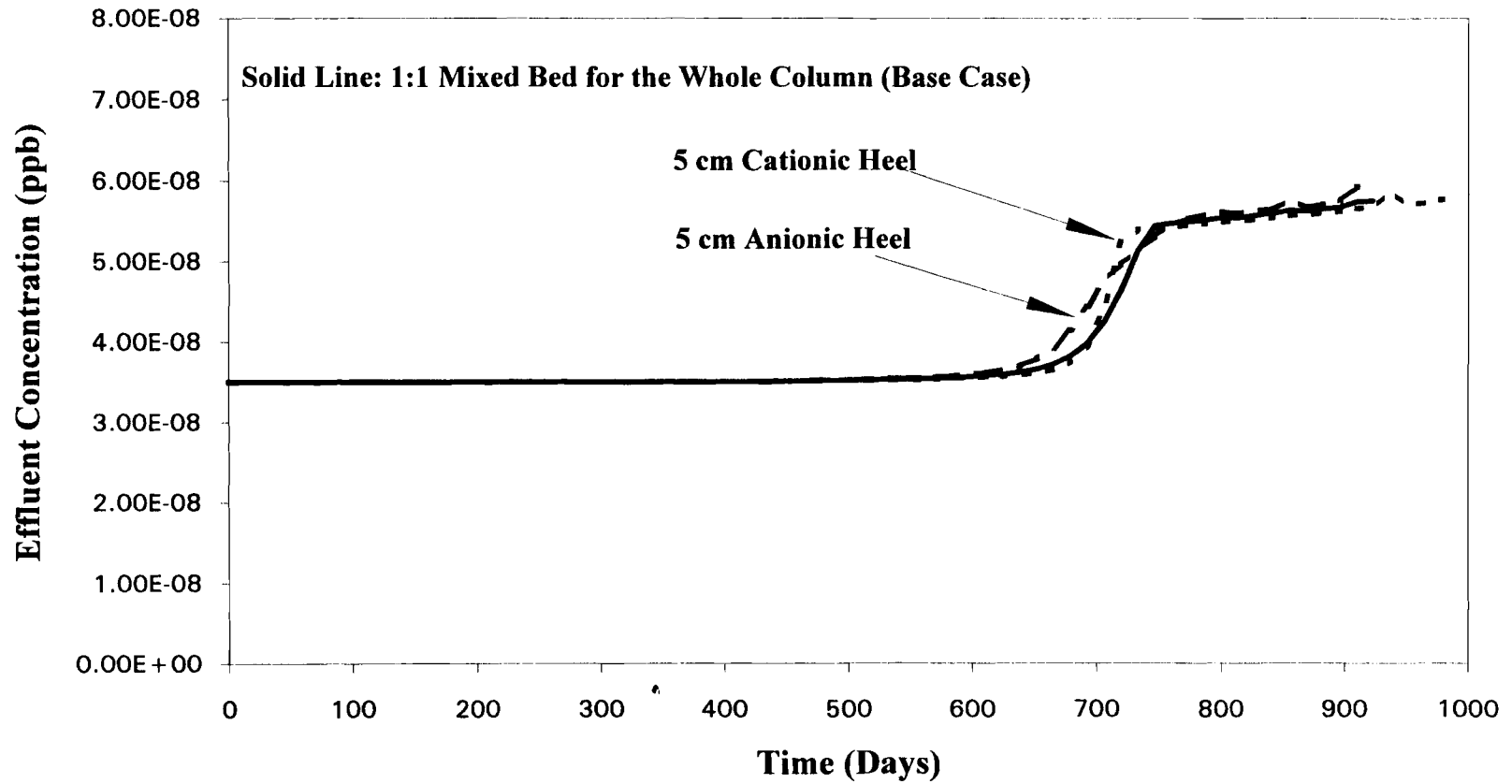


Figure 20. Effect of Anion Resin Underlay on Calcium Concentration Profile Using MBIE Model for Divalent Ions.

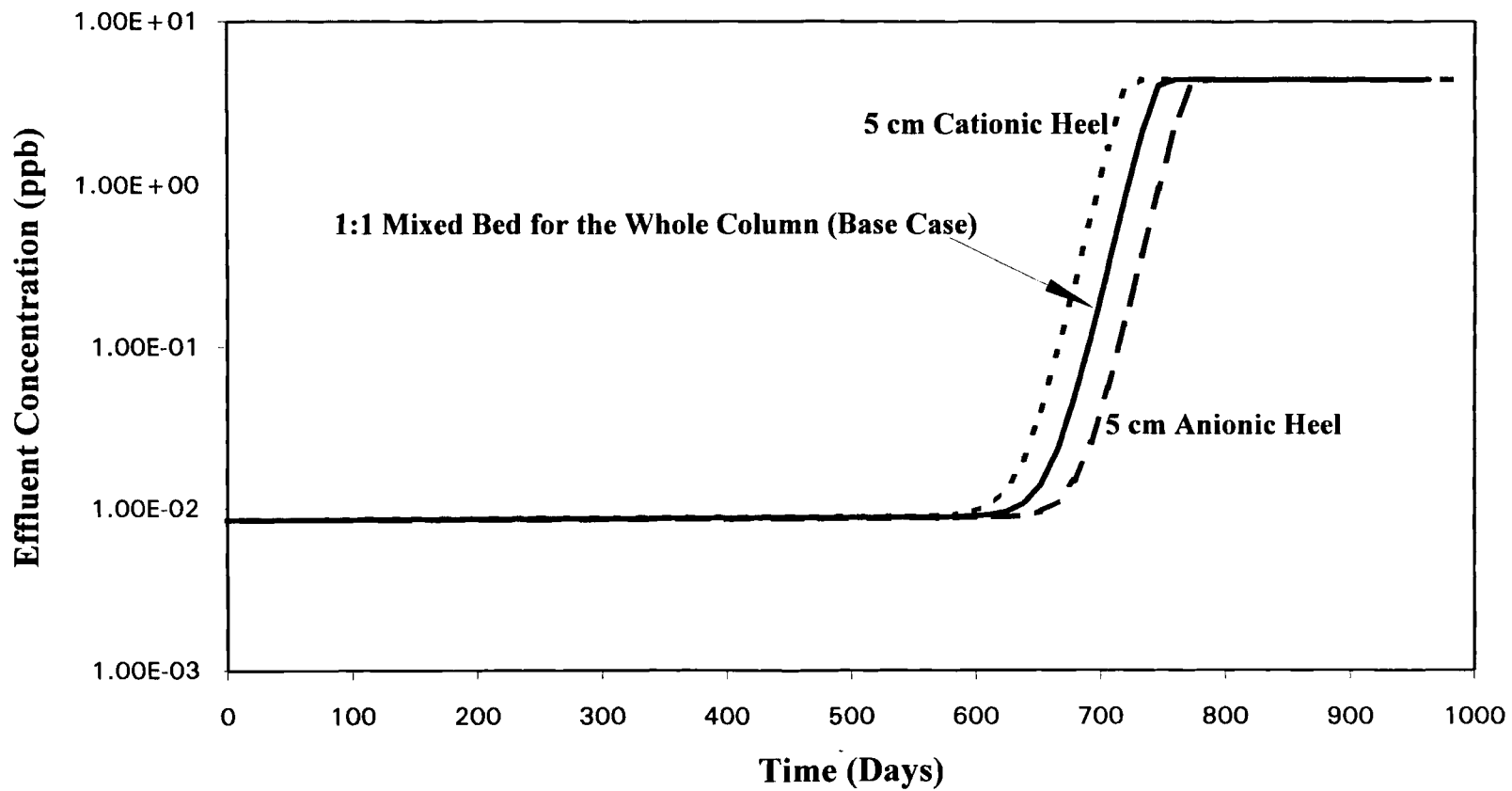


Figure 21. Effect of Anion Resin Underlay on Chloride Concentration Profile Using MBIE Model for Divalent Ions.

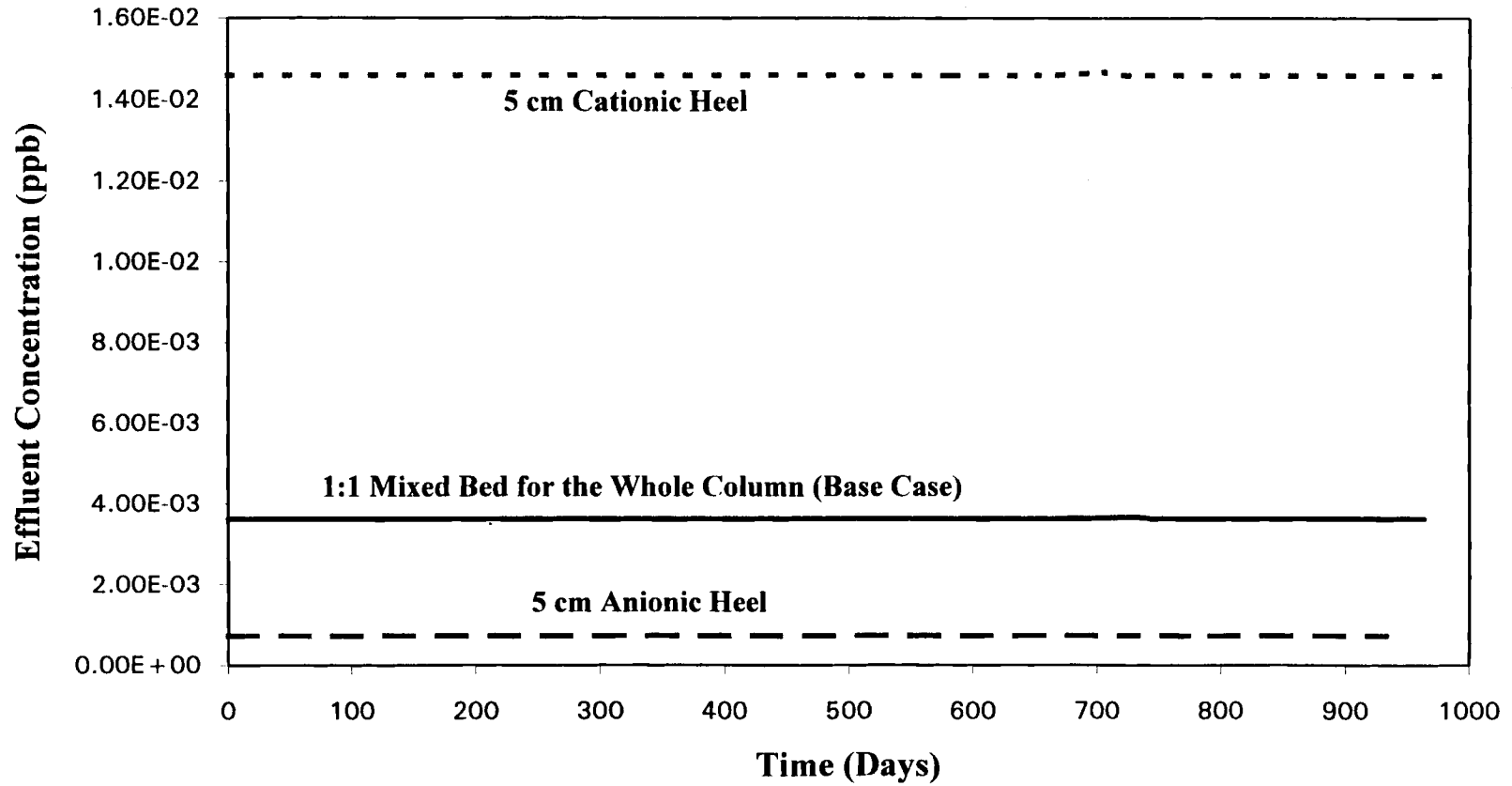


Figure 22. Effect of Anion Resin Underlay on Sulfate Concentration Profile Using MBIE Model for Divalent Ions.

Sulfur is also released from the cation resin in organic compounds such as resin fines and soluble materials such as benzene sulfonic acid. This organic sulfur is oxidized in the BWR to inorganic sulfate. The anion underlays would also act to adsorb some of these impurities, but the efficiency for adsorption of organics is not likely to be as high as ion exchange.

Calculations at PP&L indicated that inorganic sulfate release from cation-rich resin heels in the condensate polisher vessels could contribute as much as 4-5 ppb to reactor water sulfate. Additionally, the sulfate concentration would be strongly dependent on condensate temperature.

The computer simulation of the divalent model indicates that the inorganic sulfate release from polishers with well-mixed resins but without underlays would contribute 0.0023 ppb sulfate to feed water, and that the underlays would reduce that by a factor of 5. The reduction in reactor water sulfate observed at PP&L was 3-4 ppb, or about 80% of the calculated contribution from the resin heels. Thus the computer simulation is consistent with the observations at PP&L, although the actual effluent concentrations are different. The potential reasons for these differences are

- 1) Bicarbonate loading: Plant data indicated the presence of  $\text{HCO}_3^- / \text{CO}_3^{2-}$  in high quantities along with other impurities ( $\text{Mg}^+, \text{Cu}^+$ ) with anion equivalent ratios of  $0.3\text{SO}_4^{2-}:0.5\text{HCO}_3^- / \text{CO}_3^{2-}:0.2\text{Cl}^-$ . Divalent model does not currently handle bicarbonate predictions.
- 2) Organic sulfonates: Decomposition of cation ion exchange resins by the release of organic sulphonates have been studied (Stabhush, 1987, Fisher, 1987, Cutler, 1988). Plant data indicated the presence of organic sulphonates but no information is available about organic sulphonate effect on the predicted concentration levels. Divalent model does not address this effect.

The computer simulation implies that, if condensate polisher resins are well-mixed and heels are avoided, direct inorganic release of sulfate should not be a major contributor to reactor water sulfate in the BWR. The contribution of inorganic sulfate to total reactor water sulfate would be less than 1 ppb. The on-site test results and computer simulation both support the utility's decision to proceed with modifications to eliminate cation resin heels and to assure good mixing of resins in the condensate polisher vessels

### **Bed Cleaning Effects**

Figures 22 through 25 shows the effect of bed cleaning every three weeks on the predicted concentration profiles. Initial particle loading for the simulation is the same as base case. After three weeks, the bed is cleaned ultrasonically and the resin is loaded into the column. At this point an average particle loading (based on the condition of the resin on the twenty-first day) is calculated and taken as the initial particle loading for the next three weeks.

The effluent concentrations of sodium shows a significant increase for simulation with bed cleaning every three weeks. After the first three weeks, a 17.1% increase in the effluent concentrations is observed. It continues to increase to a maximum of 250% at the end of 550 days. Calcium effluent concentrations at the end of the column run time increase by more than an order of magnitude for the simulation with bed cleaning compared to the base case condition. Chloride follows the same trend as sodium but its increase in effluent concentrations are much higher (98.1% for the first three weeks). Sulfate effluent concentrations do not change significantly compared to sodium, calcium and chloride. Initial particle loading for sulfate is higher than any of the other species. Successive average particle loading of sulfate doesn't change significantly to effect the effluent concentrations.

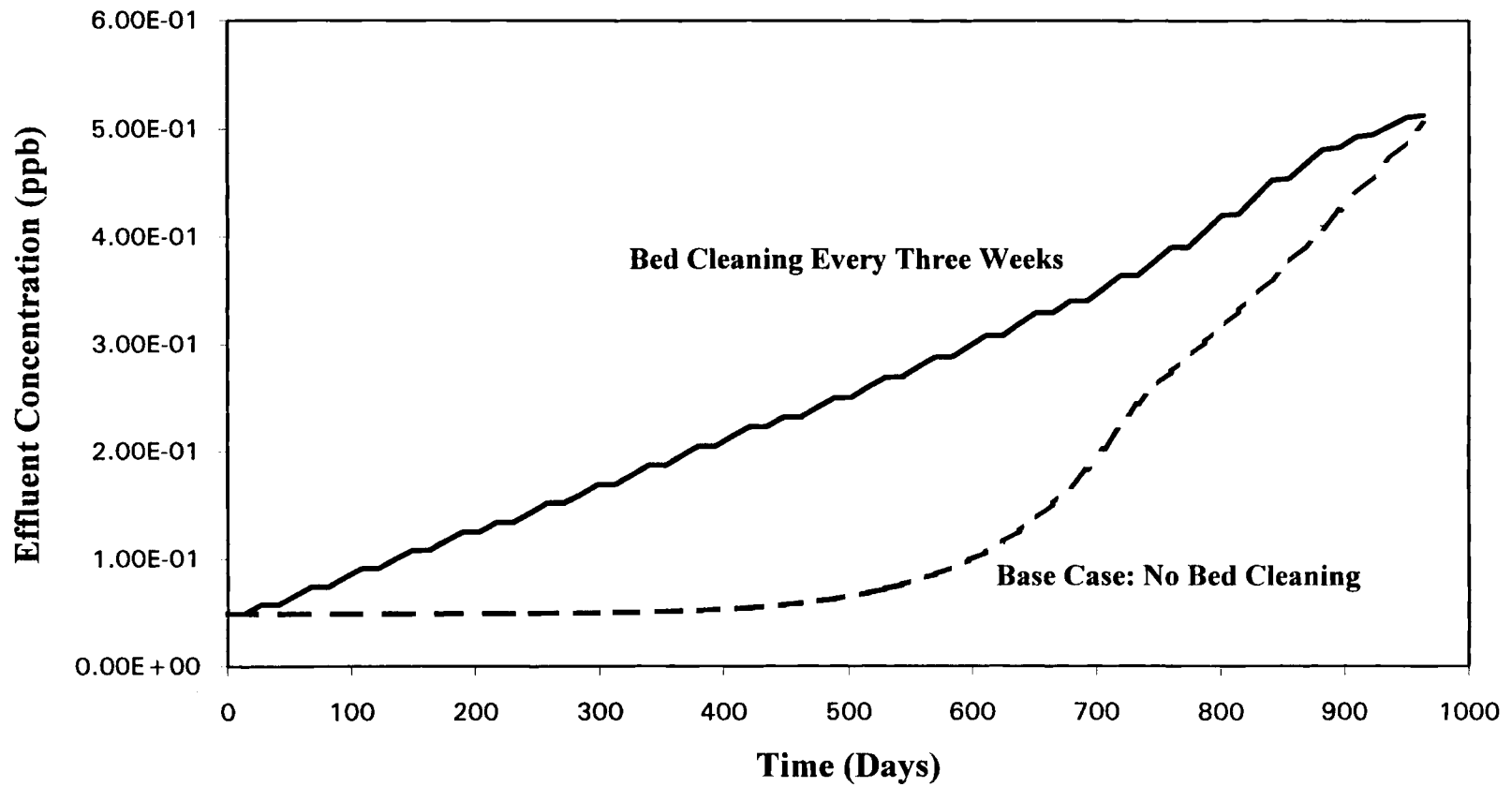


Figure 23. Effect of Bed Cleaning Every Three Weeks on Sodium Concentration Profile

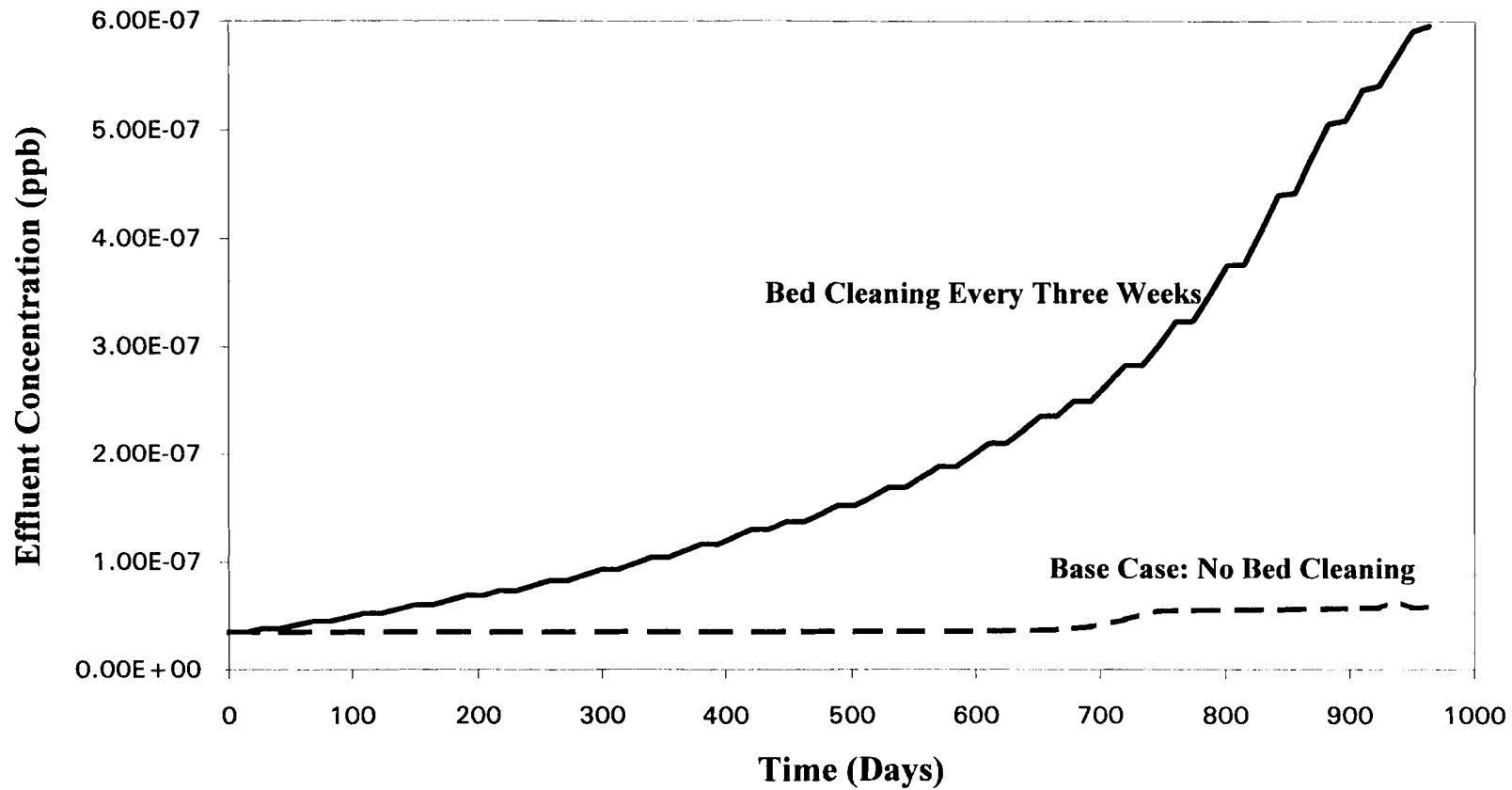


Figure 24. Effect of Bed Cleaning Every Three Weeks on Calcium Concentration Profile

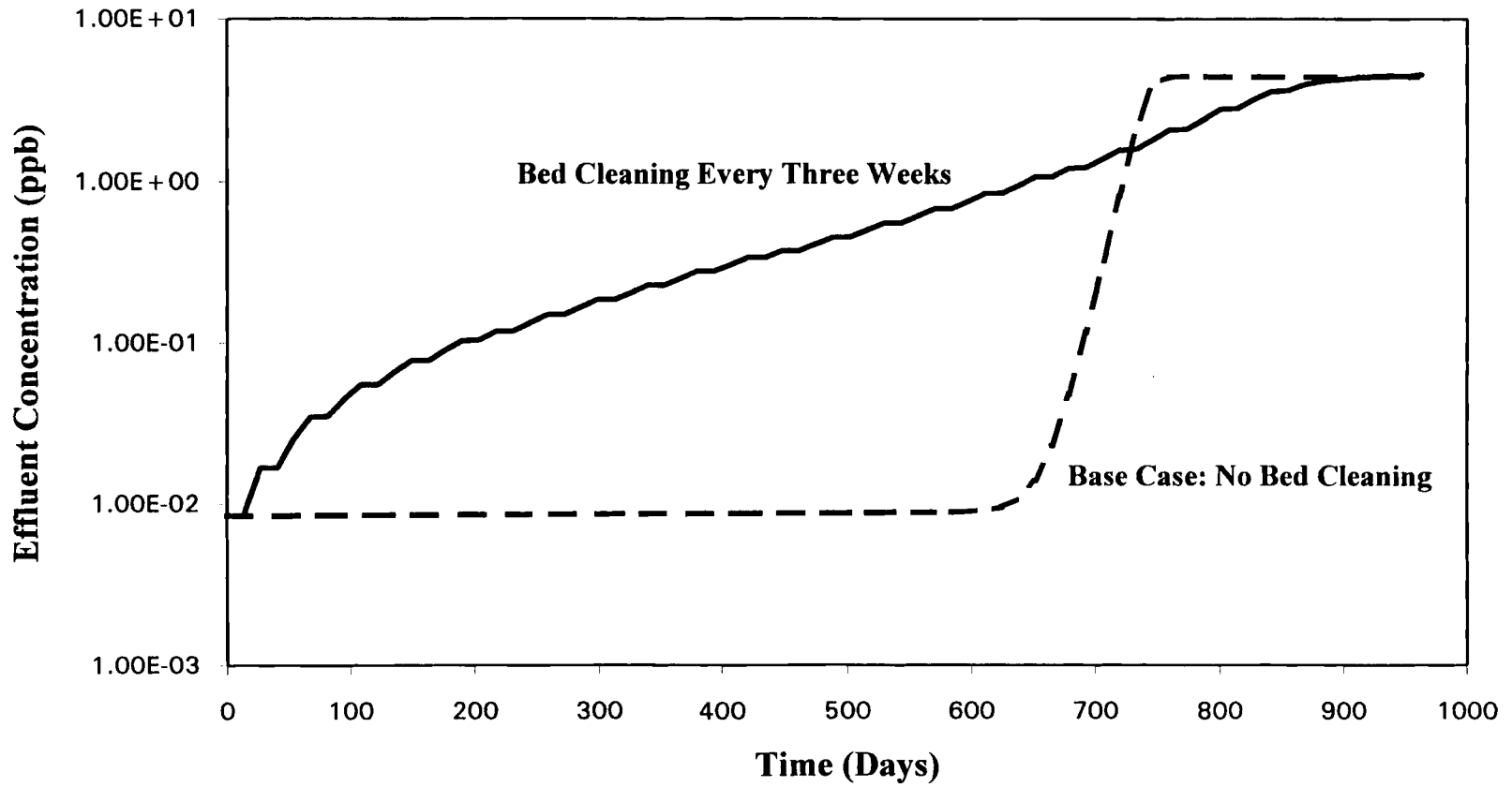


Figure 25. Effect of Bed Cleaning Every Three Weeks on Chloride Concentration Profile



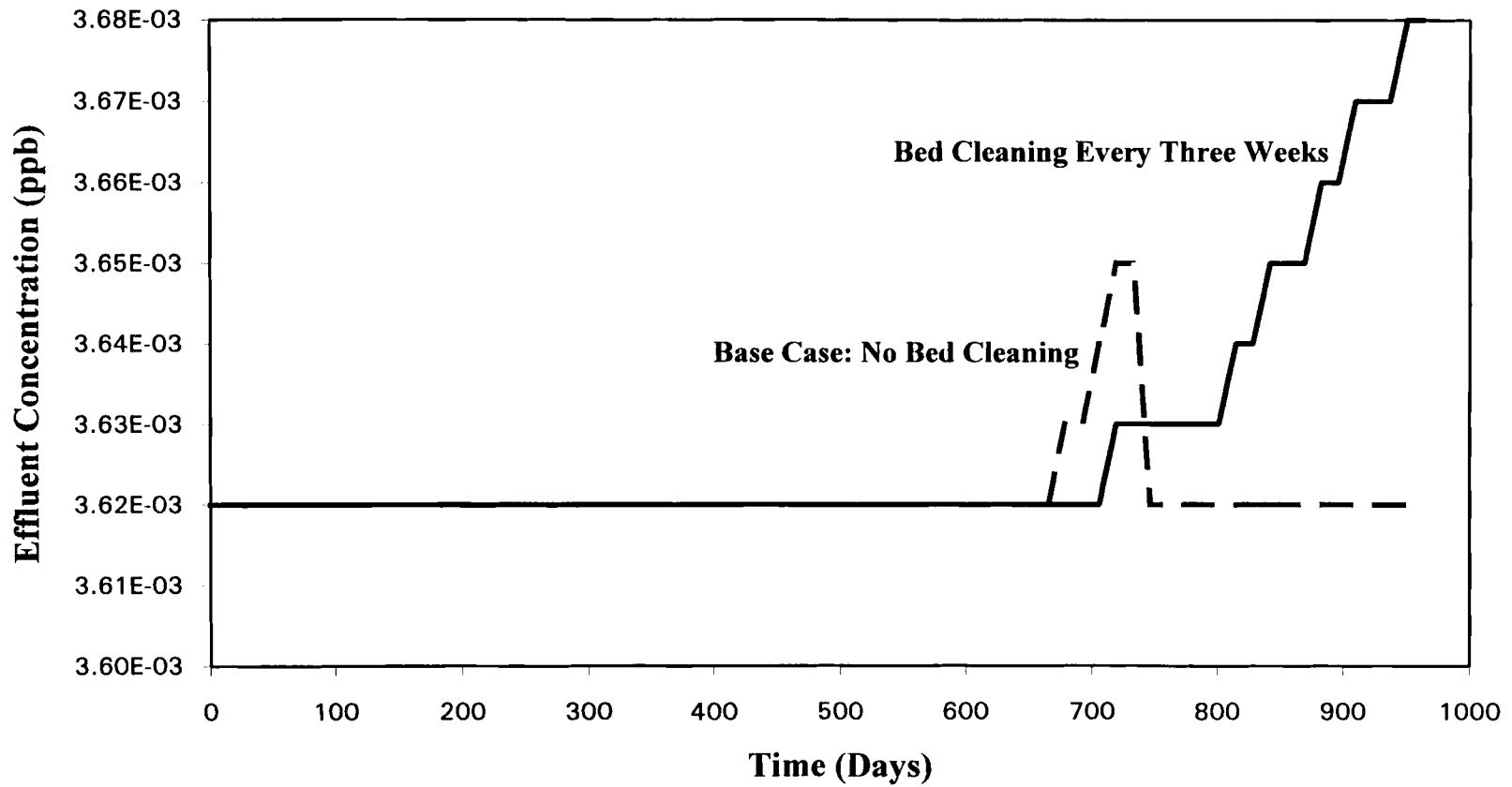


Figure 26. Effect of Bed Cleaning Every Three Weeks on Sulfate Concentration Profile

## BIBLIOGRAPHY

- Bajpai, R. K., Gupta, A. K. and Gopala Rao, M. (1974). Single particle studies of binary and ternary cation exchange kinetics. A.I.Ch.E.J., 20(5), 989-995.
- Bird, R. B., Stewart, W. E., and Lightfoot, E. N. (1960). *Transport phenomena*. John Wiley and Sons.
- Bokx, P. K. de and Boots, H. M. J. (1989). The ion exchange equilibrium. J. Phys. Chem., 93, 8243-8248.
- Bokx, P. K. de and Boots, H. M. J. (1990). The compensating-mixture model for multicomponent systems and its applications to ion exchange. J. Phys. Chem., 94, 6489-6495.
- Breslin, R. A. (1991). Condensate polisher resin optimization recommendations for in-plant tests. Internal report, PP&L.
- Calmon, C. (1986). Recent developments in water treatment by ion exchange. Reactive Polymers, 4, 131-146.
- Charles, N. H. (1988). On the existence of ternary interactions in ion exchange. A.I.Ch.E. J., 34, 702-703.
- Divekar, S. V., Foutch, G. L., and Haub, C. E. (1987). Mixed bed ion exchange at concentrations approaching the dissociation of water. Temperature effects. Ind. Eng. Chem. Res., 26(9), 1906-1909.
- Haub, C. E. and Foutch, G. L. (1986a). Mixed-bed ion exchange at concentrations approaching the dissociation of water 2. Column model applications. Ind. Eng. Chem. Fund., 25, 373-381.
- Haub, C. E. and Foutch, G. L. (1986b). Mixed-bed ion exchange at concentrations approaching the dissociation of water 2. Column model applications. Ind. Eng. Chem. Fund., 25, 381-387.
- Haub, C. E. (1984). M.S. Thesis, Oklahoma State University, Stillwater, OK.

- Helfferrich, F. G. (1967). Multicomponent ion exchange in fixed beds. Ind. Eng. Chem. Fund., 6, 362-364.
- Helfferrich, F. G. (1990). Models and physical Reality in ion-exchange kinetics. Reactive Polymers, 13, 191-194.
- Hogfeldt, E. (1990). A comparison of methods for estimating equilibrium constants in ion exchange. J. Chem. Soc. Dalton Trans., 1627-1628.
- Holloway, J. H., and James, D. B. (1989). Reduction of corrosion products in the condensate/feedwater systems at Susquehanna Steam Electric Station. Internal report, PP&L.
- Horst, J., Holl, W. H., and Eberle, S. H. (1990). Application of the surface complex formation model to the exchange equilibria on the ion exchange resins. Reactive Polymers, 13, 209-231.
- Hwang, Y. L., and F. G. Helfferrich. (1987). Generalized model for multispecies ion exchange kinetics including fast reversible reactions. Reactive Polymers, 5, 237-253.
- Ines, R. T. and Rundberg. R. S. (1987). Determination of selectivity coefficient distributions by deconvolution of ion exchange isotherms. J. Phys. Chem., 91, 5269-5274.
- Kataoka, T. and Yoshida, H. (1988). Kinetics of ion exchange accompanied by neutralization reaction. A.I.Ch.E. J., 34, 1020.
- Katoaka, T., and Yoshida, H. (1979). Ion exchange equilibria in ternary systems. J. Chem. Eng. of Japan, 13(4), 328-330.
- Kitchener, J. A. (1957). Ion exchange resins. John Wiley and Sons, N.Y.
- Kitchener, J. A. (1955). Ion exchange equilibria and kinetics-A critique of the present state of the theory. Ion exchange and its applications. Society of chemical industry.
- Klien, G., Tondeur, D., and Vermeulen, T. (1967). Multicomponent ion exchange in fixed beds. Ind. Eng. Chem. Fund., 6, 339-351.
- Kunin, R. (1960). Elements of ion exchange. Reinhold Publishing Corporation, N.Y.
- Lucas, A. D., Zarca, J., and Canizares, P. (1992). Ion-exchange equilibrium of  $\text{Ca}^{2+}$ ,  $\text{Mg}^{2+}$ ,  $\text{K}^+$ ,  $\text{Na}^+$ , and  $\text{H}^+$  ions on amberlite IR-120: Experimental

determination and theoretical prediction of the ternary and quaternary equilibrium data. Separation Science and Technology, 27(6), 823-841.

- Morgan, D. J. (1991). Modeling of mixed bed ion exchanger performance. Personal communication, PP&L.
- Morgan, D. J. (1991). Information on condensate polishing. Personal communication, PP&L.
- Nachod, F. C., and Schubert, J. (1956). *Ion exchange technology*. Academic Press INC. Publishers, N.Y.
- Noye, J. *Computational techniques for differential equations*. Elsevier Science Publishers B. V. Netherlands, North-Holland Mathematics Studies, 83.
- Perry, R. H., and Green, D. *Perry's Chemical Engineers' Handbook*. Sixth Edition. McGraw-Hill Book Company.
- Ruvarac, L. A., and Petkovic. Djordje M. (1988). Determination of the thermodynamic equilibrium constants of ion exchange processes. J. Chem. Soc. Dalton Trans., 2565-2567.
- Smith, R. P, and Woodburn, T. (1978). Prediction of multicomponent ion exchange equilibria for the ternary system  $\text{SO}_4^{2-}$  -  $\text{NO}_3^-$  - Cl from data of binary systems. A.I.Ch.E. J., 24, 577-587.
- Spires, G. V., Tombaugh, S. R., and Doebler, R. E. (1992). The effects of rubber linings in BWR condensate treatment systems. Internal report, PP&L.
- Takahashi, K., Tsuboi, K., and Takeuchi, H. (1989). Mass transfer across cation exchange membrane. J. Chem. Eng. of Japan, 22(4), 352-357.
- Tondeur, D and Klein. G. (1967). Multicomponent ion exchange in fixed beds. Ind. & Eng. Chem. Fund., 6, 351-361.
- Turner, J. C. R., Church, M. R., Johnson, A. S.W., and Snowdon, C. B. (1966). An experimental verification of the Nernst-Planck model for diffusion in an ion-exchange resin. Chem. Eng. Sci., 21, 317-325.
- Wildhagen, Gloria R. S., Qassim, Raad Y., and Rajagopal, K. (1985). Effective liquid-phase diffusivity in ion exchange. Ind. Eng. Chem. Fund., 24, 423-432.
- Yoshida, H., and Kataoka, T.,(1987). Intraparticle ion exchange mass transfer in ternary system. Ind. Eng. Chem., 26, 1179-1184.

Zecchini, E. J. (1990). Solutions to selected problems in multi-component mixed bed ion exchange modeling. Phd Thesis, 1990, Oklahoma State University.

Zecchini, E. J., and Foutch. G. L (1991). Mixed bed ion-exchange modeling with amine form cation resins. Ind. Eng. Chem. Res., 30, 1896-1892.

## APPENDIXES

## APPENDIX A

### ANION FLUX EXPRESSIONS

The anion resin flux expressions will be derived for ternary divalent exchange (one divalent ion and two univalent ions). The following derivation results from the basic principles of ion exchange using the Nernst-Planck equation. The necessary assumptions and conditions will be applied and explained as appropriate.

Haub et al. (1984) developed a binary film diffusion controlled model for application in mixed bed ion exchange. Zecchini et al (1990) improved the model to address ternary system (univalent system). The current model incorporates various modifications to address divalent ions in a ternary system.

Nernst (1904) introduced a simple model where mass transfer is by diffusion alone and no convective mixing at the surface of the particle. It assumes a static film surrounding the particle which is separated from the completely mixed bulk liquid by a sharp boundary. The model is based on linear extrapolation of the limiting concentration profile at the particle surface, where diffusion alone is effective. In the exchange of ions of different mobilities, however, an electric field arises and causes electric transference. This situation led to the development of the Nernst-Planck equation. Assuming the curvature of the film can be neglected, this expression is:

$$J_i = -D_i \left( \frac{\partial C_i}{\partial r} + \frac{C_i Z_i F}{RT} \frac{\partial \phi}{\partial r} \right)$$

Where  $\phi$  is the electrical potential and  $Z_i$  is the charge or valence on ion  $i$ . This applies to all the species taking part in the exchange process. Pseudo steady state assumption (changes with position are much more important than changes with time) enables the partial differential equations to be replaced by ordinary derivatives and vice versa.

The flux expressions used in the model are based on the film neutralization reaction. Interdiffusion within the film is treated as a quasi-stationary diffusion process across a planar layer or film. This means that the flux across the film adjusts itself rapidly to the changing boundary conditions. Though, both coions and counterions exist in the film, a reasonable assumption for avoiding a complex situation is to assume the flux of coions in the film are negligible. Film neutralization applies to systems with very low concentrations and small particle size.

There are certain conditions that must be satisfied within the film surrounding the anionic resin. These are:

$$\sum Z_i C_i = 0 \quad (\text{electro-neutrality})$$

$$J_{\text{coions}} = 0 \quad (\text{no coion flux into resin}),$$

summation of the fluxes within the film using this expression yields

$$\sum Z_i J_i = 0 \quad (\text{no net current flow})$$

the film is assumed to be very thin and curvature can be neglected. This assumption causes a relaxation in the surface condition to include the whole film as;

$$J_{\text{coions}} = 0 \quad (\text{no coion flux})$$

Applying the above criteria for a six component system with one divalent each in both the cations and anions yields:

$$C_n + C_h + 2C_b = C_c + C_o + 2C_s \quad (\text{electroneutrality}),$$

$$J_n + J_h + 2J_b = J_c + J_o + 2J_s \quad (\text{no net current flow}),$$

$$J_n = J_h = J_b = 0 \quad (\text{anion exchange; no coion flux}),$$



$$J_c = J_o = J_s = 0 \quad (\text{cation exchange; no coion flux})$$

Applying no net coion flux to the Nernst-Planck expression for each of the cation species (anion exchange) yields an expression for electrical potential  $\phi$  as:

$$\frac{d\phi}{dr} = -\frac{RT}{FC_n} \frac{dC_n}{dr} = -\frac{RT}{FC_h} \frac{dC_h}{dr} = -\frac{RT}{2FC_b} \frac{dC_b}{dr} \quad (\text{eq. A-1})$$

Now differentiating the electroneutrality condition with respect to  $r$  yields:

$$\frac{dC_n}{dr} + \frac{dC_h}{dr} + 2 \frac{dC_b}{dr} = \frac{dC_c}{dr} + \frac{dC_o}{dr} + 2 \frac{dC_s}{dr} \quad (\text{eq. A-2})$$

Now solving for each cation concentration gradient in terms of sodium gradient ( $C_n$ ) and inserting into the above equation (eq. A-2) yields:

$$\frac{dC_n}{dr} + \frac{C_h}{C_n} \frac{dC_n}{dr} + 4 \frac{C_b}{C_n} \frac{dC_n}{dr} = \frac{dC_c}{dr} + \frac{dC_o}{dr} + 2 \frac{dC_s}{dr} \quad (\text{eq. A-3})$$

The left hand side can be written as:

$$\frac{1}{C_n} \frac{dC_n}{dr} (C_n + C_h + 4C_b) = \frac{dC_c}{dr} + \frac{dC_o}{dr} + 2 \frac{dC_s}{dr} \quad (\text{eq. A-4})$$

Now using the condition of electroneutrality (eq. A-1) with the above term (eq. A-4) gives us an expression in terms of coions as:

$$\frac{1}{C_n} \frac{dC_n}{dr} = \frac{1}{(C_c + C_o + 2C_s)} \left( \frac{dC_c}{dr} + \frac{dC_o}{dr} + 2 \frac{dC_s}{dr} \right) \quad (\text{eq. A-5})$$

eq. A-5 can now be used in eq. A-1 to yield an expression for the electrical potential gradient;

$$\frac{d\phi}{dr} = -\frac{RT}{F} \left( \frac{1}{C_c + C_o + 2C_s} \right) \left( \frac{dC_c}{dr} + \frac{dC_o}{dr} + 2 \frac{dC_s}{dr} \right) \quad (\text{eq. A-6})$$

eq. A-6 allows to remove  $\phi$  from the flux expressions for chloride, sulfate, and hydroxide. The fluxes become:

$$J_c = -D_c \left( \frac{dC_c}{dr} + \left( \frac{C_c}{C_c + C_o + 2C_s} \right) \left( \frac{dC_c}{dr} + \frac{dC_o}{dr} + 2 \frac{dC_s}{dr} \right) \right) \quad (\text{eq. A-7})$$

$$J_o = -D_o \left( \frac{dC_o}{dr} + \left( \frac{C_o}{C_c + C_o + 2C_s} \right) \left( \frac{dC_c}{dr} + \frac{dC_o}{dr} + 2 \frac{dC_s}{dr} \right) \right) \quad (\text{eq. A-8})$$

$$J_s = -D_s \left( \frac{dC_s}{dr} + \left( \frac{2C_s}{C_c + C_o + 2C_s} \right) \left( \frac{dC_c}{dr} + \frac{dC_o}{dr} + 2 \frac{dC_s}{dr} \right) \right) \quad (\text{eq. A-9})$$

Using the no net current criteria with no coion flux we get:

$$\begin{aligned} & D_c \left( \frac{dC_c}{dr} + \left( \frac{C_c}{C_c + C_o + 2C_s} \right) \left( \frac{dC_c}{dr} + \frac{dC_o}{dr} + 2 \frac{dC_s}{dr} \right) \right) + \\ & D_o \left( \frac{dC_o}{dr} + \left( \frac{C_o}{C_c + C_o + 2C_s} \right) \left( \frac{dC_c}{dr} + \frac{dC_o}{dr} + 2 \frac{dC_s}{dr} \right) \right) + \\ & D_s \left( \frac{dC_s}{dr} + \left( \frac{2C_s}{C_c + C_o + 2C_s} \right) \left( \frac{dC_c}{dr} + \frac{dC_o}{dr} + 2 \frac{dC_s}{dr} \right) \right) = 0 \end{aligned} \quad (\text{eq. A-10})$$

collecting the terms and multiplying the above equation by  $(C_c + C_o + 2C_s)$  yields:

$$\begin{aligned} & (2D_c C_c + D_c C_o + 2D_c C_s + D_o C_o + 4D_s C_s) \frac{dC_c}{dr} + \\ & (D_c C_c + D_o C_c + 2D_o C_o + 2D_o C_s + 4D_s C_s) \frac{dC_o}{dr} + \end{aligned}$$

$$(2D_c C_c + D_o C_o + 2D_s C_c + 2D_s C_o + 12D_s C_s) \frac{dC_s}{dr} = 0 \quad (\text{eq. A-11})$$

eq. A-11 can be written as:

$$\begin{aligned} & \frac{d}{dr} (D_c C_c^2 + (2D_c + 2D_o) C_o C_c + (4D_c + 6D_s) C_s C_c + D_o C_o^2 \\ & + (4D_o + 6D_s) C_o C_s + 6D_s C_s^2) = 0 \end{aligned} \quad (\text{eq. A-12})$$

The term in the parentheses is a constant and represents the bulk phase parameters.

eq. A-11 can be represented as:

$$\frac{dC_o}{dr} = -\frac{1}{A} \left( B \frac{dC_c}{dr} + C \frac{dC_s}{dr} \right)$$

where

$$A = 2D_c C_c + D_c C_o + 2D_c C_s + D_o C_o + 4D_s C_s$$

$$B = D_c C_c + D_o C_c + 2D_o C_o + 2D_o C_s + 4D_s C_s +$$

$$C = 2D_c C_c + 2D_o C_o + 2D_s C_c + 2D_s C_o + 12D_s C_s$$

Using the pseudo component technique let's define

$$C_p = C_h + C_n + C_b = \sum C_i$$

applying the Nernst-Planck equation for pseudo component equation:

$$J_p = -D_p \left( \frac{dC_p}{dr} + Z \frac{FC_p}{RT} \nabla \phi \right)$$

The continuity equation within the film is

$$\frac{dC_i}{dt} + UC_i + \nabla J_i = 0$$

when the reactions are restricted to bulk phase neutralization, changes in flux w.r.t. radial position is negligible i.e.,:

$$\frac{dJ_i}{dr} = 0$$

i.e.,

$$\begin{aligned} & \frac{d^2 C_o}{dr^2} + \frac{d^2 C_c}{dr^2} + \frac{d^2 C_s}{dr^2} + \frac{d^2 C_p}{dr^2} \\ & + \frac{F}{RT} (\nabla \cdot ((C_p - C_o - C_c - C_s) \frac{d\phi}{dr})) = 0 \end{aligned} \quad (\text{eq. A-13})$$

The term in the parentheses is the charge balance i.e., equal to zero. eq. A-13 can now be written as:

$$\frac{d^2}{dr^2} (C_o + C_c + C_s) + \frac{d^2 C_p}{dr^2} = 0 \quad (\text{eq. A-14})$$

From the charge balance, eq. A-14 can be written as:

$$2 \frac{d^2 C_p}{dr^2} = 0$$

$$\text{i.e., } \frac{dC_p}{dr} = K_1 \text{ and } C_p = K_1 r + K_2 \quad (\text{eq. A-15})$$

a linear profile for coion concentration within the film. Boundary conditions are applied as:

$$C_p = C_p^* @ r = 0$$

$$C_p = C_p^o @ r = \delta$$

From the boundary condition limitation, constants  $K_1$  and  $K_2$  are found and replaced as:

$$C_p = \frac{C_p^o - C_p^*}{\delta} r + C_p^*$$

no coion flux implies that

$$\frac{d\phi}{dr} = -\frac{RT}{FC_p} \frac{dC_p}{dr}$$

from eq. A-15,

$$\frac{dC_p}{dr} = K_1$$

Substituting this in the flux expression for pseudo-component we get;

$$-J_i = D_i \left( \frac{dC_i}{dr} - Z_i \frac{C_i}{C_p} K_1 \right) \quad (\text{eq. A-16})$$

$$\text{let } y_i = \frac{C_i}{C_p}$$

Differentiating the above equation we get

$$-J_i = D_i \left( C_p \frac{dy_i}{dr} + y_i K_1 - Z_i y_i K_1 \right)$$

i.e.,

$$-J_i = D_i \left( C_p \frac{dy_i}{dr} + (1 - Z_i) y_i K_1 \right) \quad (\text{eq. A-17})$$

$J_i$  is a constant as shown by earlier applied continuity equation. Thus eq. A-17 can be separated and written in integral form to obtain an expression for the flux.

$$\frac{-J_i}{D_i} - (1 - Z_i) y_i K_1 = C_p \frac{dy_i}{dr} \quad \text{but } C_p = K_1 r + K_2$$

$$-\int_0^{\delta} \frac{dr}{(K_1 r + K_2)} = \int_{y_i^*}^{y_i^0} \frac{dy_i}{(J_i / D_i + (1 - Z_i) y_i K_i)}$$

or:

$$-2 \ln (K_1 r + K_2) \Big|_0^{\delta} = \ln (J_i / D_i + (1 - Z_i) K_i y_i) \Big|_{y_i^*}^{y_i^0}$$

Evaluating within the limits and exponentiating both sides yields:

$$\left( \frac{K_1 \delta + K_2}{K_2} \right)^{-2} = \frac{J_i / D_i + (1 - Z_i) K_i y_i^0}{J_i / D_i + (1 - Z_i) K_i y_i^*} \quad (\text{eq. A-18})$$

$$\text{LHS} = \left( \frac{C_p^*}{C_p^0} \right)^2$$

eq. A-18 can be written as:

$$\frac{J_i}{D_i} + (1 - Z_i) K_i y_i^* \left( \frac{C_p^*}{C_p^0} \right)^2 = \frac{J_i}{D_i} + (1 - Z_i) K_i y_i^0$$

$$J_i = (1 - Z_i) D_i K_i \left( \frac{y_i^0 - y_i^* \left( \frac{C_p^*}{C_p^0} \right)^2}{\left( \frac{C_p^*}{C_p^0} \right)^2 - 1} \right)$$

$$-J_i \delta = (1 - Z_i) D_i (C_p^* - C_p^0) \left( \frac{C_p^0 y_i^0 - y_i^* C_p^{*2}}{C_p^{*2} - C_p^0} \right)$$

Remembering the original definition of  $y_i$  and converting to fractional concentrations:

or:

$$-J_i \delta = (1 - Z_i) D_i \left( \frac{1 - \left(\frac{C_p^*}{C_o^*}\right) \left(\frac{C_i^*}{C_i^o}\right)}{1 + \left(\frac{C_p^*}{C_o^*}\right) \left(\frac{1}{C_i^o}\right)} \right)$$

The flux expression for any counter ion  $i$  is specified by the above expression. This expression can be used with the static film model rate expression to determine the effective diffusivity of all the species taking part in the exchanging process.

## APPENDIX B

### PARTICLE RATES

The flux expressions derived in the previous appendixes were developed so that the particle rates could be determined. The rate of change of resin phase compositions require that a model for the liquid film surrounding the resin bead be specified. The static film model will be used in preference to other available models due to its simple but accurate form and the low concentrations that this model deals with.

The static film model results in an expression of the form:

$$\frac{d \langle C_i \rangle}{dt} = K_i' a_s (C_i^o - C_i^*) \quad (\text{eq. B-1})$$

The driving force for exchange process is a simple linear relation. However, the non-linearity due to mass transfer coefficient is introduced into the relation as:

$$K_i' = D_{ei} / \delta \quad (\text{eq. B-2})$$

$D_{ei}$  is used instead of  $D_i$  because in multicomponent exchange the value for the effective diffusivity is species dependent. The rate of exchange is related to the flux of the species by:

$$\frac{d \langle C_i \rangle}{dt} = K_i' a_s (C_i^o - C_i^*) = -J_i a_s \quad (\text{eq. B-3})$$

The resin phase concentration  $\langle C_i \rangle$  can be represented as:



$$\langle C_i \rangle = y_i Q,$$

where  $Q$  is the capacity of the resin and  $y_i$  is the fraction of species in the resin.

Substituting the above expression in the rate of exchange eq,

$$\frac{dy_i}{dt} = \frac{K_i'}{Q} a_s (C_i^o - C_i^*) = -\frac{J_i}{Q} a_s \quad (\text{eq. B-4})$$

From eq. B-2 and eq. B-4, an expression for the effective diffusivity can be found as:

$$D_{ei} = -\frac{J_i \delta}{(C_i^o - C_i^*)} \quad (\text{eq. B-5})$$

This expression can be combined with the relation for  $R_i$  as defined by Pan and David (1978):

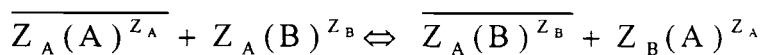
$$R_i = \left( \frac{D_{ei}}{D_i} \right)^{2/3} = \frac{K_i'}{K_i} \quad (\text{eq. B-6})$$

The right hand portion of eq. B-6 involves the calculation of the non-ionic mass transfer coefficient which is used in the rate expression. The correlation's of Carberry (1960) and Kataoka (1973) can be used to determine the non-ionic mass transfer coefficients based on the particle Reynolds number and species Schmidt number. The final rate expression reduces to

$$\frac{dy_i}{dt} = K_i R_i \frac{a_s}{Q} (C_i^o - C_i^*)$$

where  $K_i$  is the non-ionic mass transfer coefficient for species  $i$ . Interfacial concentration  $C_i^*$  is the only unknown variable. The use of selectivity coefficient allows for the determination of the interfacial concentration.

A relation for the three interfacial concentrations in a ternary system could be obtained from the selectivity coefficients. For a general reaction



Selectivity coefficients are defined as:

$$K_{A^B} = \frac{(\overline{C_B})^{Z_A} (C_A)^{Z_B}}{(\overline{C_A})^{Z_B} (C_B)^{Z_A}} \quad (\text{eq. B-7})$$

The fraction of species on the resin for a ternary anion exchange system is given by:

$$y_c + y_o + y_s = 0$$

From the definition of selectivity coefficient, the following expressions result as:

$$K_{o^c} = \frac{y_c C_o^*}{y_o C_c^*} \quad (\text{eq. B-8})$$

$$K_{o^s} = \frac{y_s C_o^{*2}}{y_o^2 C_s^*} Q \quad (\text{eq. B-9})$$

$$K_{c^s} = \frac{y_s C_c^{*2}}{y_c^2 C_s^*} Q \quad (\text{eq. B-10})$$

The film concentration relation can be applied to determine the interfacial concentrations (eq. A-12) :

$$\begin{aligned} & (D_c C_c^{*2} + (2D_c + 2D_o)C_o^* C_c^* + (4D_c + 6D_s)C_s^* C_c^* + D_o C_o^{*2} \\ & + (4D_o + 6D_s)C_o^* C_s^* + 6D_s C_s^{*2}) = \\ & (D_c C_c^{o2} + (2D_c + 2D_o)C_o^o C_c^o + (4D_c + 6D_s)C_s^o C_c^o + D_o C_o^{o2} \\ & + (4D_o + 6D_s)C_o^o C_s^o + 6D_s C_s^{o2}) = \text{RHS} \end{aligned}$$

This eq represents the anion exchange process between bulk and film taking into account the basic principles of ion exchange. From eq. B-8 - eq B-10,  $C_o^*$  and  $C_c^*$  can be eliminated and an expression for sulfate interfacial concentration can be found as:

$$AC_s^{*2} + BC_s^{*3/2} + EC_s^* - RHS = 0$$

where

$$A = 6D_s$$

$$B = \frac{((4D_c + 6D_s)K_c^{s/2} y_c + (4D_o + 6D_s)K_o^{s/2} y_o)}{y_s^{1/2} Q^{1/2}}$$

$$E = \frac{(D_c K_c^s y_c^2 + (2D_c + 2D_o)K_o^{s/2} K_c^{s/2} y_o y_c + D_o y_o^2 K_o^s)}{y_s Q}$$

Interfacial concentrations for chloride and hydroxide can be found from the definition of selectivity coefficients as:

$$C_o^* = \frac{y_o \sqrt{K_o^s}}{y_s Q} C_s^*$$

$$C_c^* = \frac{y_c \sqrt{K_c^s}}{y_s Q} C_s^*$$

The above expressions can now be used with the particle rates to describe the exchange process.

## APPENDIX C

### COLUMN MATERIAL BALANCES

Material balance equations around the column are required for determining the effluent concentration profiles. These material balances will use previously determined rate expressions for individual species. The overall column material balance for species  $i$  is given as:

$$\frac{u_s}{\epsilon} \frac{\partial C_i}{\partial Z} + \frac{\partial C_i}{\partial t} + \frac{(1-\epsilon)}{\epsilon} \frac{\partial q_i}{\partial t} = 0 \quad (\text{eq. C-1})$$

where :

$u_s$  = superficial velocity, and  $\epsilon$  = void fraction.

This expression can be simplified by using dimensionless variables in time and distance.

The dimensionless expressions are expressed as:

$$\tau = \frac{K_i C_T^f}{d_p Q} \left( t - \frac{\epsilon Z}{u_s} \right) \quad (\text{eq. C-2})$$

and,

$$\xi = \frac{K_i(1-\epsilon)}{u_s} \frac{Z}{d_p} \quad (\text{eq. C-3})$$

$K_i$  is the non-ionic mass transfer coefficient for species  $i$ ,  $d_p$  is the particle diameter,  $Q$  is the resin capacity and  $C_T^f$  is the total cationic feed concentration. The above expressions are differentiated with respect to time and distance respectively to yield:

$$\frac{\partial \tau}{\partial t} = \frac{K_i C_T^f}{d_p Q}, \quad \frac{\partial \tau}{\partial Z} = \frac{K_i C_T^f \epsilon}{d_p Q u_s},$$

$$\frac{\partial \xi}{\partial t} = 0 \quad \text{and} \quad \frac{\partial \xi}{\partial Z} = \frac{K_i C_T^f \epsilon}{d_p Q u_s}$$

Now using the chain rule the original derivatives are expressed as:

$$\frac{\partial C_i}{\partial Z} = \frac{\partial C_i}{\partial \xi} \left( \frac{\partial \xi}{\partial Z} \right) + \frac{\partial C_i}{\partial \tau} \left( \frac{\partial \tau}{\partial Z} \right) = \frac{K_i (1 - \epsilon)}{u_s d_p} \left( \frac{\partial C_i}{\partial \xi} \right) - \frac{K_i C_T^f \epsilon}{d_p u_s Q} \left( \frac{\partial C_i}{\partial \tau} \right)$$

$$\frac{\partial q_i}{\partial t} = \frac{\partial q_i}{\partial \tau} \left( \frac{\partial \tau}{\partial t} \right) + \frac{\partial q_i}{\partial \xi} \left( \frac{\partial \xi}{\partial t} \right) = \frac{K_i C_T^f}{d_p Q} \frac{\partial q_i}{\partial \tau} + 0 \frac{\partial q_i}{\partial \xi}$$

Replacing these into the material balance yields:

$$\frac{\partial C_i}{\partial \xi} + \frac{C_T^f}{Q} \frac{\partial q_i}{\partial \tau} = 0$$

This expression is easier to handle. Introducing the fractions in liquid phase and resin phase as:

$$x_i = C_i / C_T^f, \quad \text{and} \quad q_i = Q y_i$$

This substitution into the material balance equation yields:

$$\frac{\partial x_i}{\partial \xi} + \frac{\partial y_i}{\partial \tau} = 0$$

In the current code, chloride is selected as the reference species. Since all the material balance is to be solved using same steps in  $\tau$  and  $\xi$ , expressions for the base species result as:

$$\tau = \tau_c = \frac{K_c C_T^f}{d_{pa} Q_a} \left( t - \frac{\epsilon Z}{u_s} \right), \text{ and } \xi = \xi_c = \frac{K_c (1 - \epsilon) Z}{u_s d_{pa}}$$

This expression is easier to handle. Introducing the fractions in liquid phase and resin phase where the additional subscript a denotes the anion resin. The corresponding change in all the species with respect to the base species is:

$$\frac{\partial x_n}{\partial \xi} = \frac{\partial x_n}{\partial \xi_c} \left( \frac{\partial \xi_c}{\partial \xi} \right) = \frac{K_c}{K_n} \frac{d_{pc}}{d_{pa}} \frac{\partial x_n}{\partial x_c},$$

$$\frac{\partial y_n}{\partial \tau} = \frac{\partial y_n}{\partial \tau_c} \left( \frac{\partial \tau_c}{\partial \tau} \right) = \frac{K_c}{K_n} \frac{d_{pc}}{d_{pa}} \frac{Q_c}{Q_a} \frac{\partial y_n}{\partial \tau_c},$$

$$\frac{\partial x_b}{\partial \xi} = \frac{\partial x_b}{\partial \xi_c} \left( \frac{\partial \xi_c}{\partial \xi} \right) = \frac{K_c}{K_b} \frac{d_{pc}}{d_{pa}} \frac{\partial x_b}{\partial x_c},$$

$$\frac{\partial y_b}{\partial \tau} = \frac{\partial y_b}{\partial \tau_c} \left( \frac{\partial \tau_c}{\partial \tau} \right) = \frac{K_c}{K_b} \frac{d_{pc}}{d_{pa}} \frac{Q_c}{Q_a} \frac{\partial y_b}{\partial \tau_c}, \text{ and}$$

$$\frac{\partial x_s}{\partial \xi} = \frac{\partial x_s}{\partial \xi_c} \left( \frac{\partial \xi_c}{\partial \xi} \right) = \frac{K_c}{K_s} \frac{\partial x_s}{\partial x_c}$$

$$\frac{\partial y_s}{\partial \tau} = \frac{\partial y_s}{\partial \tau_c} \left( \frac{\partial \tau_c}{\partial \tau} \right) = \frac{K_c}{K_s} \frac{\partial y_s}{\partial \tau_c}.$$

Replacing into the general material balance equation and introducing the cation (FCR) and anion (FCA) resin volume fractions within the bed:

$$\frac{\partial x_n}{\partial \xi_c} + \text{FCR} \frac{\partial y_n}{\partial y_c} = 0$$

$$\frac{\partial x_b}{\partial \xi_c} + \text{FCR} \frac{\partial y_b}{\partial y_c} = 0$$

$$\frac{\partial x_c}{\partial \xi_c} + \text{FCA} \frac{\partial y_c}{\partial y_c} = 0$$

$$\frac{\partial x_s}{\partial \xi_c} + \text{FCA} \frac{\partial y_s}{\partial y_c} = 0$$

The rate equations that were developed earlier need to be modified to incorporate the dimensionless variables that have been introduced. This involves changing from  $t$  to  $\tau_c$  as the basis for the individual species equations.

$$\frac{\partial y_i}{\partial t} = K_i \left( \frac{D_{ei}}{D_i} \right)^{2/3} \frac{a_s C_i^o}{Q} \left( 1 - \frac{C_i^*}{C_i^o} \right)$$

Changing from  $t$  to  $\tau$  yields:

$$\frac{\partial y_i}{\partial \tau} = d_p a_s R_i \left( \frac{C_i^o}{C_f^*} - \frac{C_i^*}{C_f^*} \right)$$

where  $R_i$  is equal to the two thirds power of the diffusivity ratio. It is important to note that the product of  $d_p a_s$  is equal to six. so:

$$\frac{\partial y_i}{\partial \tau} = 6 R_i \left( \frac{C_i^o}{C_T} - \frac{C_i^*}{C_T} \right)$$

again changing the basis from  $\tau$  to  $\tau_x$  four different equations yields

$$\frac{\partial y_c}{\partial \tau_c} = 6 R_c (x_c^o - x_c^*)$$

$$\frac{\partial y_s}{\partial \tau_c} = 9 R_s \frac{K_s}{K_c} (x_s^o - x_s^*)$$

$$\frac{\partial y_n}{\partial \tau_c} = 6 R_n \frac{K_n}{K_c} \frac{d_{pa}}{d_{pc}} \frac{Q_a}{Q_c} (x_n^o - x_n^*)$$

$$\frac{\partial y_b}{\partial \tau_c} = 9 R_b \frac{K_b}{K_c} \frac{d_{pa}}{d_{pc}} \frac{Q_a}{Q_c} (x_b^o - x_b^*)$$

These represent the rate equations that describe the exchange process. These are combined with the material balance equations and solved simultaneously to determine the effluent concentration profiles of each exchanging species. The numerical methods used to solve them are described in Appendix D.



## APPENDIX D

### NUMERICAL METHODS

The material balance equations outlined in Appendix C for all the exchanging species are a system of partial differential equations that need to be solved for finding the concentration profile history for MBIE column. Constant time and distance steps are used to calculate the particle loading and bulk phase liquid concentrations down the column. As seen in Appendix C, rate equation in general form is represented as

$$\frac{\partial x}{\partial \xi} = -\frac{\partial y}{\partial \tau} = \text{Rate} = f(y) \quad (\text{eq. D-1})$$

These system of partial differential equations are solved as ordinary differential equations keeping one of the parameters as constant while the other is evaluated. This involves the application of any numerical method using initial value problems.

The application of numerical methods for the divalent model is classified into two categories based upon its function:

- 1) Predicting liquid phase concentrations using the distance parameter along the column.
- 2) Predicting particle loading using the time parameter.

The model is solved for effluent concentrations using backward differentiation formulas for stiff initial value problems. Backward Euler method of first order (also called Adams-Moulton method) is used for predicting particle loading.

Backward differentiation formulas are the most common method of solution for stiff systems. They are linear multi step methods of the form

$$\sum_{j=0}^k \alpha_j y_{n+j} = h \beta_k f_{n+k}$$

where

$$\alpha_k = 1, \alpha_0 \neq 0 \text{ and } \beta_k \neq 0$$

Their order, is equal to step number  $k$ , and for orders of one to six they are stiffly stable. The first order method is the backward Euler method, and it, together with the second and third order methods, is absolutely stable in the right half plane not particularly far from the origin. The higher-order methods do not suffer this problem, but instead are not absolutely stable in a region of the left half-plane near the imaginary axis.

The backward differentiation formulas are implemented in the same variable order variable-step manner as the Adam's formulas. A  $p^{\text{th}}$  order predictor of the form

$$y_{n+k}^0 = h \beta_k^* f_{n+k-1} - \sum_{j=0}^{k-1} \alpha_j^* y_{n+j}$$

is used to provide the initial estimates for the corrector method described above. The model cannot use this method for the following reasons.

- 1) The predictor-corrector loop involves iterative procedure and this changes the interfacial concentration, which is controlled by kinetics of ion-exchange.
- 2) An iterative procedure on the interfacial concentration involves the already imposed Newton Raphson iterative method for finding interfacial concentration and this method may not converge at all.

Hence as a first estimate a fourth order Runge Kutta method is used in combination with the backward differentiation predictor in the model to predict the liquid

phase concentrations as a function of the bed depth (and consequently effluent concentrations).

Table D-I

Coefficients of backward differentiation formulas (Noye, J., 1984).

Order	$\beta_k$	$\alpha_0$	$\alpha_1$	$\alpha_2$	$\alpha_3$	$\alpha_4$	$\alpha_5$	$\alpha_6$
1	1	-1	1					
2	2/3	1/3	-4/3	1				
3	6/11	-2/11	9/11	-18/11	1			
4	12/25	3/25	-16/25	36/25	-48/25	1		
5	60/137	-12/137	75/137	-200/137	300/137	-300/137	1	
6	60/147	10/147	-72/147	225/147	-400/147	450/147	-360/147	1

## APPENDIX E

### INLET CONDITIONS AND MODEL PARAMETER VALUES

The system parameters used for different test conditions are summarized below. The values are based on the data provided by Pennsylvania Power & Light (PPL).

#### **Base Case Parameters:**

Initial Particle loading:

Sodium: 0.01,

Calcium: 0.1,

Chloride: 0.01,

Sulfate: 0.2,

Flow rate = 42 gallons per minute,

Temperature = 140°F,

Cation to Anion resin ratio = 1:1,

Cation Particle Diameter = 0.08 cm,

Anion Particle Diameter = 0.06 cm,

Void fraction of the bed = 0.35

Cation resin capacity = 2.1 meq/ml

Anion resin capacity = 1.0 meq/ml

Test Runs:

Temperatures: 120°F and 90°F,

Flow rates: 50 gpm and 57 gpm,

Resin ratios: Cation/Anion = 0.4:0.6; Cation/Anion = 0.6:0.4

Particle size: Cation = 0.065 cm ; Anion = 0.055 cm

Mass Transfer Coefficients: Anion mass transfer coefficients were reduced by half in the program to compare the effluent profiles with the base case results.

Influent concentrations: Sulfate concentration was 3.3 ppb. Sodium feed concentration was 1:1 ppb (  $\text{SO}_4^{2-}/3$  ) and cation equivalent ratios of 0.2  $\text{Na}^+$  : 0.8  $\text{Ca}^{+2}$  were used.

Chlorine was adjusted to meet electroneutrality criteria. Changes in the system parameters affected the electroneutrality and consequently changes in the influent concentrations were done for the affected run. Table E-1 shows the numerical values in the concentrations of the exchanging species which were affected due to the changes in system parameters.

Table E-1  
Values adjusted for Electroneutrality Criteria

Run Type	Sodium (meq/ml)	Calcium (meq/ml)	Chloride (meq/ml)	Sulfate (meq/ml)	pH
Base Case	0.229E-7	0.917E-7	0.575E-7	0.687E-7	6.50
Temperature at 32.2° C	0.229E-7	0.917E-7	0.458E-7	0.687E-7	6.88
Temperature at 48.9° C	0.229E-7	0.917E-7	0.458E-7	0.687E-7	6.64

APPENDIX F  
COMPUTER CODE FOR CHAPTER III

THIS PROGRAM IS USED FOR PREDICTING THE EFFLUENT  
 CONCENTRATIONS FOR DIVALENT SPECIES.  
 MULTIVALENT TERNARY ION-EXCHANGE CODE (DIVALENT MODEL)  
 EMPHASIS ON SULFATE PREDICTIONS INCORPORATING THE  
 DESULPHONATION OF STRONGLY ACIDIC CATION EXCHANGE  
 RESIN.

SYSTEM : TERNARY SYSTEM

PARTICIPATING IONS:

CATIONS :	SODIUM (N)	ANIONS:	CHLORIDE(C)
	CALCIUM(B)		SULFATE (S)
	HYDROGEN(H)		HYDROXIDE(O)

IMPLICIT INTEGER (I-N), REAL\*8 (A-H,O-Z)  
 REAL\*8 KLN, YNC(4,5000),XNC(4,5000),YBC(4,5000),KLS,  
 1 RATN(4,5000),RATC(4,5000),XSA(4,5000),KLC,KLB,  
 2 YCA(4,5000),XCA(4,5000),YSA(4,5000),RATB(4,5000),  
 3 RATS(4,5000),RATEN,RATEC,XBC(4,5000),RATEB, RATES

\*

\* Correlations-kataoka & carberry:

\*

$$F1(R,S) = 1.15 * VS / (VD * (S^{2/3}) * (R^{0.5}))$$

$$F2(R,S) = 1.85 * VS * ((VD / (1 - VD))^{1/3}) /$$

$$1 (VD * (S^{2/3}) * (R^{2/3}))$$

\*

\* READING THE DATA

\*

```

OPEN(UNIT=9,FILE='s.d',STATUS = 'UNKNOWN')
READ(9,*)KPBK, KPPR, TIME
READ(9,*)YNO, YCO, YBO, YSO
READ(9,*)PDC, PDA, VD
READ(9,*)FR, DIA, CHT
READ(9,*)TAU, XI, FCR, TMP
READ(9,*)DEN, QC, QA, FAR
READ(9,*)TKSO, TKSC, TKCO, TKCS
READ(9,*)TKNH, TKNB, TKBN, TKBH
READ(9,*)CNF,CBF,CCF,CSF,PH

```

c-----

```

WRITE (6,10)
WRITE (6,11)
WRITE (6,12) YNO,YSO

```

WRITE (6,13) PDC,VD  
 WRITE (6,14) QC,QA

C-----

-----

\*

\* CALCULATIONS OF DIFFUSION COEFFICIENTS AND NON IONIC MASS  
 \* TRANSFER COEFFICIENTS

\*

---

CP = 1.43123+TMP\*(0.000127065\*TMP-0.0241537  
 ALOGKW = 4470.99/(TMP+273.15)-6.0875+0.01706\*(TMP+273.15)  
 DISS = 10\*\*(-ALOGKW)  
 CHII = ((10.)\*\*(-PH))  
 COII = DISS/CHII  
 CFCAT = CNF + CBF + CHII  
 CFANI = CCF + CSF + COII  
 IF(ABS(CFCAT-CFANI).LE.(CFCAT/10000))GO TO 446  
 IF(CFCAT.GT.CFANI) THEN  
 WRITE(\*,444)  
 444 FORMAT('TOTAL CATIONS IS GREATER THAN TOTAL ANIONS.')

GO TO 448  
 ELSE  
 WRITE(\*,447)  
 447 FORMAT(' TOTAL ANIONS IS GREATER THAN TOTAL CATIONS.')

ENDIF  
 448 WRITE(\*,445)COII,CHII  
 445 FORMAT(' COII = ',E12.5,'CHII = ',E12.5)  
 446 CONTINUE  
 IF(CFCAT.GE.CFANI) THEN  
 CF = CFCAT  
 ELSE  
 CF = CFANI  
 ENDIF  
 WRITE (6,15) CF,FR,DIA,CHT  
 RTF = (8.931D-10)\*(TMP+273.16)  
 DN = RTF\*(23.00498+1.06416\*TMP+0.0033196\*TMP\*TMP)  
 DO = RTF\*(104.74113+3.807544\*TMP)  
 DC = RTF\*(39.6493+1.39176\*TMP+0.0033196\*TMP\*TMP)  
 DH = RTF\*(221.7134+5.52964\*TMP-0.014445\*TMP\*TMP)  
 DS = RTF\*(2.079\*TMP+35.76)/2.  
 DB = RTF\*(1.575\*TMP+23.27)/2.  
 AREA = 3.1415927\*(DIA\*\*2)/4.  
 VS = FR/AREA  
 REC = PDC\*100.\*VS\*DEN/((1.-VD)\*CP)      !REYNOLD'S NUMBER  
 REA = PDA\*100.\*VS\*DEN/((1.-VD)\*CP)



```

SCN = (CP/100.)/DEN/DN
SCA = (CP/100.)/DEN/DC
SSA = (CP/100.)/DEN/DS
SSB=(CP/100.)/DEN/DB
  IF (REC.LT.20.) THEN
    KLN = F2(REC,SCN)
    KLB = F2(REC,SSB)
  ELSE
    KLN = F1(REC,SCN)
    KLB = F1(REC,SSB)
  ENDIF
  IF (REA.LT.20.) THEN
    KLC = F2(REA,SCA)
    KLS = F2(REA,SSA)
  ELSE
    KLC = F1(REA,SCA)
    KLS = F1(REA,SSA)
  ENDIF

```

```

*
* -----
* CALCULATE TOTAL NUMBER OF STEPS IN DISTANCE (NT) DOWN
* COLUMN:SLICES
*
* -----

```

```

      CHTD = KLC*(1.-VD)*CHT/(VS*PDA)    !distance dimensionless
      NT = CHTD/XI

```

```

*
* -----
* PRINT CALCULATED PARAMETERS
*
* -----

```

```

WRITE (6,16) DN,DS,DH
WRITE (6,117)DC,DB,DO
WRITE (6,17) CP,DEN.TMP
WRITE (6,18)
WRITE (6,19)
WRITE (6,20)
WRITE (6,21) TAU,XI,NT
WRITE (6,22) REC,KLN
WRITE (6,88) KLB,KLC
WRITE (6,*)'SULFATE COEFFICIENT : ',KLS
WRITE (6,23) VS

```

```

*
* -----
* SET INITIAL RESIN LOADING THROUGHOUT THE ENTIRE COLUMN

```

\*  

---

```

MT = NT + 1
DO 100 M=1,MT
YNC(1,M)=YNO
YBC(1,M)=YBO
YCA(1,M)=YCO
YSA(1,M)=YSO

```

100 CONTINUE

\*  

---

```

* CALCULATE DIMENSIONLESS PROGRAM TIME LIMIT
*   BASED ON INLET CONDITIONS (AT Z=0)

```

\*  

---

```

TMAXC = QC*3.142*(DIA/2.)**2.*CHT*FCR/(FR*CF*60.)
TMAXA = QA*3.142*(DIA/2.)**2.*CHT*FAR/(FR*CF*60.)
IF(TMAXC.GE.TMAXA) THEN
  TMAX = TMAXC
ELSE
  TMAX = TMAXA
ENDIF

```

```

TAUMAX = KLC*CF*(TMAX*60.)/(PDA*QA)
DMAX=TMAX/1440.

```

WRITE(6,\*)

WRITE(6,\*)

WRITE(6,222)

WRITE(6,223)DMAX

WRITE(6,224)

222 FORMAT(' PROGRAM RUN TIME IS BASED ON TOTAL RESIN CAPACITY')

223 FORMAT(' AND FLOW CONDITIONS. THE PROGRAM WILL RUN

FOR',F12.1)

224 FORMAT(' DAYS OF COLUMN OPERATION FOR THE CURRENT  
CONDITIONS.')\*  

---

\* PRINT BREAKTHROUGH CURVE HEADINGS

\*  

---

IF (KPBK.NE.1) GO TO 50

WRITE (6,24)

WRITE (6,25)

WRITE (6,26)

WRITE (6,27)

WRITE (6,28)

50 CONTINUE

\*  

---

\* PRINT CONCENTRATION PROFILE HEADINGS

\*  

---

```

      T = 0.
      TAUPR = KLC*CF*(TIME*60.)/(PDA*QA)
      IF (KPPR.NE.1) GO TO 60
      WRITE (6,30)
      WRITE (6,31) TIME
      WRITE (6,32)
      WRITE (6,33)
      WRITE (6,34)
60 CONTINUE
*
* -----
* INITIALIZE VALUES PRIOR TO ITERATIVE LOOPS
*
* -----
      J = 1
      JK = 1
      TAUTOT = 0.
      JFLAG = 0
      KK = 1
      KPRINT = 1500
*
* -----
* DEFINING THE DESULPHONATION TERM(FISHER'S DATA)
* -- CONTEXT TO CODE
*
* -----
      S1 = (7.5E+6*EXP(-10278.6/(TMP+273.16))*CHTD
1      *3.1415927*(DIA**2.)*2.1)*(VS*PDA)*FCR
1      /(NT*3600.*4.0*FR*KLC*(1.-VD))
*
* -----
* TIME STEP LOOP WITHIN WHICH ALL COLUMN CALCULATIONS ARE
* IMPLEMENTED TIME IS INCREMENTED AND OUTLET CONCENTRATION
CHECKED
*
* -----
1 CONTINUE
  IF (TAUTOT.GT.TAUMAX) GOTO 138
  IF (J.EQ.4) THEN
    JD = 1
  ELSE
    JD = J + 1
  ENDIF
*
* -----
* SET INLET LIQUID PHASE FRACTIONAL CONCENTRATIONS FOR EACH
* SPECIES IN THE MATRIX
*
* -----
      COO = COII
      CHO = CHII
      XCA(J,1) = CCF/CF
      XNC(J,1) = CNF/CF

```

XBC(J,1) = CBF/CF

XSA(J,1) = CSF/CF

\*

\* LOOP TO INCREMENT DISTANCE (BED LENGTH) AT A FIXED TIME

\*

DO 400 K=1,NT

    CNO = XNC(J,K)\*CF

    CBO = XBC(J,K)\*CF

    CCO = XCA(J,K)\*CF

    CSO = XSA(J,K)\*CF

\*

\* CALL ROUTINES TO CALCULATE RN, RB, CNI, CBI(INTERFACIAL

\* CONCENTRATIONS

\* & COEFFICIENTS)

\*

    CALL KUM1(DN,DH,DB,CNO,CHO,CBO,TKBH,TKBN, YNC(J,K), YBC(J,K),  
1    QC,CNI,CHI,CBI,RN,RB)

    XNI = CNI/CF

    XBI = CBI/CF

    CALL KUM(DC,DO,DS,CCO,COO,CSO,TKSO,TKSC, YCA(J,K), YSA(J,K),  
1    QA,CCI,COI,CSI,RC,RS)

    XCI = CCI/CF

    XSI = CSI/CF

IF (K .EQ. 1) THEN

RATN(J,1) = 6.\*RN\*(XNC(J,1) - XNI)\*KLN\*PDA/(KLC\*PDC)

RATC(J,1) = 6.\*RC\*(XCA(J,1)-XCI)

RATS(J,1) = 9.\*RS\*(XSA(J,1)-XSI)\*KLS/KLC

RATB(J,1) = 9.\*RB\*(XBC(J,1)-XBI)\*KLB\*PDA/(KLC\*PDC)

    YNC(JD,1) = YNC(J,1)+TAU\*RATN(J,1)\*QA/QC

    YBC(JD,1) = YBC(J,1)+TAU\*RATB(J,1)\*QA/QC

    YCA(JD,1) = YCA(J,1)+TAU\*RATC(J,1)

    YSA(JD,1) = YSA(J,1)+TAU\*RATS(J,1)

ENDIF

IF ((YNC(JD,1)+YBC(JD,1)).GT.1.0)THEN

CALL CORRECT(Ybc(JD,1),Ync(JD,1),Ybc(J,1),Ync(J,1),TAU,

1    RATEb,RATEn)

    RATB(J,1)=RATEB\*QC/QA

    RATN(J,1)=RATEN\*QC/QA

ENDIF

IF ((YCA(JD,1)+YSA(JD,1)).GT.1.0)THEN

CALL CORRECT(YSA(JD,1),YCA(JD,1),YSA(J,1),YCA(J,1),TAU,

1    RATES,RATEC)

    RATS(J,1)=RATES

    RATC(J,1)=RATEC

ENDIF

---

\*  
 \* IMPLEMENT IMPLICIT PORTION OF THE BACKWARD DIFFERENCES  
 \* METHOD FROM THE PREVIOUS FUNCTION VALUES. FOR THE FIRST  
 \* THREE STEPS (ALONG THE DISTANCE) USE FOURTH-ORDER RUNGE  
 \* KUTTA METHOD

---

IF (K.LE.3) THEN

F1N = XI\*6.\*RN\*(XNC(J,K)-XNI)\*FCR\*KLN\*PDA/(KLC\*PDC)  
 F2N = XI\*6.\*RN\*((XNC(J,K)+F1N/2.)-XNI)\*FCR\*KLN\*PDA/(KLC\*PDC)  
 F3N = XI\*6.\*RN\*((XNC(J,K)+F2N/2.)-XNI)\*FCR\*KLN\*PDA/(KLC\*PDC)  
 F4N = XI\*6.\*RN\*(XNC(J,K)+F3N-XNI)\*FCR\*KLN\*PDA/(KLC\*PDC)  
 XNC(J,K+1) = XNC(J,K) - (F1N+2.\*F2N+2.\*F3N+F4N)/6.  
 F1B = XI\*9.\*RB\*(XBC(J,K)-XBI)\*FCR\*KLB\*PDA/(KLC\*PDC)  
 F2B = XI\*9.\*RB\*((XBC(J,K)+F1B/2.)-XBI)\*FCR\*KLB\*PDA/(KLC\*PDC)  
 F3B = XI\*9.\*RB\*((XBC(J,K)+F2B/2.)-XBI)\*FCR\*KLB\*PDA/(KLC\*PDC)  
 F4B = XI\*9.\*RB\*(XBC(J,K)+F3B-XBI)\*FCR\*KLB\*PDA/(KLC\*PDC)  
 XBC(J,K+1) = XBC(J,K) - (F1B+2.\*F2B+2.\*F3B+F4B)/6.  
 F1C = XI\*6.\*RC\*(XCA(J,K)-XCI)\*FAR  
 F2C = XI\*6.\*RC\*((XCA(J,K)+F1C/2.)-XCI)\*FAR  
 F3C = XI\*6.\*RC\*((XCA(J,K)+F2C/2.)-XCI)\*FAR  
 F4C = XI\*6.\*RC\*(XCA(J,K)+F3C-XCI)\*FAR  
 XCA(J,K+1) = XCA(J,K) - (F1C+2.\*F2C+2.\*F3C+F4C)/6.  
 F1S = XI\*9.\*RS\*(XSA(J,K)-XSI)\*FAR\*KLS/KLC  
 F2S = XI\*9.\*RS\*((XSA(J,K)+F1S/2.)-XSI)\*FAR\*KLS/KLC  
 F3S = XI\*9.\*RS\*((XSA(J,K)+F2S/2.)-XSI)\*FAR\*KLS/KLC  
 F4S = XI\*9.\*RS\*(XSA(J,K)+F3S-XSI)\*FAR\*KLS/KLC  
 XSA(J,K+1) = XSA(J,K) - (F1S+2.\*F2S+2.\*F3S+F4S)/6.+(S1/CF)

ELSE

COEN=3.\*XNC(J,K-3)/25. -16.\*XNC(J,K-2)/25. +  
 1 36.\*XNC(J,K-1)/25. -48.\*XNC(J,K)/25.  
 XNC(J,K+1) =-XI\*12.\*FCR\*RATN(J,K)/25.-COEN  
 COEB=3.\*XBC(J,K-3)/25. -16.\*XBC(J,K-2)/25. +  
 1 36.\*XBC(J,K-1)/25. -48.\*XBC(J,K)/25.  
 XBC(J,K+1) =-XI\*12.\*FCR\*RATB(J,K)/25.-COEB  
 COEC=3.\*XCA(J,K-3)/25. -16.\*XCA(J,K-2)/25. +  
 1 36.\*XCA(J,K-1)/25. -48.\*XCA(J,K)/25.  
 XCA(J,K+1) =- XI\*12.\*FAR\*RATC(J,K)/25.-COEC  
 COES=3.\*XSA(J,K-3)/25. -16.\*XSA(J,K-2)/25. +  
 1 36.\*XSA(J,K-1)/25. -48.\*XSA(J,K)/25.  
 XSA(J,K+1) = - XI\*12.\*FAR\*RATS(J,K)/25.-COES+(S1/CF)

ENDIF

---

\*  
 \* DETERMINE CONCENTRATIONS FOR THE DISTANCE STEP AND  
 RECALCULATE  
 \* BULK PHASE EQUILIBRIA

\*

---

```

CNO = XNC(J,K+1) * CF
CBO = XBC(J,K+1) * CF
CCO = XCA(J,K+1) * CF
CSO = XSA(J,K+1) * CF
CALL EQB(DISS,CNO,CBO,CCO,CSO,COO,CHO)

```

\*

```

* DETERMINE RATES AT CONSTANT XI FOR SOLUTIONS OF THE TAU
* MATERIAL BALANCE

```

\*

---

```

CALL
KUM1(DN,DH,DB,CNO,CHO,CBO,TKBH,TKBN,YNC(J,K+1),YBC(J,K+1),
1   QC,CNI,CHI,CBI,RN,RB)
    XNI = CNI/CF
    XBI = CBI/CF
    CALL KUM(DC,DO,DS,CCO,COO,CSO,TKSO,TKSC,YCA(J,K+1),YSA(J,K+1),
1   QA,CCI,COI,CSI,RC,RS)
    XCI = CCI/CF
    XSI = CSI/CF
RATN(J,K+1) = 6.*RN*((XNC(J,K+1)) - XNI)*KLN*PDA/(KLC*PDC)
RATB(J,K+1) = 9.*RB*KLB*((XBC(J,K+1))-XBI)*PDA/(KLC*PDC)
RATC(J,K+1) = 6.*RC*((XCA(J,K+1))-XCI)
RATS(J,K+1) = 9.*RS*KLS*((XSA(J,K+1))-XSI)/(KLC)

```

\*

```

* INTEGRATE Y USING ADAMS BASHFORTH (CALCULATE NEXT PARTICLE
* LOADING FOR THE SAME DISTANCE STEP)

```

\*

---

```

YNC(JD,K+1) = YNC(J,K+1) + TAU*RATN(J,K+1)*QA/QC
YBC(JD,K+1) = YBC(J,K+1) + TAU*RATB(J,K+1)*QA/QC
YCA(JD,K+1) = YCA(J,K+1) + TAU*RATC(J,K+1)
YSA(JD,K+1) = YSA(J,K+1) + TAU*RATS(J,K+1)

```

\*

```

* CHECK VALUES WITHIN BOUNDS

```

\*

---

```

IF ((YNC(JD,K+1)+YBC(JD,K+1)).GT.1.0)THEN
CALL CORRECT(Ybc(JD,K+1),Ync(JD,K+1),Ybc(J,K+1),
1   Ync(J,K+1),TAU,RATB(J,K+1),RATN(J,K+1))
    RATB(J,K+1)=RATB(J,K+1)*QC/QA
    RATN(J,K+1)=RATN(J,K+1)*QC/QA
    ENDIF
IF ((YCA(JD,K+1)+YSA(JD,K+1)).GT.1.0) THEN
CALL CORRECT(YSA(JD,K+1),YCA(JD,K+1),YSA(J,K+1),
1   YCA(J,K+1),TAU,RATS(J,K+1),RATC(J,K+1))
    ENDIF

```

```

400 CONTINUE

```

```

*
* _____
* PRINT BREAKTHROUGH CURVES
*
* _____
  IF (KPBK.NE.1) GO TO 450
    PN = CNO/1.E-6*23.
    PC = CCO/1.E-6*35.5
    PS = CSO/1.E-6*48.
    PB = CBO/1.E-6*40.
    TAUTIM = TAUTOT*PDA*QA/(KLC*CF*60.)/1440.
    pH = 14.+LOG10(COO)
    IF (KPRINT.NE.1500) GOTO 450
    IF(KNC.EQ.2)KNC = 0
77  WRITE(6,139) TAUTIM,PN,PB,PC,PS,PH
139 FORMAT(1x,F11.6,2X,E12.7,2X,E12.7,2X,E12.7,4X,E12.7,4X,F4.2)
*
* _____
* STORE EVERY THOUSAND FIVE HUNDREDTH ITERATION TO THE PRINT
* FILE
*
* _____
  KPRINT = 0
450 CONTINUE
  KPRINT = KPRINT+1
  JK = J
  IF (J.EQ.4) THEN
    J = 1
  ELSE
    J = J+1
  ENDIF
*
* _____
* END OF LOOP RETURN TO BEGINNING AND STEP IN TIME
*
* _____
  IF (JFLAG.EQ.1) STOP
  TAUTOT = TAUTOT + TAU
  GOTO 1
*
* _____
* PRINT OUT FORMATS
*
* _____
10 FORMAT (' MIXED BED SYSTEM PARAMETERS:')
11 FORMAT (' ')
12 FORMAT (' RESIN REGENERATION',2X,': YNO =',F5.3,
  1 ' YSO =',F5.3)
13 FORMAT (' RESIN PROPERTIES',4X,': PDC =',F6.4,5X,'VD =',F6.4)
14 FORMAT (' RESIN CONSTANTS',5X,': QC =',F6.4,5X,'QA =',F6.4)
15 FORMAT (' COLUMN PARAMETERS',3X,': CF =',E10.4,' FR =',E10.5,3X,
  1 'DIA =',F6.2,2X,'CHT =',F5.1)
16 FORMAT (' IONIC CONSTANTS',5X,': DN =',E10.4,2X,'DS =',E10.4,

```

```

1      2X,'DH =' ,E10.4)
117 FORMAT (' IONIC CONSTANTS',5X,': DC =' ,E10.4,2X,'DB =' ,E10.4,
1      2X,'DO =' ,E10.4)
17 FORMAT (' FLUID PROP.',8X,': CP =' ,F7.5,4X,' DEN =' ,F6.3,
1      4X,' TEMP =' ,F6.1)
18 FORMAT (' ')
19 FORMAT (' CALCULATED PARAMETERS :')
20 FORMAT (' ')
21 FORMAT (' INTEGRATION INCREMENTS : TAU =' ,F7.5,5X,'XI =' ,F7.5,
1      5X,'NT =' ,I6)
22 FORMAT (' TRANSFER COEFFICIENTS : REC=' ,E10.4,' KLN =' ,E10.4)
88 FORMAT (' ,25X,' KLB =' ,E10.4,2x,'KLC =' ,E10.4)
23 FORMAT (' SUPERFICIAL VELOCITY : VS =' ,F7.3)
24 FORMAT (' ')
25 FORMAT (' BREAKTHROUGH CURVE RESULTS:')
26 FORMAT (' ')
27 FORMAT (6x,' Time',6X,'SODIUM',6x,'CALCIUM',8X,'CHLORIDE',
1      8X,'SULFATE',6x,'pH')
28 FORMAT (' ,6X,'Days'.7x,'ppb',11X,'ppb',11X,'ppb',13x,'ppb')
29 FORMAT (' ,4(4X,E8.3),5X.F4.2)
30 FORMAT (' ')
31 FORMAT (' CONCENTRATION PROFILES AFTER ',F5.0,' MINUTES')
32 FORMAT (' ')
33 FORMAT (' ,5X,'Z',7X,'XNC',7X,'YNC',
1      7X,'YCA')
34 FORMAT (' ')
35 FORMAT (' ,6(2X,E8.3))
138 STOP
      END

```

```

* -----
* THE SULFATE SUBROUTINE-> (CALCULATION OF ANIONIC
INTERFACIAL
* CONCENTRATIONS)
* -----
      SUBROUTINE KUM(DC,DO,DS,CCO,COO,CSO,TKSO,TKSC,YC,YS,
1      QA,CCI,COI,CSI,RC,RS)
      IMPLICIT REAL*8(A-H, O-Z)
      EPSILON = 1.0E-14
      EPN = 2./3.
      S = DC*CCO**2+((2.*DC)+(2.*DO))*COO*CCO
1      +((4.*DC)+(6.*DS))*CSO*CCO+DO*COO**2.
1      +((4.*DO)+(6.*DS))*COO*CSO+6.*DS*CSO**2.
      YO = 1. - YC - YS
      YO=ABS(YO)
      A =6.*DS

```



```

      B = ((4.*DC)+(6.*DS))*YC*SQRT(TKSC)
1   +((4.*DO)+(6.*DS))*YO*SQRT(TKSO)/SQRT(YS * QA)
      E = (DC*TKSC*YC**2.+((2.*DC)+(2.*DO))*YO*YC*SQRT(TKSO*TKSC)
1   +DO*TKSO*YO**2.)/(YS*QA)
      X0 = E
      X = X0 -((A*X0**4.) + (B*X0**3.) + (E*X0**2.) - S)/
1   ((4.*A*X0**3.) + (3.*B*X0**2.) + 2.*E*X0)
      DO WHILE ((ABS(X-X0)/X).GT.EPSILON)
      X0 = X
      X = X0 -((A*X0**4.) + (B*X0**3.) + (E*X0**2.) - S)/
1   ((4.*A*X0**3.) + (3.*B*X0**2.) + 2.*E*X0)
      END DO
      IF(X.LT.0.0) THEN
      X = 0.0
      ENDIF
      CSI = X**2.
      COI = YO*SQRT((TKSO * CSI)/(YS*QA))
      IF(COI.LT.0.0)COI=0.0
      CCI = YC*SQRT(TKSC*CSI/(YS*QA))
      IF(CCI.LT.0.0)CCI=0.0
      CTI = CSI + COI + CCI
      CTO = CSO + COO + CCO
C-----
C   CALCULATE TERNARY DIFFUSIVITIES
C-----
      IF(ABS(CSO - CSI).GE.(CSO/100000.)) GO TO 52
      DESS = 0.0
      GOTO 53
52  DESS = 3.*(CTI/CTO*CSI/CSO-1.)/
1   (1.+CTI/CTO)/(1.-CSI/CSO)
53  IF(ABS(CCO - CCI).GE.(CCO/100000.)) GOTO 59
      DEC = 0.0
      GOTO 61
59  DEC = 2.*(CTI/CTO*CCI/CCO-1)/(1.+CTI/CTO)/(1.-CCI/CCO)
61  CONTINUE
      RS = (ABS(DESS))**EPN
      RC = (ABS(DEC))**EPN
      RETURN
      END
* -----
*   INTERFACIAL CONCENTRATIONS FOR CATIONS : 1 DIVALENT AND 2
MONOVALENT
*   BASED SIMILAR TO SULFATE SUBROUTINE   :
* -----
      SUBROUTINE KUM1(DN,DH,DB,CNO,CHO,CBO,TKBH,TKBN,YN,YB,

```

```

1      QC,CNI,CHI,CBI,RN,RB)
      IMPLICIT REAL*8 (A-H, O-Z)
      EPSILON = 1.0E-14
      EPN = 2./3.
      S = DN*CNO**2+((2.*DN)+(2.*DH))*CHO*CNO
1  +((4.*DN)+(6.*DB))*CBO*CNO+DH*CHO**2.
1  +((4.*DH)+(6.*DB))*CHO*CBO+6.*DB*CBO**2.
      YH = 1. - YN - YB
      A = 6.*DB
      B = ((4.*DN)+(6.*DB))*YN*SQRT(TKBN)
1  +((4.*DH)+(6.*DB))*YH*SQRT(TKBH)/SQRT(YB * QC)
      E = (DN*TKBN*YN**2.+((2.*DN)+(2.*DH))*YH*YN*SQRT(TKBH*TKBN)
1  +DH*TKBH*YH**2.)/(YB*QC)
      X0 =E
      X = X0 -((A*X0**4.) + (B*X0**3.) + (E*X0**2.) - S)/
1  ((4.*A*X0**3.) + (3.*B*X0**2.) + 2.*E*X0)
      DO WHILE ((ABS(X-X0)/X).GT.EPSILON)
      X0 = X
      X = X0 -((A*X0**4.) + (B*X0**3.) + (E*X0**2.) - S)/
1  ((4.*A*X0**3.) + (3.*B*X0**2.) + 2.*E*X0)
      END DO
      IF(X.LT.0.0) THEN
      X=0.0
      ENDIF
      CBI =X**2.
      CHI = YH*SQRT((TKBH * CBI)/(YB*QC))
      IF(CHI.LT.0.0)CHI=0.0
      CNI = YN*SQRT(TKBN*CBI/(YB*QC))
      IF(CNI.LT.0.0)CNI=0.0
      CTI = CBI + CHI + CNI
      CTO = CBO + CHO + CNO
C-----
C  CALCULATE TERNARY DIFFUSIVITIES
C-----
      IF(ABS(CBO - CBI).GE.(CBO/100000.)) GO TO 52
      DEBB = 0.0
      GOTO 53
52  DEBB = 2.*(CTI/CTO*CBI/CBO-1.)/
1  (1.+CTI/CTO)/(1.-CBI/CBO)
53  IF(ABS(CNO - CNI).GE.(CNO/100000.)) GOTO 59
      DEN = 0.0
      GOTO 61
59  DEN = 1.*(CTI/CTO*CNI/CNO-1)/(1.+CTI/CTO)/(1.-CNI/CNO)
61  CONTINUE
      RB = (ABS(DEBB))**EPN

```

```

      RN = (ABS(DEN))**EPN
RETURN
END

```

```

      SUBROUTINE EQB(DISS,CNO,CBO,CCO,CSO,COO,CHO)

```

```

*

```

```

* Subroutine to calculate bulk phase concentrations
* based on amine equilibrium

```

```

IMPLICIT REAL*8 (A-H,O-Z)
V1=(CNO+CBO-CCO-CSO)**2.+4.*DISS
COO=(CNO+CBO-CCO-CSO+(V1**0.5))/2.
CHO=DISS/COO
RETURN
END

```

```

*

```

```

      SUBROUTINE CORRECT(YSA,YCA,YSAOLD,YCAOLD,TAU,
1          RATES,RATEC)

```

```

*

```

```

* Subroutine to correct the bulk concentration when the
* calculated loading exceeds 1.0 on the resin

```

```

IMPLICIT REAL*8 (A-H,O-Z)
YYY=YSA+YCA-1.0
IF (ysa.GE.yca) THEN
  IF (YSA.GT.1.0) THEN
    YSA=0.999999
    YCA=0.0000005
    GOTO 120
  ELSE
    YCA=YCA-YYY
    IF (YCA.LE.0.0) THEN
      YCA=0.0000005
      YSA=0.999999
    ENDIF
  ENDIF
ELSE
  IF (YCA.GT.1.0) THEN
    YCA=0.999999
    YSA=0.0000005
    GOTO 120
  ELSE
    YSA=YSA-YYY
    IF (YSA.LE.0.0) THEN
      YSA=0.0000005
      YCA=0.999999
    ENDIF
  ENDIF
ENDIF

```

```
ENDIF  
120  RATES=(YSA-YSAOLD)/TAU  
    RATEC=(YCA-YCAOLD)/TAU  
RETURN  
END
```

## VITA

Sudhir K. Pondugula

Candidate for the Degree of

Master of Science

Thesis: MIXED BED ION EXCHANGE MODELING FOR DIVALENT  
IONS IN A TERNARY SYSTEM

Major Field: Chemical Engineering

Biographical:

Personal Data: Born in Vijayawada, India, March 01, 1970, the son of Rajyalakshmi and Ramaiah Venkata Pondugula.

Education: Graduated from Kendriya Vidyalaya Central School, Visakhapatnam, AP, India, in May 1988; received Bachelor of Technology Degree in Chemical Engineering from Andhra University in May 1992; completed requirements for the Master of Science degree at Oklahoma State University in May, 1995.

Professional Experience: Employed as a research assistant, School of Chemical Engineering, Oklahoma State University, September 1992 to May 1994.